2014

Pyrolysis and catalytic pyrolysis of protein- and lipid-rich feedstock

Kaige Wang
Iowa State University

Pyrolysis and catalytic pyrolysis of protein- and lipid-rich feedstock

by

Kaige Wang

A dissertation submitted to the graduate faculty

in partial fulfillment of the requirements for the degree of

DOCTOR OF PHILOSOPHY

Co-Majors: Mechanical Engineering; Biorenewable Resources and Technology

Program of Study Committee:
Robert Brown, Major Professor
Song-Charng Kong
Terry Meyer
Shihwu Sung
Tong Wang

Iowa State University

Ames, Iowa

2014

DEDICATION

Dedicated to my dear Mama (Mom) Baba (Dad)

TABLE OF CONTENTS

ACKNOWLEDGEMENTS

I am glad to take the opportunity to express my gratitude to all those people who contributed towards the successful completion of this work directly or indirectly. Foremost, I would like to thank my supervisor Dr. Robert C. Brown for his trust, motivation, and support in numerous ways in last four years.

I would like to thank my committee members Dr. Song-Charng Kong, Dr. Terry Meyer, Dr. Tong Wang, and Dr. Shihwu Sung, for their guidance and support throughout my PhD program.

In addition, I would also like to thank my friends and colleagues in Center for Sustainable Environmental Technologies (CSET). I am grateful to the help and discussion from staff members in particular Ryan Smith, Patrick Johnston, Marjorie Rover. I would also like to thank previous CSET staffs Weihua Deng and Sunith Sadula for their help and friendship. I am grateful to CSET colleagues including Mark Mba Wright, Pushkaraj Patwardhan, Pedro Ortiz, Katherine Brewer, Dustin Dalluge, Karl Broer, Nice Creager, Patrick Woolcock, Yanan Zhang, Bernardo del Campo, Matt Kiefer, Martin Haverly, Yan Zheng, Juan Peron, Tannon Daugaard, Chamila Thilakaratne, Longwen Ou, KwangHo Kim and Joe Polin. Their friendship and help makes my time at Iowa State University a wonderful experience. I would also like to thanks Dr. Zhiyou Wen, Dr. Tristan Brown and Dr. Jackie Shanks for their guidance, discussions and help during the PhD program.

Finally, I would like to thank my families, who constantly support and encourage me. Special thanks to my grandparents for their love and encouragement in my life.

CHAPTER 1 INTRODUCTION

Biomass and renewable fuel production

Advancing America's technologies for the production of renewable transportation fuels is a critical element in our country's efforts to reduce foreign energy dependence and to mitigate environmental problems caused by fossil fuel usage [1, 2]. The United States currently imports approximately two-thirds of its petroleum. In an effort to reduce this level of dependence and to promote cleaner fuels, the U.S. Energy Independence and Security Act (EISA) of 2007 established minimum production requirements for domestic alternative fuels[3, 4]. EISA's Renewable Fuel Standard (RFS) requires renewable transportation fuel production to reach 36 billion gallons a year nationally by 2022. This ambitious target demands the development of cost-effective processes and an expansion of feedstock production.

Biomass derived from trees, grasses, and aquatic crops are versatile and important renewable feedstocks for the production of biofuels. Based on the types of feedstock used, biofuels can be classified into first and second generations [5]. First-generation biofuels are produced from the sugars and lipids found in arable crops such as corn, sugarcane, rapeseed, etc. In comparison, second-generation biofuels are made from non-food biomass including lignocellulose, microalgae and municipal solid waste.

First-generation biofuel production

The two main types of first-generation biofuels used commercially are biodiesel and bioethanol, of which large quantities have been produced worldwide. The production processes for bioethanol and biodiesel are considered "established technology" [1, 5]. Biodiesel is a substitute for diesel and is produced through transesterification of vegetable

oils, residual oils, and fat. Bioethanol is derived from sugar or starch through fermentation [5].

Biodiesel production utilizes the lipid in oilseeds, leaving lipid-extracted press cakes as a by-product. The press cakes contain large amounts of edible or non-edible protein. The edible protein can provide essential amino acids for animal and human consumption. However, some of the oil-seed press cakes, such as those produced from jatropha, neem, karanja, etc. are non-edible for either livestock or humans [6, 7]. Production of bioethanol, especially corn-based bioethanol, also produces large amounts of protein-rich residuals. The U.S. corn ethanol industry has continuously expanded over the past decade; domestic corn ethanol production increased eight-fold between 2000 and 2012 [8, 9]. The production of corn ethanol utilizes the starch present in the corn, leaving protein, crude fat, and fibers as a leftover product called dry distillers grains with solubles (DDGS). With every gallon of ethanol produced, approximately 2.6 kg of DDGS are produced [7]. In 2011, the U.S. ethanol industry produced 36 million metric tons of DDGS, which is an increase of nearly 32 million metric tons over the past decade [7, 8]. Currently, DDGS is primarily used as enriched feed for livestock [10]. As the biofuel industry grows, however, the increasing supply of DDGS may saturate or eventually surpass the demand from the livestock feed market. Moreover, there is a concern that the demand from the livestock industry may become constrained due to certain negative effects of feeding DDGS, including growth depression of animals and undesirable meat quality [10]. Studies have also shown that feeding DDGS to beef cattle results in a net increase of greenhouse gas emission due to an increase in the cattle's nitrogen excretion [11].

Second-generation biofuel production

Although production technologies for first-generation biofuels are well established, these technologies have garnered a fair amount of skepticism among scientists [5]. The technologies offer limited reduction in greenhouse gas emissions, which limits the development of first-generation biofuels [4, 5]. Another disadvantage of first-generation biofuels is the food-versus-fuel debate. Increases in the production of first-generation biofuels have been blamed for rising food prices. These multiple limitations of first-generation biofuels have led to the development of second-generation biofuels, also known as advanced biofuels.

Feedstocks for second-generation biofuel production include lignocellulosic biomass and microalgae biomass, both of which have been extensively investigated in recent years [3]. lignocellulosic feedstocks were identified as a significant source of biomass by the U.S. Department of Energy [12], and many pathways are currently under consideration for the production of biofuels and bio-based chemicals from lignocellulosic biomass. While lignocellulosic biomass consists of cellulose, hemicellulose, and lignin, microalgae biomass consists mainly of proteins, lipids, and carbohydrates. Microalgae have captured the interests of researchers around the world, who are intrigued by the algae's high biomass yield and ability to synthesize and accumulate large quantities of neutral lipids [13]. Viable products generated from microalgae range from gases, such as hydrogen, to alcohols and alkanes; among these, lipid-based biodiesel is the most well-investigated product [3, 13].

One of the great challenges for microalgae biodiesel production is the question of how to utilize the remnants that remain after lipid extraction. These remnants represent about 30-80 wt% of the algal feedstock, depending on the microalgae strains and the growth

conditions [13]. While the market for advanced biofuels is growing fast, the same is not happening for the abundant by-products. Historically, the remnants have been used for animal feed supplementation, but microalgae's effectiveness in capturing and concentrating heavy metals and the relatively small size of the animal feed market compared to energy markets has limited this market's potential to address the problem of microalgal remnants. If microalgae were to replace petroleum as the feedstock for the U.S. gasoline supply, 750 million tons of algal remnants would be produced annually. That's 50 times the amount of feed supplement required by the 100 million cattle in the U.S. So far, no clear strategy has emerged for utilizing the remnants after oil extraction.

Thermochemical conversion of protein-rich biomass

As discussed above, current biorefining technologies utilize only one component in biomass while leaving protein and other components as residuals. The full potential of protein-rich biomass has not been well explored, but improper disposals protein-rich biomass will lead to economic and ecological problems for current first- and second- generation biofuels production [6, 14, 15].

Thermochemical biomass conversion offers an alternative that can utilize the entire energy content of the biomass in a matter of seconds. Thus, thermochemical conversion of protein-rich biomass into biofuel and bio-based chemicals may enhance the economic and environmental sustainability of the current biorefinery. Generally, thermochemical biofuel pathways can be classified into gasification, hydrothermal liquefaction, and pyrolysis.

Gasification

Gasification uses oxygen-starved conditions and elevated temperatures (typically 750-1500°C) to convert carbon-rich materials into flammable gas mixtures consisting of

carbon monoxide, hydrogen, methane, nitrogen, carbon dioxide, and smaller quantities of higher hydrocarbons and inorganic contaminants such as hydrogen sulfide and ammonia [1]. The gas mixture, which is sometimes called syngas, can be used not only for generation of heat and power, but also as a feedstock for production of liquid fuels and chemicals. Gasification has been well-explored for lignocellulosic biomass [16]. Protein-rich biomass has inherently high energy content, making it suitable for direct combustion or gasification for energy production. The potentials of algal biomass and DDGS as feedstocks for gasification have been explored by various researchers [17-22]. Davies et al. [19] also demonstrated electricity generation by combining a steam engine system and gasifier, using DDGS as feedstock. Gasification of algal biomass has produced syngas with higher yield and heating value than that produced from the less-protein-rich lignocellulosic biomass [20, 22]. The cost of the fuel produced through the gasification pathway is expected to be two times higher than conventional gasoline due to high capital costs of syngas production from lignocellulose and syngas synthesis [23, 24]. This analysis could also hold true for protein-rich biomass.

Hydrothermal liquefaction

Hydrothermal liquefaction exploits enhanced solvent properties in compressed or supercritical water. Aquatic biomass, especially microalgal biomass, is a preferred feedstock for hydrothermal processing due to its massive water content. The major product of this process is “bio-crude,” which has a high energy content and can be upgraded to diesel fuel. Extensive studies have been conducted to explore the potential of hydrothermal liquefaction of wet algal biomass [25-31]and it is considered a promising technological approach. However, more research - including pilot-scale evaluations and techno-economic analyses -

is needed before hydrothermal liquefaction of algae can become a commercially viable option.

Pyrolysis

Pyrolysis, the thermal conversion of materials in the absence of oxygen, also has potential for converting protein-rich biomass into bio-oil for upgrading to fuels and chemicals. Fast pyrolysis has already been developed for converting lignocellulosic biomass into advanced biofuels [32]. Fast Pyrolysis yields three products: gas, solid, and liquid. Pyrolysis gas is a flammable mixture of carbon monoxide, hydrogen, carbon dioxide, and light hydrocarbons suitable for generating process heat [32]. The solid biochar product is primarily composed of reduced aromatic carbon and contains most of the mineral components of the feedstock [32, 33]. Biochar has various potential applications, including usage as a soil amendment and a carbon sequestration agent [33]. The liquid bio-oil product is a high viscosity, dark-brown liquid composed of numerous organic components along with up to 15–20 wt% water. Bio-oil can be upgraded to drop-in fuels through hydroprocessing and catalytic cracking [32, 33]. Compared to the pyrolysis of lignocellulosic biomass with low-protein content, relatively little is known about the pyrolysis of biomass with high-protein and lipid content.

Wood et al. [34, 35] examined pyrolysis of corn DDGS to produce bio-oil and bio-char as a potential opportunity for expanding markets for DDGS and improving the sustainability of the corn ethanol industry. Their study showed that the yields of bio-oil produced from DDGS were comparable to those produced from lignocellulosic biomass [34, 35]. The gas chromatography/mass spectrometry (GC/MS) analysis indicated that the bio-oil from microwave pyrolysis of DDGS contained a series of aliphatic and aromatic

hydrocarbons [36]. Boateng's [37, 38] group pyrolyzed barley-derived DDGS, pennycress press cake, and other protein-rich biomass in a fluidized bed reactor. Relatively higher yields of bio-oil with high-energy density were obtained from DDGS, compared with those obtained from lignocellulosic biomass. Boateng's group also found that bio-oil from high-protein biomass exhibited better thermal stability than that from low-protein biomass [38]. The few studies that have been performed [39, 40] suggest that pyrolysis of protein-rich microalgae can also produce bio-oil that, in some respects, is superior to bio-oil from lignocellulosic biomass. Miao et al. [40] reported that bio-oil from microalgae was characterized by lower oxygen content and a higher heating value than bio-oil from lignocellulosic biomass. Bio-oil yields of 18% and 24% for pyrolysis of *Chlorella protothecoides* and *Microcystis aeruginosa* were achieved, respectively. Another study by this group showed that controlling microalgal growth conditions could tailor the yield and composition of the resulting bio-oil [39]. They reported a 57.9% yield of bio-oil from the fast pyrolysis of heterotrophic *C. protothecoides*. Grierson et al. [41] compared pyrolysis of six species of microalgae in a tube reactor under slow heating conditions; calculations of the process energy requirements indicated that the process was self-sustaining.

In spite of these appealing advantages, bio-oil from those protein-rich biomass feedstocks contains a high content of nitrogen, which may poison catalysts during bio-oil upgrading and produce unacceptable nitrogen oxide emissions during combustion [32, 34, 36, 42, 43]. Therefore, methods to remove nitrogen must be devised if transportation fuels are the final products from DDGS. Catalytic pyrolysis

The high oxygen content and instability during storage of bio-oil impedes commercial deployment of pyrolysis technology. Catalytic pyrolysis has emerged as a means for

improving the quality of bio-oil [44-49]. Although alkali in biomass can catalytically react with solid biomass [50, 51], most heterogeneous catalysts appear to react with the vapor products released from pyrolyzing biomass [44, 45, 52-55].

Catalytic pyrolysis can be performed in the presence of transition-metal or precious-metal catalysts and gaseous hydrogen to promote hydrodeoxygenation, which is referred to hydropyrolysis process[48, 49]. Otherwise, zeolite catalysts such as HZSM-5 are used to deoxygenate pyrolysis vapors through decarbonylation, decarboxylation, and dehydration to produce aromatics and olefins [45, 52, 53]. Catalytic pyrolysis with zeolites is attractive for several reasons. Zeolites are relatively inexpensive and robust compared to the transition-metal and precious-metal catalysts. They can be readily regenerated to remove deposits of coke. They do not require hydrogen or other reactive agents and can be used at atmospheric pressure. Thus, zeolites are very attractive for catalytic conversion of pyrolysis vapors into partially or fully deoxygenated molecules that can be refined with crude oil to produce transportation fuels

Although significant research has been devoted to catalytic pyrolysis processes that deoxygenate these compounds in order to produce higher quality bio-oil, limited studies have been conducted on catalytic pyrolysis of protein- and lipid-rich biomass. Milne et al. [56] first proposed the catalytic conversion of whole microalgae over HZSM-5, but claimed that the results were ambiguous. Another study in 2010 showed that HZSM-5 increased the hydrocarbon fraction in the bio-oil from *Nannochloropsis sp.* in a fixed bed reactor [57], but no quantitative results were reported and the fate of the nitrogen during this process was not addressed.

Thesis scope

The objective of this thesis is to explore the potential of protein- and lipid-rich biomass for biofuel and bio-based chemicals production. Both pyrolysis and catalytic pyrolysis are explored in this study. A comparative study of lignocellulosic biomass and protein-rich biomass is also performed. In this work, protein-rich biomass, including microalgal biomass and by-product from bioethanol plant (DDGS), are used. Model compounds for individual components in the biomass are used to investigate the reaction mechanism.

This dissertation is organized into eight chapters, including this Chapter 1 introduction. Chapter 2 describes fast pyrolysis of microalgae remnants in a bench-scale fluidized bed reactor for bio-oil and bio-char production. The properties of bio-oil and biochar produced from the protein-rich biomass are characterized.

Chapter 3 explores the potential for catalytic pyrolysis of microalgae to improve the properties of bio-oil. After the addition of zeolite catalyst, the reaction network of algae pyrolysis changed. The nitrogen- and oxygen-containing compounds were eliminated and aromatic hydrocarbons were generated. The result indicates that protein-derived nitrogen compounds can be converted to aromatic hydrocarbons in the same way that oxygenates from lignocellulosic biomass are converted. In this process, nitrogen in the microalgae was released as ammonia, which suggests the potential to recycle nitrogen as a nutrient for microalgae cultivation.

Chapters 4 and 5 discuss the chemistry of catalytic pyrolysis using the individual components of both lignocellulosic and protein-rich biomass. Protein, lipid, cellulose, hemicellulose, and lignin were used as feedstock for catalytic pyrolysis. Performances of the

individual components in catalytic pyrolysis were distinct from each other. The interactions between the individual components during catalytic pyrolysis were also investigated. DDGS was explored as a feedstock for catalytic pyrolysis.

Chapter 6 discusses two types of catalytic pyrolysis in a micro-reactor system: *in-situ* and *ex-situ*. Various reaction parameters were evaluated for those two processes. The product distributions from the two types of catalytic pyrolysis were compared. The results show that mass and heat transfer significantly affect product distribution from catalytic pyrolysis.

Chapter 7 is dedicated to techno-economic analysis of an integrated corn biorefinery combing ethanol production and DDGS conversion to hydrocarbons from catalytic pyrolysis.The result suggests that the minimum-fuel-selling-price for the integrated biorefinery is comparable to the conventional ethanol plant with selling DDGS as by-product. Moreover, modest improvement in yield of hydrocarbons from catalytic pyrolysis could make the integrated biorefinery competitive with conventional ethanol plant. General conclusions and directions for future work are discussed in Chapter 8.

References

[1] R.C. Brown, Biorenewable Resources: Engineering New Products from Agriculture, Ames,IA, 2003.

[2] R. Brown, C, T. Brown, R, Why are We Producing Biofuels?, Brownia LLC 2012.

[3] U. DOE, National algal biofuels technology roadmap, US Department of Energy, Office of Energy Efficiency and Renewable Energy, Biomass Program, (2010).

[4] N.R.C.C.o. Economic, E.I.o.I.B. Production, Renewable Fuel Standard: Potential Economic and Environmental Effects of US Biofuel Policy, National Academies Press, 2011.

[5] S.N. Naik, V.V. Goud, P.K. Rout, A.K. Dalai, Production of first and second generation biofuels: A comprehensive review, Renewable and Sustainable Energy Reviews, 14 (2010) 578-597.

[6] Y.-X. Huo, D.G. Wernick, J.C. Liao, Toward nitrogen neutral biofuel production, Current opinion in biotechnology, 23 (2012) 406-413.

[7] T.M. Lammens, M.C.R. Franssen, E.L. Scott, J.P.M. Sanders, Availability of protein-derived amino acids as feedstock for the production of bio-based chemicals, Biomass and Bioenergy, 44 (2012) 168-181.

[8] C.W.K.M.K.A. Rosentrater, Pyrolysis of Distillers Grains, in: Agricultural and Biosystems Engineering Presentations and Posters, 2012.

[9] C.W.K.M.K.A. Rosentrater, Optimization of the Pyrolysis of Distillers Dried Grains with Solubles, in: Agricultural and Biosystems Engineering Presentations and Posters, 2013.

[10] R. Song, Lipid peroxidation in corn dried distillers grains with solubles (DDGS) and effects of feeding a highly oxidized DDGS source to swine, in, THE UNIVERSITY OF MINNESOTA, 2013.

[11] M. Hünerberg, S.M. Little, K.A. Beauchemin, S.M. McGinn, D. O'Connor, E.K. Okine, O.M. Harstad, R. Kröbel, T.A. McAllister, Feeding high concentrations of corn dried distillers' grains decreases methane, but increases nitrous oxide emissions from beef cattle production, Agricultural Systems, (2014).

[12] R.D. Perlack, L.L. Wright, A.F. Turhollow, R.L. Graham, The technical feasibility of a billion-ton annual supply, in, Oak Ridge National Laboratory, 2005.

[13] Q. Hu, M. Sommerfeld, E. Jarvis, M. Ghirardi, M. Posewitz, M. Seibert, A. Darzins, Microalgal triacylglycerols as feedstocks for biofuel production: perspectives and advances, The Plant Journal, 54 (2008) 621-639.

[14] M. Appl, Ammonia, in: Ullmann's Encyclopedia of Industrial Chemistry, Wiley-VCH Verlag GmbH & Co. KGaA, 2000.

[15] G.W. Huber, S. Iborra, A. Corma, Synthesis of transportation fuels from biomass: chemistry, catalysts, and engineering, Chem. Rev., 106 (2006) 4044-4098.

[16] V. Kirubakaran, V. Sivaramakrishnan, R. Nalini, T. Sekar, M. Premalatha, P. Subramanian, A review on gasification of biomass, Renewable and Sustainable Energy Reviews, 13 (2009) 179-186.

[17] A. Kumar, K. Eskridge, D.D. Jones, M.A. Hanna, Steam–air fluidized bed gasification of distillers grains: Effects of steam to biomass ratio, equivalence ratio and gasification temperature, Bioresour. Technol., 100 (2009) 2062-2068.

[18] A. Tavasoli, M.G. Ahangari, C. Soni, A.K. Dalai, Production of hydrogen and syngas via gasification of the corn and wheat dry distiller grains (DDGS) in a fixed-bed micro reactor, Fuel Processing Technology, 90 (2009) 472-482.

[19] A. Davies, R. Soheilian, C. Zhuo, Y.A. Levendis, Pyrolytic Conversion of Biomass Residues to Gaseous Fuels for Electricity Generation, Journal of Energy Resources Technology, 136 (2013) 021101-021101.

[20] A. Hirano, K. Hon-Nami, S. Kunito, M. Hada, Y. Ogushi, Temperature effect on continuous gasification of microalgal biomass: theoretical yield of methanol production and its energy balance, Catalysis Today, 45 (1998) 399-404.

[21] S. Amin, Review on biofuel oil and gas production processes from microalgae, Energy Conversion and Management, 50 (2009) 1834-1840.

[22] L. Sanchez-Silva, D. López-González, A.M. Garcia-Minguillan, J.L. Valverde, Pyrolysis, combustion and gasification characteristics of Nannochloropsis gaditana microalgae, Bioresource Technology, 130 (2013) 321-331.

[23] R.M. Swanson, A. Platon, J.A. Satrio, R.C. Brown, Techno-economic analysis of biomass-to-liquids production based on gasification, Fuel, 89 (2010) S11-S19.

[24] P.L. Spath, D.C. Dayton, Preliminary screening-technical and economic assessment of synthesis gas to fuels and chemicals with emphasis on the potential for biomass-derived syngas, in, DTIC Document, 2003.

[25] P. Biller, A. Ross, Potential yields and properties of oil from the hydrothermal liquefaction of microalgae with different biochemical content, Bioresource technology, 102 (2011) 215-225.

[26] D. López Barreiro, W. Prins, F. Ronsse, W. Brilman, A critical review on microalgae hydrothermal liquefaction (HTL): state of the art and evaluation for different algal strains, in: ANQUE's International congress of Chemical Engineering 2012 (ANQUE ICCE 2012), ANQUE, 2012, pp. T8-111-T118-112.

[27] P. Duan, P.E. Savage, Hydrothermal Liquefaction of a Microalga with Heterogeneous Catalysts, Ind. Eng. Chem. Res., 50 (2010) 52-61.

[28] T.M. Brown, P. Duan, P.E. Savage, Hydrothermal liquefaction and gasification of Nannochloropsis sp, Energy & Fuels, 24 (2010) 3639-3646.

[29] P.J. Valdez, J.G. Dickinson, P.E. Savage, Characterization of product fractions from hydrothermal liquefaction of Nannochloropsis sp. and the influence of solvents, Energy & Fuels, 25 (2011) 3235-3243.

[30] R.B. Levine, T. Pinnarat, P.E. Savage, Biodiesel production from wet algal biomass through in situ lipid hydrolysis and supercritical transesterification, Energy & Fuels, 24 (2010) 5235-5243.

[31] P. Duan, P.E. Savage, Catalytic hydrotreatment of crude algal bio-oil in supercritical water, Applied Catalysis B: Environmental, 104 (2011) 136-143.

[32] D. Mohan, C.U. Pittman, P.H. Steele, Pyrolysis of Wood/Biomass for Bio-oil: A Critical Review, Energy & Fuels, 20 (2006) 848-889.

[33] D.A. Laird, R.C. Brown, J.E. Amonette, J. Lehmann, Review of the pyrolysis platform for coproducing bio‐oil and biochar, Biofuels, Bioproducts and Biorefining, 3 (2009) 547-562.

[34] C. Wood, K. Muthukumarappan, K.A. Rosentrater, Pyrolysis of Distillers Grains, in: Agricultural and Biosystems Engineering Presentations and Posters, 2012.

[35] C. Wood, K. Muthukumarappan, K.A. Rosentrater, Optimization of the Pyrolysis of Distillers Dried Grains with Solubles, in: Agricultural and Biosystems Engineering Presentations and Posters, 2013.

[36] H.W. Lei, S.J. Ren, L. Wang, Q. Bu, J. Julson, J. Holladay, R. Ruan, Microwave pyrolysis of distillers dried grain with solubles (DDGS) for biofuel production, Bioresour. Technol., 102 (2011) 6208-6213.

[37] A.A. Boateng, C.A. Mullen, N.M. Goldberg, Producing Stable Pyrolysis Liquids from the Oil-Seed Presscakes of Mustard Family Plants: Pennycress (Thlaspi arvense L.) and Camelina (Camelina sativa)†, Energy & Fuels, 24 (2010) 6624-6632.

[38] C. Mullen, A. Boateng, Production and Analysis of Fast Pyrolysis Oils from Proteinaceous Biomass, Bioenerg. Res., 4 (2011) 303-311.

[39] X. Miao, Q. Wu, High yield bio-oil production from fast pyrolysis by metabolic controlling of< i> Chlorella protothecoides</i>, Journal of Biotechnology, 110 (2004) 85-93.
[40] X. Miao, Q. Wu, C. Yang, Fast pyrolysis of microalgae to produce renewable fuels, Journal of analytical and applied pyrolysis, 71 (2004) 855-863.

[41] S. Grierson, V. Strezov, G. Ellem, R. Mcgregor, J. Herbertson, Thermal characterisation of microalgae under slow pyrolysis conditions, Journal of Analytical and Applied Pyrolysis, 85 (2009) 118-123.

[42] C.A. Mullen, A.A. Boateng, K.B. Hicks, N.M. Goldberg, R.A. Moreau, Analysis and Comparison of Bio-Oil Produced by Fast Pyrolysis from Three Barley Biomass/Byproduct Streams, Energy & Fuels, 24 (2010) 699-706.

[43] K. Wang, R.C. Brown, Catalytic pyrolysis of microalgae for production of aromatics and ammonia, Green Chemistry, (2013).

[44] T.R. Carlson, J. Jae, Y.-C. Lin, G.A. Tompsett, G.W. Huber, Catalytic fast pyrolysis of glucose with HZSM-5: The combined homogeneous and heterogeneous reactions, Journal of Catalysis, 270 (2010) 110-124.

[45] T.R. Carlson, G. Tompsett, W. Conner, G. Huber, Aromatic Production from Catalytic Fast Pyrolysis of Biomass-Derived Feedstocks, Topics in Catalysis, 52 (2009) 241-252.
[46] A.A. Lappas, K.G. Kalogiannis, E.F. Iliopoulou, K.S. Triantafyllidis, S.D. Stefanidis, Catalytic pyrolysis of biomass for transportation fuels, Wiley Interdisciplinary Reviews: Energy and Environment, 1 (2012) 285-297.

[47] E.F. Iliopoulou, S. Stefanidis, K. Kalogiannis, A.C. Psarras, A. Delimitis, K.S. Triantafyllidis, A.A. Lappas, Pilot-scale validation of Co-ZSM-5 catalyst performance in the catalytic upgrading of biomass pyrolysis vapours, Green Chemistry, (2013).

[48] T.L. Marker, L.G. Felix, M.B. Linck, M.J. Roberts, Integrated hydropyrolysis and hydroconversion (IH2) for the direct production of gasoline and diesel fuels or blending components from biomass, part 1: Proof of principle testing, Environmental Progress & Sustainable Energy, 31 (2012) 191-199.

[49] V.K. Venkatakrishnan, J.C. Degenstein, A.D. Smeltz, W.N. Delgass, R. Agrawal, F.H. Ribeiro, High-pressure fast-pyrolysis, fast-hydropyrolysis and catalytic hydrodeoxygenation of cellulose: production of liquid fuel from biomass, Green Chemistry, (2013).

[50] P.R. Patwardhan, J.A. Satrio, R.C. Brown, B.H. Shanks, Influence of inorganic salts on the primary pyrolysis products of cellulose, Bioresource Technol, 101 (2010) 4646-4655.
[51] P.R. Patwardhan, R.C. Brown, B.H. Shanks, Product Distribution from the Fast Pyrolysis of Hemicellulose, ChemSusChem, 4 (2011) 636-643.

[52] H. Zhang, T.R. Carlson, R. Xiao, G.W. Huber, Catalytic fast pyrolysis of wood and alcohol mixtures in a fluidized bed reactor, Green Chemistry, 14 (2012) 98-110.
[53] K. Wang, K.H. Kim, R.C. Brown, Catalytic pyrolysis of individual components of lignocellulosic biomass, Green Chemistry, (2013).

[54] X. Li, H. Zhang, J. Li, L. Su, J. Zuo, S. Komarneni, Y. Wang, Improving the aromatic production in catalytic fast pyrolysis of cellulose by co-feeding low-density polyethylene, Applied Catalysis A: General, 455 (2013) 114-121.

[55] D.J. Mihalcik, C.A. Mullen, A.A. Boateng, Screening acidic zeolites for catalytic fast pyrolysis of biomass and its components, Journal of Analytical and Applied Pyrolysis, 92 (2011) 224-232.

[56] T.A. Milne, R.J. Evans, N. Nagle, Catalytic conversion of microalgae and vegetable oils to premium gasoline, with shape-selective zeolites, Biomass, 21 (1990) 219-232.

[57] P. Pan, C. Hu, W. Yang, Y. Li, L. Dong, L. Zhu, D. Tong, R. Qing, Y. Fan, The direct pyrolysis and catalytic pyrolysis of Nannochloropsis sp. residue for renewable bio-oils, Bioresource Technol, 101 (2010) 4593-4599.

CHAPTER 2 FAST PYROLYSIS OF MICROALGAE REMNANTS IN A FLUIDIZED BED REACTOR FOR BIO-OIL AND BIOCHAR PRODUCTION

A paper published by *Bioresource Technology*

Kaige Wang, Robert C.Brown, Sally Homsy, Liliana Martinez, and Sukh S. Sidhu

Abstract

In this study, pyrolysis of microalgal remnants was investigated for recovery of energy and nutrients. Chlorella vulgaris (C.vulgaris) biomass was first solvent-extracted for lipid recovery then the remnants were used as the feedstock for fast pyrolysis experiments using a fluidized bed reactor at 500^{o}C. Yields of bio-oil, biochar and gas were 53, 31, and 10wt.%, respectively. Bio-oil from C.vulgaris remnants was a complex mixture of aromatics and straight-chain hydrocarbons, amides, amines, carboxylic acids, phenols and other compounds with molecular weights ranging from 70Da to 1200Da. Structure and surface topography of the biochar were analyzed.The high inorganic content (potassium, phosphorous, and nitrogen) of the biochar suggests it may be suitable to provide nutrients for crop production. The bio-oil and biochar represented 57 and 36% of the energy content of the microalgae remnant feedstock, respectively.

Keywords: microalgae, pyrolysis, *Chlorella vulgaris,* bio-oil, biochar

Introduction

There is growing interest in utilizing microalgae as a feedstock for next-generation biofuels production due to its high biomass yield, its high lipid content, and the prospects of avoiding competition with arable land and recovering nutrients for use in conventional agriculture[58, 59]. Based on the photosynthetic efficiency and growth potential for algae, oil

yields per hectare for certain algal strains are projected to be at least 60 times higher than those for soybean, which currently accounts for 90% of biodiesel production feedstock in the US[58]. Many algal biofuel studies have focused on producing biodiesel (fatty acid methyl esters) from microalgae species with high lipid contents[60]. Such a production scheme will result in large quantities of lipid-extracted algal remnants. How to best use these algal remnants is one of the greatest challenges for algal biorefineries[58].The remnants, which contain protein, carbohydrates and a small amounts of lipids, have potential for use as an animal feed. At the scale of replacing petroleum with microalgae as the feedstock for the U.S. gasoline supply, however, 750 million tons of algal remnants would be produced annually--50 times the amount of feed supplement required by the 100 million cattle in the U.S. Furthermore, algae are effective at capturing and concentrating heavy metals, which could potentially make its use as an animal feed problematic [61].

Pyrolysis, the thermal conversion of materials in the absence of oxygen, has potential for converting algal remnants into bio-oil for upgrading to fuels and other value-added products; fast pyrolysis has already been developed for converting lignocellulosic biomass into advanced biofuels [62].Pyrolysis yields three products: gas, solid, and liquid. Pyrolysis gas is a flammable mixture of carbon monoxide, hydrogen, carbon dioxide and light hydrocarbons suitable for generating process heat. The solid biochar product is primarily reduced aromatic carbon and contains most of the feedstock's mineral components. Biochar has various potential applications including use as a soil amendment and a carbon sequestrationagent.The liquid bio-oil product is a high viscosity, dark-brown liquid composed of numerous organic components along with up to15-20wt.% water. Bio-oil can be upgraded to drop-in fuels through hydroprocessing and catalytic cracking [62].

Compared to the pyrolysis of lignocellulosic biomass, relatively little is known about the pyrolysis of whole or lipid-extracted microalgae. The few studies [40, 63, 64]that have been performed suggest that pyrolysis of microalgae can produce bio-oil that, in some respects, is superior to bio-oil from lignocellulosic biomass. Miao et al. [40]reported that bio-oil from microalgae was characterized by lower oxygen content and a higher heating value than bio-oil from lignocellulosic biomass. Bio-oil yields of 18% and 24% for pyrolysis of *Chlorella protothecoides* and *Microcystisaeruginosa* were achieved, respectively. Miao and Wu [64] showed that controlling microalgal growth conditions can tailor the yield and composition of resulting bio-oil. They reported a 57.9% yield of bio-oil from the fast pyrolysis of heterotrophic *Chlorella protothecoides*. Microwave-assisted pyrolysis of *Chlorella spin* in a batch reactor also showed promise for advanced renewable fuel production [63]. Grierson et al. [65]compared pyrolysis of six species of microalgae in a tube reactor under slow heating conditions; calculations of the process energy requirements indicated that the process was self-sustaining. The kinetics of microalgae pyrolysis have also been reported [66, 67]

One disadvantage of algal biomass as a pyrolysis feedstock is its high nitrogen content, which can then appear in the bio-oil product. Most of this nitrogen exists as protein in fast-growing, autotrophic microalgae [61]. Other nitrogenous constituents of microalgae include chlorophyll, nucleic acids, glucoseamides and cell wall materials, albeit at relatively low levels (less than 0.6 wt.%) compared to protein (10 wt.%) [61]. By comparison, the amount of nitrogen in lignocellulosic crops is generally less than 1wt.%.

The goal of this research was to investigate the yields and compositions of bio-oil, biochar, and non-condensable gas from the pyrolysis of extracted microalgae remnants. Of particular interest was the fate of nitrogen in the feedstock.

Materials and methods

Algal cultivation and harvest

A strain of *Chlorella vulgaris* (C.*vulgaris*) obtained from the University of Texas algae culture collection was autographically cultivated in an indoor 3800L closed tubular photobioreactor. C.*vulgaris* was grown in Bold's Basal Medium (BBM) at room temperature with continuous illumination (338 $\mu molm^{-2}s^{-1}$) and constant purging with CO_2 and air. Flow rates of CO_2 and air were 3 and 25 litre per minute respectively. Spectrophotometry of UV-vis with 550 nm wavelength was used to monitor the algal growth rate.The algae was harvested by an in-line continuous solid bowl centrifuge when maximum optical density was reached. The dewatered algal biomass was then freeze-dried and stored at room temperature.

Pre-pyrolysis processing of harvested microalgae

Lipids were removed from the dried algal biomass using solvent extraction; dry algae (1 kg) was mixed with 8 L ethanol at room temperature for 10 h in a 19 L constantly stirred tank. The slurry was then centrifuged and the ethanol-soluble extract saved for further processing. The raffinate was subjected to a second extraction with a reduced stirring time of 1.25 h. The raffinate from this extraction, referred to here as the remnants, was freeze dried to remove all solvent and milled to a particle size of 420-700 μm.

Pyrolysis experiments

Pyrolysis of C.*vulgaris* remnants was performed with a lab-scale,atmospheric-pressure fluidized bed reactor. The reactor consisted of a 316 stainless steel tube 0.31 m in length and 38.1 mm in diameter. The fluidization media was 100 g of silica particles with an average diameter of 0.55mm. Clamshell heaters maintained the pyrolysis reactor temperature at 500^{o}C. Two gas cyclones were used to collect 99% of the char. The bio-oil condensation system consisted of two condensers at 20^{o}C, followed by an electrostatic precipitator (ESP), and one final condenser at 1^{o}C. Bio-oils collected at these four condensers are referred to as stage fractions: SF1, SF2, SF3 and SF4, respectively. Non-condensable gases (NCG) were analyzed by a micro-GC (Varian-CP-4900) equipped with two columns: a Varian Molsieve 5A for hydrogen(H_2), oxygen(O_2), nitrogen(N_2), carbon monoxide(CO) and methane(CH_4), and a VarianPoraplot Q for carbon dioxide(CO_2), ethylene(C_2H_4), ethane(C_2H_6) and propane (C_3H_6). The cumulative volume of NCG was measured by a drum-type gas meter (Ritter, Germany).The biomass feeder was calibrated to a feed rate of 100g/h.

Yields of bio-oil and biochar were determined gravimetrically by weighing the char catch and condensation system before and after each experiment. NCG yield was calculated using the measured cumulative volume and the ideal gas law, and an apparent NCG molecular weight was derived from the gas composition measured by the micro-GC.

Characterization of pyrolysis products

CHN elemental analysis of the feedstock, bio-oils and biochars was performed using a TRUSPEC-CHN elemental analyzer (LECO, USA). Oxygen content was calculated by difference. Inorganic element content was measured using inductively coupled plasma atomic emission spectrometry (ICP-AES; Thermo, Franklin, MA, USA) after microwave

acid digestion. Proximate analysis was performed using a thermogravimetric analysis (TGA) system (Mettler Toledo, USA) following ASTM D5142. Higher heating values (HHV) were measured using an oxygen bomb calorimeter (Parr Instrument Company, USA). Protein content was approximated by multiplying elemental N concentrations by a factor of 6.25 [68]. Lipid content was measured according to the Bligh and Dyer method. The carbohydrates mass fraction (mf, %)was determined by difference:

$$mf_{carbohydrate} = 100 - mf_{protein} - mf_{lipid} - mf_{moisture} - mf_{ash}$$

Moisture content of the bio-oil was measured using a MKS-500Karl Fischer Moisture Titrator (Kyoto Electronics Measurement, Japan) following ASTM E203-96. Compounds in bio-oil detectable by GC were analyzed on a gas chromatograph with mass spectrometry flame ionization detection (GC-MS/FID) system (Varian CP 3800GC and Saturn 2200 MS) using a ZB-FFAP column (30m×0.25mm, 0.25 μm film thickness with nitroterepthalic acid modified polyethylene glycol as the stationary phase). Helium was employed as the carrier gas at a flow rate of 1ml/min. The GC oven was programmed for a 3 min hold at 40^{o}C followed by heating (5^{o}C/min) to 250^{o}C and hold for 9 min. The injector temperature was 250^{o}C and the injector split ratio set to 100:1. The compounds were identified by mass spectra comparison with the NIST library.

Gel permeation chromatography (GPC) of the bio-oils was performed using a Dionex Ultimate 3000 high performance liquid chromatograph (HPLC) with refractive index detection. A Meso Pore (3μm, 300×7.5 mm) column and a PL gel (3μm, 100 Å, 300×7.5 mm) column were used in series at 25^{o}C. Tetrahydrofuran (THF) was used as the mobile phase at flow rate of 1 ml/min. Samples (approximately 1 ml) were dissolved in THF and

filtered through a 0.25 µm PTFE filter prior to injection. The GPC columns were calibrated using nine polystyrene standards over the molecular weight range of 162 to 10,110 Da.

Brunauer-Emmet-Teller (BET) surface area of the biochars was determined using a NOVA 4200e surface area analyzer (Quantachrome Instruments, Boyton Beach, FL). Prior to analysis, samples were vacuum degassed at 300^{o}C for 12 h. Biochar particle structure and surface topography were analyzed using an FEI variable pressure scanning electron microscope(SEM).

Results and discussion

Feedstock characterization

Proximate and biochemical compositions of the whole microalgal biomass and the microalgal remnants are given in Table 1. Data for switchgrass and loblolly pine slash are also presented for a comparison to lignocellulosic biomass. In general, the main components of microalgae are protein, lipid and carbohydrate, while the three main components of lignocellulosic biomass are cellulose, hemicellulose and lignin. Protein contents were 41.51and 61.24wt.% for *C.vulgaris* and *C.vulgaris* remnants, respectively. The total lipid content of *C.vulgaris* was only 15.67wt.%, although the amount is strongly dependent upon the algae species and growth conditions [60]. Due to the incomplete extraction of the algal lipids by the method used in this study, 5.71wt.% lipid still remained in the remnants. The ash content of *C.vulgaris* (15.64wt.%) and *C.vulgaris* remnants (8.34wt.%) were much higher than that of pine and switchgrass due to the accumulation of inorganic salts in the cells from the culture media during the growth phase (Table 1). This high ash content is in agreement with previous study [69]. Despite the high ash content, the heating values of *C.vulgaris* and *C.vulgaris* remnants were comparable to those of switchgrass and pine

because of the relatively higher energy contents of proteins and lipids compared to carbohydrates [70].

Table 1. Proximate and biochemical compositions, and higher heating values (HHV)of fast pyrolysis feedstocks (as received).

Feedstock	Proximate analysis (wt.%)					Biochemical composition(wt.%)		
	Moisture	Volatile	Fixed Carbon	Ash	HHV (MJ/kg)	Lipid	Protein	Carbohydrate
C.vulgaris	6.18	66.56	11.62	15.64	16.80	15.67	41.51	20.99
C.vulgaris remnant	4.39	72.68	14.59	8.34	19.44	5.71	61.24	20.34
Switchgrass	5.25	76.69	14.36	3.70	16.69	-	-	-
Pine[a]	2.71	75.49	18.17	2.63	19.51	-	-	-

[a]Data taken from reference [71]

Results of ultimate and trace elemental analyses are given in Table 2. *C.vulgaris* and *C.vulgaris* remnants had similar C and H contents to lignocellulosic biomass while the N content of the microagal biomass was much higher. As shown in Table 2, the mineral contents of algal biomass, especially P, K and Mg, were several orders of magnitude higher than those found in lignocellulosic biomass. This high content of inorganic metals in microalgae may exert a significant effect on the pyrolysis product distribution as has been demonstrated for carbohydrate pyrolysis [50].

Table 2. Elemental and inorganic content of fast pyrolysis feedstocks (dry basis).

Feedstock	Elemental analysis (wt.%)				Elemental analysis (mg/kg)				
	C	H	N	O	P	K	Na	Mg	Ca
C.vulgaris	42.51	6.77	6.64	27.95	32500	11140	593	13460	19960
C.vulgaris remnants	45.04	6.88	9.79	29.42	15520	8416	118	3670	1766
Switchgrass	44.82	6.57	0.56	44.35	726	3438	269	1386	2716
Pine[a]	47.32	6.16	0.31	42.47	390	1810	76	460	3070

[a]Data taken from reference [71]

Pyrolysis product yields and distribution

Bio-oil, biochar and gas yields for fluidized bed pyrolysis of *C.vulgaris* remnant are shown in Fig.1.Data for pine pyrolysis in a fluidized bed reactor at 520^{o}C is also given for comparision [71]. The total bio-oil yield from *C.vulgaris* remnants was 53wt.%. Although higher than bio-oil yields reported for pyrolysis of algal biomass by other researchers (21 wt.% to 48 wt.%) [40, 57, 64], this yield is still somewhat lower than the bio-oil yield for pyrolysis of lignocellulosic biomass in a fluidized bed reactor(>60wt. %) [62].

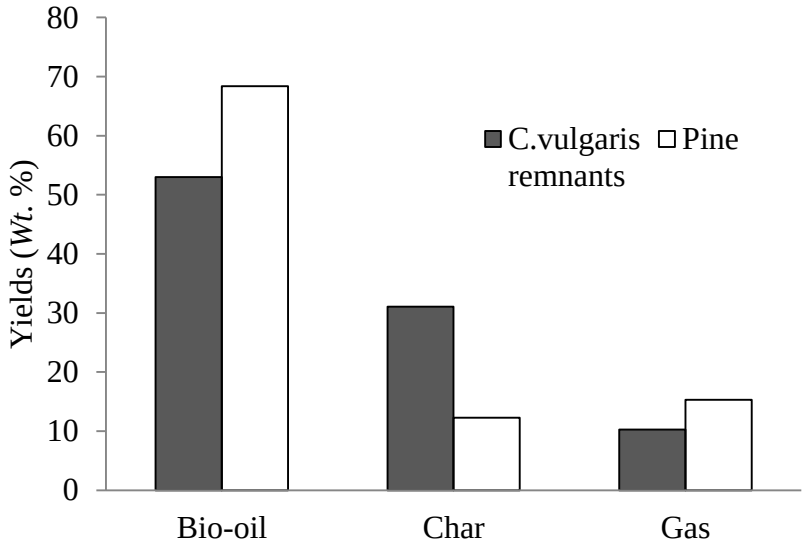

Figure 1. Comparison of fast pyrolysis product yields for C.vulgaris remnants (this study) and pine wood [71].

The largest amount of bio-oil (28.2 wt.%) was collected from stage fraction 3 (the ESP). Yields of SF1 and SF2 were only 14.3 wt.% and 4.7 wt.%, respectively. This indicates that a large portion of the bio-oil exits the pyrolyzer as aerosols which does not condense in the first two stages of the bio-oil recovery system. Bio-oil from the first three fractions were similar both in physical and chemical properties and are collectively referred to as the oily

phase. With a water content as high as 90wt.%, SF4 is referred to as the aqueous phase. The total oily phase yield was 47wt.%, while the aqueous-phase yield was only 6wt.%.

The biochar yield was 31wt.%, which is much higher than the typical 10-15 wt.% biochar yield observed for the fast pyrolysis of lignocellulosic biomass and may be partially due to the higher ash content in the algal remnants. The gas yield was 10wt.%, which is comparable to the gas yield for lignocellulosic biomass. The overall mass balance for the experiment was 94wt.%. This incomplete mass balance closure was attributed to some undetectable components of the non-condensable gases, such as ammonia and molecular nitrogen, which previously have been reported in the literature as products of the pyrolysis of proteinaceous biomass [72-74] .

Bio-oil properties and composition

Table3 provides the CHNO elemental analysis, water content, and heating value of selected stage fractions of the bio-oil produced from *C.vulgaris* remnants. For comparison, the typical composition of the bio-oil from pyrolyzed wood collected as a single fraction (whole bio-oil) is also included in the table [75]. Whole bio-oil from wood pyrolysis contains around 35-40wt.% oxygen; the oxygen content of SF3 from *C.vulgaris* remnants was only 27.5wt.%. Reduced oxygen content is thought to be beneficial for the stability of bio-oil and reduces the amount of hydrogen required for catalytic upgrading to drop-in biofuels [38].

Table 3. Elemental content, water content, and higher heating value (HHV) of bio-oil obtained from the fast pyrolysis of *C.vulgaris* remnants and woody biomass.

Properties	Feedstock		
	C.vulgaris remnants		Wood[a]
	SF 3	SF 4	Whole bio-oil
C(wt.%)	51.4	5.02	54-58
H(wt.%)	8.34	10.56	5.5-7.0
N(wt.%)	12.8	1.78	0-0.2
O(wt.%)	27.46	82.64	35-40
Moisture (wt.%)	15.89	90.02	15-30
HHV (MJ/Kg)	24.57	-	16-19

[a]Data taken from reference.[75]

While whole bio-oil from wood pyrolysis contains less than 0.2 wt.% nitrogen, the SF3 fraction of bio-oil from algal remnants was 12.8 wt.%, reflecting the high protein content of the microalgae remnant feedstock. Overall, the four stage fractions contained 60% of the feedstock nitrogen, which is unacceptably high if the bio-oil is to be catalytically upgraded to fuels. On the other hand, if this nitrogen could be extracted at some point in the process, it might be used as fertilizer. The balance of nitrogen is thought to leave the pyrolyzer in the gas phase (ammonia) or as part of the biochar (as heteroatoms in the aromatic carbon rings). Ammonia readily absorbs into water as it condenses in SF4. Ion chromatography of this aqueous phase showed it to contain up to 11.5g/L of ammonia. Small amounts of amines and other nitrogenous compounds were also present in SF4 bio-oil.

Table 4. Compounds identified by GC/MS in bio-oil (SF3)from the pyrolysis of *C.vulgaris* remnants at 500°C.

Categories	Compounds	Formula	Area[a](%)
Carbohydrate-derived			
2,5-dimethyl, furan		C_6H_8O	0.78
furfural		$C_5H_4O_2$	1.04
levoglucosenone		$C_6H_6O_3$	1.31
levoglucosan		$C_6H_{10}O_5$	2.29
3,methyl-pentanoic acid		$C_6H_{12}O_2$	0.44
5-methyl-2-furancarboxaldehyde		$C_6H_6O_2$	1.35
acetic acid		$C_2H_4O_2$	1.32
Protein-derived			
benzenepropanenitrile		C_9H_9N	0.98
benzyl nitrile		C_8H_7N	0.3
propanenitrile		C_3H_5N	0.62
4-methyl-pentanenitrile		$C_6H_{11}N$	0.45
toluene		C_7H_8	5.09
styrene		C_8H_8	0.65
enthylbenzene		C_8H_{10}	0.61
phenol			1.53
4-methyl-phenol		C_7H_8O	4.74
4-ethyl-phenol		$C_8H_{10}O$	0.7
pyridine		C_5H_5N	0.59
pyrrole		C_4H_5N	0.38
2-methyl-1H-pyrrole		C_5H_7N	0.77
3-methyl-1H-pyrrole		C_5H_7N	0.57
2,3-dimethyl,1-H-pyrrole		C_6H_9N	0.38
2,4-dimethyl,1-H-pyrrole		C_6H_9N	0.49
2,3,5-trimethyl-1H-pyrrole		$C_7H_{11}N$	0.44
4-ethyl-2-methyl-pyrrole		$C_7H_{11}N$	0.8
4-ethyl-2,3-dimethyl-pyrrole		$C_8H_{13}N$	0.31
acetamide		C_2H_5NO	0.73
picolinamide		$C_6H_6N_2O$	0.78
3-pyridinol		C_5H_5NO	0.59
indole		C_8H_7N	2.89
4-methyl-1H-indole		C_9H_9N	1.08
succinmide		$C_4H_5NO_2$	1.18
pyrrolos		$C_7H_{10}N2O_2$	1.76
Lipid-derived			
3,7,11,15-tetramethyl-2-hexadecen		$C_{20}H_{40}O$	8.25
n-hexadecanoic acid		$C_{16}H_{32}O_2$	5.34
Z-11,hexadecenoic acid		$C_{16}H_{30}O_2$	1.09
cis-vaccenic acid		$C_{18}H_{34}O_2$	3.2
9,12-octadecadienoic acid (Z,Z)		$C_{18}H_{32}O_2$	4.75
9,12,15-octadecatrienoic acid (Z,Z,Z)		$C_{18}H_{30}O_2$	2.38

[a]Based on peak area of GC chromatograph.

As can be seen in Table 4, the N content in the GC-identified bio-oil compounds was just around 1.5%, which is significantly lower than the elemental nitrogen content (12.8 wt.%) of the algal bio-oil. Most of the nitrogen is likely contained in non-volatile, high molecular weight compounds that are undetectable by GC. The bio-oil was analyzed by GPC to determine the molecular weight distribution of the non-volatile compounds. Fig. S 1 shows that the molecular weight of the bio-oil ranged from 70 Da to over 1200 Da, with a maximum peak at 230 Da and smaller peaks at 457 Da and 908 Da. The number average molecular weight and the weight average molecular weight were 220 Da and 324 Da respectively, both of which are much lower than that of bio-oil typically obtained from lignocellulosic biomass [62].

Compounds identified by GC/MS in SF3 after the pyrolysis of *C. vulgaris* remnants at 500^{o}C are shown in Table 4. Despite the absence of lignin in the microalgae remnants, which usually contributes significantly to the diversity of products in lignocellosic biomass pyrolysis bio-oil, the resulting microalgal remnant bio-oil displays a wide variety of compounds including aromatics, amides, amines, carboxylic acids, and phenols. These compounds are categorized in Table 4 according to their likely source.

Carbohydrate-derived compounds found in the bio-oil included anhydrosugars (levoglucosan and levoglucosenone), furfural, furans and carboxylic acids [62, 76]. Concentrations of these oxygenated compounds were comparatively low in the bio-oil from *C. vulgaris* remnants as a result of this feedstock containing only a few weight percent of carbohydrates.

Protein-derived compounds found in the bio-oil included aromatic hydrocarbons, nitrogen-containing analogs of aromatic hydrocarbons, nitriles, pyrrolesand phenols. Many of these products are derived from the amino acids making up in the original proteins [77, 78]. The generation of toluene and other aromatic hydrocarbons was associated with the presence of aromatic amino acids such as tyrosine and phenylalanine in the micoalgal protein[79].Pyrroles probably originated from proline, which was present in the *C. vulgaris*remnants. Pyrolysis of tryptophan reportedly results in the generation of indole and alkyl indoles [79].Phenol and alkyl phenols were also present in the bio-oil and are believed to be the main products of the decomposition of tyrosine found in the *C.vulgaris* remnants. In contrast, phenolic compounds from the pyrolysis of lignocellulosic biomass originate mainly from lignin [62]. Heterocyclic amines were also detected in the microalgal remnant bio-oil that may have been generated from pyrolysis of protein and amino acids [80]. The interaction of nitrogenous compounds with sugars in the feedstock could also generate heterocyclic amines [79] .

Another group of abundant products in microalgal remnant bio-oil are fatty acids including n-hexadecanoicacid, oleic acid, cis-vacenic acid, and 9,12-octadecandienoic acid. These compounds are beneficial to bio-oil quality from the prospective of energy content and ease of upgrading to fuels.

Biochar analysis

Fig. S.2 compares the SEM images of the *C.vulgaris* remnants and the biochar derived their pyrolysis. Fig.S.2 a and b clearly reveal the single-celled structure of *C.vulgaris* remnants where the cells are slightly broken and aggregated together from the lipid-extraction process. Fig. S.2 c and d suggest that the resulting biochar particles are compact

and irregular, and do not resemble the structure of the feedstock before pyrolysis. The cell wall structure appears to have been totally destroyed and there is evidence of melting and re-solidification of cell structures. This is in contrast with biochars from lignocellusosic biomass which clearly retain the feedstock's plant structure [81, 82]. The surface area of the biochar was only 2.4m^2/g, which is relatively low compared to biochar obtained from lignocellulosic biomass [81, 82].

Results from the elemental and proximate analyses of the biochar are shown in Table 5. Biochar from *C.vulgaris* remnants is comparatively low in C, and high in N and minerals. Around 30% of the original N content in *C.vulgaris* remnants was fixed in the biochar, though the form of this N is uncertain. Some may exist as ammonium or nitrate; a large portion, however, likely exists as high molecular weight N-heterocyclic compounds condensed on the biochar surface or inside the biochar pores. Table 5 also presents the inorganic content of the biochar as determined by ICP. The biochar contained higher concentrations of trace elements than biochar from lignocellulosic biomass, in particular plant nutrients such as N, P, K, Ca and Mg. This suggests that biochar produced from algae pyrolysis has good prospects as fertilizer.

Table 5. Results from the proximate, elemental, higher heating value (HHV) and inorganic mineral analyses of biochar derived from the fast pyrolysis of *C.vulgaris* remnants.

Proximate analysis (wt%)		Elemental analysis (wt%)		Inorganic mineral content (mg/kg)	
Moisture	3.38	C	61.96	P	15360
Volatile	23.46	H	3.87	K	30100
Fixed carbon	54.20	N	9.43	Mg	5786
Ash	19.96	O	4.78	Ca	7337
HHV (MJ/kg)	23.04			Na	176

Pyrolysis gas characterization

The non-condensable gases consisted mainly of CO_2 and CO with concentrations of 71.7v% and 14.7v%, respectively. Around 12 v% of light hydrocarbons was observed also in the gaseous product; CH_4 was the dominant light hydrocarbon at 6.6 v%, while around 5 v% total of C_2H_4, C_2H_6 and C_3H_8 were also detected. Based on the heating value and concentration of each component, the heating value of the NCG mixture was calculated to be 5.1MJ/kg, which is comparable to that of the gas product from lignocellulosic biomass pyrolysis [83].

Energy and elemental mass balances

Based on the product yields and the elemental analysis of individual products, the energy and elemental (C, N) mass balances for the pyrolysis of *C.vulgaris* remnants were calculated (Table 6). Energy recovery was defined as the HHV of one product divided by the HHV of the original *C.vulgaris* remnant feedstock. Elemental recovery was defined as the ratio of the amount of the element in the pyrolysis product to the amount of the element in the *C.vulgaris* remnant feedstock.

Table 6. Elemental and energy recovery in products from the fast pyrolysis of *C.vulgaris* remnants.

Recovery (%)	Carbon	Nitrogen	Hydrogen	Energy
Bio-oil	52.3	60.3	66.8	57.4
Biochar	42.5	29.6	17.4	36.8
Gas	7.34	-	4.36	2.69

About 52.3% of the C in the algal remnants was recovered in the bio-oil while 42.6% of the C was recovered in the biochar. Of the original N content, 60.3% ended up in the bio-oil while approximately 30% ended up in the biochar. Nitrogen in gaseous products, such as

ammonia and hydrogen cyanide, was not directly measured but was estimated to be about10% based on mass balance. Taken together, bio-oil and biochar represent an energy recovery of 94.2%. Only around 3% of the energy in the feedstock appeared in the non-condensable gas fraction, giving an overall energy recovery of 97%.

Conclusions

Fast pyrolysis of *C.vulgaris* remnants using a fluidized bed reactor demonstrates the potential to recover energy and nutrients from microalgal remnants after lipid extraction. The bio-oil yield was 53wt.% and contained aromatics, amides, amines, carboxylic acids, phenols, fatty acids as well as other organic compounds. The high nitrogen content of the bio-oil (12.8 wt.%) was attributable to the high protein content of the feedstock. The biochar yield was 31wt.%. Around 94% of the energy content of *C.vulgaris* remnant was recovered in the bio-oil and biochar products.

Acknowledgements

The authors would like to acknowledge financial support from the Iowa Energy Center (Grant No.: 10-02). The authors would also like to thank Catherine Brewer, Dustin Dalluge, Marge Rover, and Sunitha Sadula at the Center for Sustainable Environmental Technologies for assistance in performing the experiments and analyzing the bio-oil and biochar.

References

[1] DOE, National Algal Biofuels Technology Roadmap in, 2010.

[2] P.J.L. Williams, L.M.L. Laurens, Microalgae as biodiesel & biomass feedstocks: Review & analysis of the biochemistry, energetics & economics, Energy Environ. Sci., 3 (2010) 554-590.

[3] Q. Hu, M. Sommerfeld, E. Jarvis, M. Ghirardi, M. Posewitz, M. Seibert, A. Darzins, Microalgal triacylglycerols as feedstocks for biofuel production: perspectives and advances, Plant J., 54 (2008) 621-639.

[4] E.W. Becker, Micro-algae as a source of protein, Biotechnol Adv, 25 (2006) 207-210.

[5] D. Mohan, C.U. Pittman, P.H. Steele, Pyrolysis of wood/biomass for bio-oil: A critical review, Energ Fuel, 20 (2006) 848-889.

[6] Z. Du, Y. Li, X. Wang, Y. Wan, Q. Chen, C. Wang, X. Lin, Y. Liu, P. Chen, R. Ruan, Microwave-assisted pyrolysis of microalgae for biofuel production, Bioresource Technol, 102 (2011) 4890-4896.

[7] X. Miao, Q. Wu, C. Yang, Fast pyrolysis of microalgae to produce renewable fuels, J Anal Appl Pyrol, 71 (2004) 855-863.

[8] X. Miao, Q. Wu, High yield bio-oil production from fast pyrolysis by metabolic controlling of Chlorella protothecoides, J Biotechnol, 110 (2004) 85-93.

[9] S. Grierson, V. Strezov, G. Ellem, R. McGregor, J. Herbertson, Thermal characterisation of microalgae under slow pyrolysis conditions, J Anal Appl Pyrol, 85 (2009) 118-123.

[10] Z. Shuping, W. Yulong, Y. Mingde, L. Chun, T. Junmao, Pyrolysis characteristics and kinetics of the marine microalgae Dunaliella tertiolecta using thermogravimetric analyzer, Bioresource Technol, 101 (2010) 359-365.

[11] W.M. Peng, Q.Y. Wu, P.G. Tu, N.M. Zhao, Pyrolytic characteristics of microalgae as renewable energy source determined by thermogravimetric analysis, Bioresource Technol, 80 (2001) 1-7.

[12] AOAC, Official methods of analysis, Washington D.C, 1990.

[13] Ö. Tokuşoglu, M.K. üUnal, Biomass Nutrient Profiles of Three Microalgae: Spirulina platensis, Chlorella vulgaris, and Isochrisis galbana, J Food Sci, 68 (2003) 1144-1148.

[14] J.M.A. Nazer, C.T. Young, F.G. Giesbrecht, Pyrolysis-GC Analysis as an Identification Method of Fats and Oils, J Food Sci, 50 (1985) 1095-1100.

[15] R.D. Kasparbauer, The effects of biomass pretreatments on the products of fast pyrolysis in: MecEn, Iowa State University, Ames, 2009.

[16] P.R. Patwardhan, J.A. Satrio, R.C. Brown, B.H. Shanks, Influence of inorganic salts on the primary pyrolysis products of cellulose, Bioresource Technol, 101 (2010) 4646-4655.

[17] P. Pan, C. Hu, W. Yang, Y. Li, L. Dong, L. Zhu, D. Tong, R. Qing, Y. Fan, The direct pyrolysis and catalytic pyrolysis of Nannochloropsis sp. residue for renewable bio-oils, Bioresource Technol, 101 (2010) 4593-4599.

[18] Q. Ren, C. Zhao, X. Chen, L. Duan, Y. Li, C. Ma, NOx and N2O precursors (NH3 and HCN) from biomass pyrolysis: Co-pyrolysis of amino acids and cellulose, hemicellulose and lignin, Proceedings of the Combustion Institute, 33 (2011) 1715-1722.

[19] S. Yuan, Z.-j. Zhou, J. Li, X.-l. Chen, F.-c. Wang, HCN and NH3 Released from Biomass and Soybean Cake under Rapid Pyrolysis, Energ Fuel, 24 (2010) 6166-6171.

[20] K.-M. Hansson, J. Samuelsson, C. Tullin, L.-E. Åmand, Formation of HNCO, HCN, and NH3 from the pyrolysis of bark and nitrogen-containing model compounds, Combustion and Flame, 137 (2004) 265-277.

[21] S. Czernik, A.V. Bridgwater, Overview of Applications of Biomass Fast Pyrolysis Oil, Energ Fuel, 18 (2004) 590-598.

[22] C. Mullen, A. Boateng, Production and Analysis of Fast Pyrolysis Oils from Proteinaceous Biomass, BioEnergy Research, 4 (2011) 303-311.

[23] R.C. Brown, Thermochemical Processing of Biomass: Conversion into Fuels, Chemicals and Power, Wiley, 2011.

[24] M. Langhammer, I. Lüderwald, A. Simons, Analytical pyrolysis of proteins, Fresenius' Journal of Analytical Chemistry, 324 (1986) 5-8.

[25] W.T. Smith, T.B. Harris, J.M. Patterson, Pyrolysis of soybean protein and an amino acid mixture having the same amino acid composition, J. Agric. Food Chem., 22 (1974) 480-483.
[26] C.M. Serban, Analytical Pyrolysis of Natural Organic Polymers, Elsevier, 1998.

[27] E.B. Higman, I. Schmeltz, W.S. Schlotzhauer, Products from the thermal degradation of some naturally occurring materials, J. Agric. Food Chem., 18 (1970) 636-639.

[28] C. Brewer, R. Unger, K. Schmidt-Rohr, R. Brown, Criteria to Select Biochars for Field Studies based on Biochar Chemical Properties, BioEnergy Research, 4 (2011) 312-323.

[29] C.E. Brewer, K. Schmidt-Rohr, J.A. Satrio, R.C. Brown, Characterization of biochar from fast pyrolysis and gasification systems, Environmental Progress & Sustainable Energy, 28 (2009) 386-396.

[30] C.A. Mullen, A.A. Boateng, N.M. Goldberg, I.M. Lima, D.A. Laird, K.B. Hicks, Bio-oil and bio-char production from corn cobs and stover by fast pyrolysis, Biomass and Bioenergy, 34 (2010) 67-74.

CHAPTER 3 CATALYTIC PYROLYSIS OF MICROALGAE FOR PRODUCTION OF AROMATICS AND AMMONIA

A paper Published by *Green Chemistry*

Kaige Wang and Robert C. Brown

Abstract

We report an economically- and environmentally-promising microalgae biorefinery pathway, which uses catalytic pyrolysis with HZSM-5 catalyst to convert whole microalgae into aromatic hydrocarbons. This process produces valuable petrochemicals and ammonia, the latter of which can be recycled as a fertilizer for microalgae cultivation. We tested samples of lipid-lean green microalgae, *Chlorella vulgaris*, at various reaction temperatures and catalyst loads. We also tested samples of lignocellulosic biomass, red oak, for comparison. Our results demonstrated that catalytic pyrolysis of microalgae produces better aromatic yields and better aromatic distributions than catalytic pyrolysis of red oak. The maximum carbon yield of aromatics from microalgae was 24%, while that from red oak was 16.7%. Moreover, catalytic pyrolysis of microalgae produced more monocyclic aromatics than were produced by catalytic pyrolysis of lignocellulosic biomass. Microalgae present many advantages as a feedstock for biofuel. With the promise catalytic pyrolysis offers for solving some of microalgae's disadvantages, microalgae biorefineries move one step closer to economic and environmental feasibility.

Introduction

The potential for microalgae as a feedstock for biofuels has captured the interest of researchers and the public alike. Microalgae's high biomass yield and ability to accumulate

large quantities of neutral lipids[60] give them much promise as a source of biofuels. Moreover, with their photosynthetic efficiency and growth potential, certain strains of microalgae are projected capable of delivering oil yields per hectare at least 60 times higher than those for soybeans, the feedstock that currently accounts for 90% of biodiesel production in the United States.[58] This high productivity, combined with microalgae's inherent advantage of avoiding competition with arable land, has motivated researchers to study the production of biodiesel from microalgae.[59, 60]

While results have been promising, researchers have also identified several challenges. For example, most microalgae strains have thick cell walls, which make the wall disruption and lipid extraction processes energy-intensive and expensive. Researchers have also identified a trade-off between lipid yield and microalgae growth rate: Higher lipid content correlates to much lower and more unstable biomass productivity.[59, 84]

Finally, the nitrogen content of microalgal biomass can be as high as 10%, indicating that a large amount of nitrogen is consumed during algal cultivation and would need to be regularly replenished. Nitrogen fertilizer is artificially produced through Haber-Bosch synthesis, an energy-intensive process that contributes significantly to the nitrogen cycle of the planet.[14] Huge amounts of energy would be consumed in the production of nitrogen fertilizer if algae-based biofuel were to replace petroleum fuel on a large scale without some provision for recycling the nitrogen in the biomass. In fact, considering the impact of microalgae's nitrogen requirements on energy use and greenhouse gas emissions, the feasibility of microalgae-based biofuel is questionable. The nitrogen fertilizer is assimilated by algal species to make proteins and nucleic acids, neither of which are used in current biofuels production. Production of lipid-based biofuels from microalgae will result in large

quantities of lipid-extracted algal remnants, for which disposal or utilization represents a significant challenge to the industry.[58] Historically, these nitrogen-rich residuals have potential as animal feed.[6, 58] However, due to the relatively small size of animal feed markets compared to transportation fuel markets, this application has limited potential to address the microalgal remnants problem.[6, 85] All of these issues combine to make current methods for algae-based biofuel production relatively inefficient and potentially unsustainable. As a result, while researchers continue to explore microalgae's advantages and challenges, commercial-scale facilities for producing biofuels from microalgae have yet to emerge.[58, 59]

Fast pyrolysis, the thermal conversion of biomass into bio-oil, biochar, and gases, is proving to be a promising pathway for converting lignocellulosic biomass into advanced biofuels.[62] We hypothesized that fast pyrolysis technology could also provide a feasible pathway for the conversion of microalgae. Fast pyrolysis has the potential to convert whole microalgae into bio-oil for upgrading to fuels and other value-added products, but microalgae's nitrogen content presents difficulties for this pathway. During the pyrolysis process, nitrogen in the microalgae, mainly arising from proteins and amino acids, is converted to various nitrogenous compounds, including pyrroles, nitriles, indoles, pyridines, and poly-heteroaromatics.[85-87] Nitrogen content in microalgae-derived bio-oils can vary from 5% to 12% depending on the feedstock.[40, 57, 64, 85] This large amount of nitrogen can have deleterious effects on catalysts during bio-oil upgrading processes and is undesirable from a fuel combustion perspective. Some methods for removing nitrogen during pyrolysis, therefore, must be devised if whole microalgae are to be pyrolytically converted into transportation fuels.

Bio-oil from lignocellulosic biomass contains many oxygenated organic compounds, including furans, phenols, anhydrosugars, and aldehydes.[62] Significant research has been devoted to catalytic pyrolysis processes that deoxygenate these compounds in order to produce higher quality bio-oil.[88] Various types of catalysts have been tested, including metal oxides, zeolites, and transition metals.[88-90] Among these catalysts, zeolites have been extensively investigated because of their ability to convert biomass-derived oxygenates into aromatic hydrocarbons.[44, 89-91] Specifically, HZSM-5 has shown the best performance in terms of bio-oil aromatic fraction yield.[92] We hypothesize that zeolite catalysts are also capable of converting protein-derived nitrogenous compounds into aromatic hydrocarbons while releasing the nitrogen as ammonia, which can then be used as a nitrogen fertilizer. These two process changes would greatly enhance the economics of a microalgae biorefinery.

In 1990, Milne et al. first proposed the catalytic conversion of whole microalgae over HZSM-5, but claimed that the results were ambiguous.[56] A study in 2010 showed that HZSM-5 increased the hydrocarbon fraction in the bio-oil from *Nannochloropsis sp.* in a fixed bed reactor,[57] but no quantitative results were reported. A more recent study with a Py/GC-MS confirmed that HZSM-5 increased hydrocarbon production from microalgae,[93] but the fate of nitrogen was not addressed. Here, we report the product distribution and the fate of nitrogen in catalytic fast pyrolysis of microalgal biomass over HZSM-5. For comparison purposes, catalytic pyrolysis of lignocellulosic biomass was also investigated in this study.

Experimental

Feedstock preparation

A strain of *Chlorella vulgaris* (*C.vulgaris*) obtained from The University of Texas algae culture collection was autographically cultivated in an indoor 3800L closed tubular photo bioreactor. *C.vulgaris* was grown in Bold's Basal Medium (BBM) at room temperature with continuous illumination (338 μmol m^{-2} s^{-1}) and constant introduction of CO_2 and air. Spectrophotometry was used to monitor algal growth rate, and algae were harvested by means of centrifugation when the algal growth rate substantially declined. The dewatered algal biomass was then freeze-dried and stored at room temperature until further processing.

Bark-free red oak (*Quercus rubra*) was purchased from Wood Residual Solutions, LLC of Montello, Wisconsin.. Both *C.vulgaris* and red oak were ground and sifted to < 200 mesh before the experiment. We chose commercially-available zeolite catalyst ZSM-5 (CBV2314 with SiO_2/Al_2O_3 ratio of 23, Zeolyst, USA) for our study. The catalyst was calcined at 550^{o}C for 5 hours in a muffle furnace to activate it prior to use. Calcined catalyst was mixed with biomass before the pyrolysis experiment. Approximately 500μg of biomass were used for a typical run.

Elemental analysis of the feedstock, bio-oils, and biochars was performed using a TrusPec Carbon/Hydrogen/Nitrogen elemental analyzer (LECO, USA). Oxygen content was calculated by difference. Proximate analysis was performed using a thermogravimetric analysis (TGA) system (Mettler Toledo, USA) following ASTM D5142. Higher heating values (HHV) were measured using an oxygen bomb calorimeter (Parr Instrument Company, USA). Lipid was extracted from *C.vulgaris* in a mixture of chloroform and methanol under high-power ultrasonication. The resulting lipid was esterified to fatty acid methyl esters,

which were then analyzed with a gas chromatograph (GC) (Hewlett-Packard HP-5890, USA). Total fatty acid (TFA) is a convenient proxy for the lipid content of the microalgae. Protein content was approximated by multiplying elemental N concentrations by a factor of 6.25.[68] The mass fraction (mf) of carbohydrate in *C.vulgaris* (mf, %) was determined by difference:

$$mf_{carbohydrate} = 100 - mf_{protein} - mf_{\mathrm{TFA}} - mf_{moisture} - mf_{ash}$$

Pyrolysis Experiment

Pyrolysis experiments were conducted in a micro-furnace pyrolyzer (PY-2020iS, Frontier Laboratories, Japan), which was equipped with an auto-shot sampler (AS-1020E, Frontier Laboratories, Japan). The micro-pyrolyzer contains a quartz pyrolysis tube that can be temperature controlled in the range of 40-800^{o}C. It also includes an interface heater operated at 100-400^{o}C and a deactivated needle that inserts into the injector of the GC. Samples of approximately 0.5 mg were loaded in deactivated stainless steel cups, which were automatically lowered into the preheated furnace. Helium carrier gas was used to sweep pyrolysis vapor into the GC (Varian CP3800, USA). The vapor was separated in a GC capillary ZB-FFAP column (30m×0.25mm, 0.25 µm film thickness using nitroterepthalic-acid-modified polyethylene glycol as the stationary phase). Helium was employed as the carrier gas at a flow rate of 1ml/min. The GC oven was programmed for a 3-minute hold at 40^{o}C followed by heating (10^{o}C/min) to 250^{o}C, after which temperature was held constant for 9 minutes. The injector temperature was 260^{o}C and the injector split ratio was set to 100:1. Separated pyrolysis vapors were analyzed either by a mass spectrometer (MS) or a Flame Ionization Detector (FID). The MS (Saturn 2200, Varian, USA) was used for molecular identification. After the peaks were identified, standards were prepared to quantify

the results using FID. CO and CO_2 concentrations in the split stream from GC were recorded as real-time measurements by a De-Jaye gas analyzer (Des Moines, USA).

Separate pyrolysis experiments were performed for ammonia (NH_3) analysis. The pyrolyzer was separated from the GC and the pyrolyzer needle was inserted into a plastic bottle containing NH_3 100mmol/L of hydrochloric acid (HCl) to absorb NH_3. Ammonium ion ($NH4^+$) in the solution was analyzed at the end of the tests using an ammonia-selective electrode (Fisher Scientific, USA).

Collection of hydrogen cyanide was carried out in separate experiments using the same method described above for ammonia, except that sodium hydroxide (NaOH) solution was used as the absorbent. Cyanide ion (CN^-) concentrations were analyzed using ion chromatography (Dionex, USA) with separation column of IonPac AS 15 (Dionex, USA). The carbon and nitrogen content (%C, %N) in the residue (char/coke) after pyrolysis was quantified by elemental analysis using a PE 2100 Series II combustion analyzer (Perkin Elmer Inc., USA).

Final product distribution was reported as carbon yield or nitrogen yield, which was defined as the molar ratio of carbon or nitrogen in a certain product to the carbon or nitrogen in the feedstock. All experiments were run at least in duplicates to check the reproducibility of the data.

Results and Discussion

Feedstock characterization

The proximate, ultimate and biochemical analyses of *C.vulgaris* are shown in Table 1. Data for red oak are also presented for a comparison to lignocellulosic biomass. The ash content of *C.vulgaris* (15.64 wt%) was much higher than that of red oak due to the

accumulation of inorganic salts in the cells from the culture media during the growth phase. The heating value of *C.vulgaris* was slightly lower than that of red oak because of the extremely high content of ash in *C.vulgaris*. Microalgal biomass has carbon and hydrogen content similar to those of lignocelluloses, but the nitrogen content of microalgal biomass is much higher. Nitrogen content of *C.vulgaris* was 6.64 wt%, while that of red oak was only 0.06 wt%. Most of the nitrogen in the algal biomass exists as protein. Other nitrogenous constituents of microalgae may include

Table 1. Characterization of *C.vulgaris* and red oak (as received)

Feedstock	C.vulgaris	Red Oak
Proximate Analysis (wt%)		
Moisture	6.18	4.75
Volatiles	66.56	83
Fixed carbon	11.62	0.73
Ashes	15.64	11.52
Higher Heating Value (MJ kg^{-1})	16.8	19.51
Elemental Analysis (wt%)		
C	42.54	45.19
H	6.77	6.36
N	6.64	0.06
O	27.95	47.66
Biochemical Composition (wt%)		
TFA	4.68	n.d.
Protein	42.51	n.d.
Carbohydrates	20.99	83.62
Lignin	n.d.	13.02

chlorophyll, nucleic acids, glucoseamides, and cell wall materials, all with relatively low levels of nitrogen compared to the levels in the protein.[61] These constituents are not discussed here due to their relatively low occurrence.

In general, the main components of microalgae are protein, lipids, and carbohydrates. Protein content of *C.vulgaris* was 42.5 wt%. Total fatty acid content was only 4.68 wt%. Such low content of fatty acid in *C.vulgaris* suggests that it is not an optimal feedstock for algal lipid-based biodiesel production. Carbohydrate content of microalgae is highly dependent upon the species and their cultivation conditions. Extensive study suggests that carbohydrates in microalgae contain various acidic and neutral sugars, among which glucose and galactose are the most common.[94] In contrast, in lignocellulosic biomass, protein and lipids are negligible and carbohydrates and lignin are the predominant components. The carbohydrates in lignocellulose are mainly hemicellulose and cellulose, occurring at concentrations of 41.01 wt% and 42.61 wt%, respectively, for the red oak in this study[95]. The overall lignin content of the red oak was 13 wt%. Lignin is a major component of lignocellulosic biomass, but it is absent in microalgae biomass.[58, 69]

Effect of HZSM-5 catalyst on microalgae pyrolysis

The direct pyrolysis of *C.vulgaris* at 700^{o}C, in the absence of zeolite catalyst, produced a wide range of nitriles, pyrroles, phenols, furfurals, and other nitrogen- and oxygen-containing compounds, all of which are detectable by GC (see Table S 1). Moreover, our previous work on fast pyrolysis of micoralgal biomass in a lab-scale fluidized bed reactor showed that most of the nitrogen in pyrolysis vapor likely exists in non-volatile, high-molecular-weight compounds undetectable by GC.[85] This also agrees with other researchers' studies on pyrolysis of microalgal biomass.[57, 93]

With the addition of HZSM-5 catalyst with temperature of 700^{o}C, the reaction network changed dramatically: the nitrogen- and oxygen-containing compounds detected in direct pyrolysis were completely eliminated from the products and aromatic hydrocarbons were generated. The gas chromatograph in Figure S 1 shows the significant effect of the catalyst on the pyrolysis products. This result confirms that HZSM-5 catalyst has an effect on pyrolysis of microalgae similar to that for lignocellulosic biomass: the removal of heteronuclear atoms (oxygen and nitrogen) from the organic compounds in the feedstock and their conversion into aromatic hydrocarbons.

Aromatic hydrocarbons generated from *C.vulgaris* over HZSM-5 catalyst at 700^{o}C were quantified in Table 2. Benzene, toluene, and xylene (BTX) were the most abundant products, with a combined carbon yield of 15%. Napthalene and alkylnapthalenes were the second major group of aromatic hydrocarbons, with carbon yields of 1.38% and 2.23%, respectively. Moderate amounts of alkylbenzene, indanes, and indenes were also detected. Polycyclic aromatic hydrocarbons with three benzene rings were produced, but in amounts too small to be considered significant. For example, the carbon yield of anthracene was less than 0.1%. In addition to the aromatic hydrocarbons, large amounts of carbon monoxide (CO) and carbon dioxide (CO_2) were also generated, with carbon yields of 28.34% and 13.90%, respectively. The pyrolytic residue also contained carbon; carbon in the residue (coke/char) was as high as 33.1%. The total carbon balance was around 98%. Olefins were not detected in this experiment.

Table 2. Products from catalytic pyrolysis of C.vulgaris (reaction temperature = 700oC, HZSM-5: biomass = 20) quantified by GC analysis.

Compounds	Formula	Carbon yield/%	Aromatic selectivity*/%
benzene	C_6H_6	4.24	18.5
toluene	C_7H_8	6.72	29.3
xylene	C_8H_{10}	6.03	26.3
propyl-benzene	C_9H_{12}	0.02	0.1
1-ethyl-2-methyl-benzene	C_9H_{12}	0.4	1.7
Trimethyl-benzene	C_9H_{12}	0.59	2.6
4-ethyl-1,2-dimethyl-benzene	$C_{10}H_{14}$	0.05	0.2
indane	C_9H_{10}	0.24	1.0
1-propynyl-benzene	C_9H_8	0.35	1.5
1,methyl-Indan	$C_{10}H_{12}$	0.23	1.0
methyl-1H-Indene	$C_{10}H_{10}$	0.25	1.1
napthalene	$C_{10}H_8$	1.38	6.0
2-methyl-napthalene	$C_{11}H_{10}$	1.62	7.1
ethyl-napthalene	$C_{12}H_{12}$	0.07	0.3
dimethyl-napthalene	$C_{12}H_{12}$	0.54	2.4
fluorene	$C_{13}H_{10}$	0.02	0.1
anthracene	$C_{14}H_{10}$	0.09	0.4
2-methylanthracene	$C_{15}H_{12}$	0.07	0.3
Total aromatics		22.95	100.0
Carbon monoxide	CO	13.90	-
Carbon dioxide	CO_2	28.34	-
Residue (Coke/char)	-	33.10	-
Total Carbon balance	-	98.29	-

* Aromatics selectivity is defined as moles of carbon in an aromatic hydrocarbon to total moles of carbon in the aromatic products.

Effect of catalyst loading and reaction temperatures

To explore the effects of reaction temperature on product distribution, pyrolysis was performed at temperatures of 400°C, 500°C, 600°C, 700°C, and 800°C. As illustrated in Figure 1, carbon yields of aromatics increased from 14% to 24% in increasing temperature from 400°C to 800°C, but the increase becomes negligible above 600°C. At low reaction temperatures, most carbon remained in the residue.

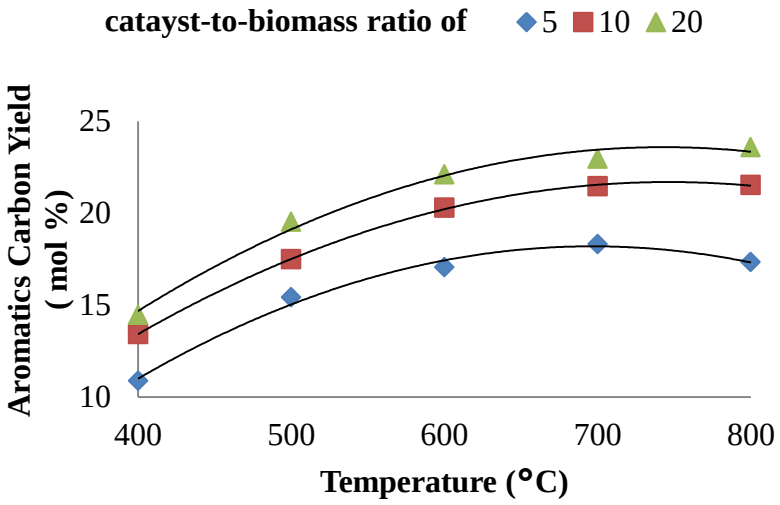

Figure 1. Effect of reaction temperature and catalyst-to-biomass ratio on aromatic hydrocarbon yields for the catalytic fast pyrolysis of *C.vulgaris* using HZSM-5.

Figure 1 also shows the effect of catalyst loading on the aromatic yields for biomass-to-catalyst ratios of 5, 10, and 20. Aromatic hydrocarbon production was favored under conditions of high catalyst-to-biomass ratio and high temperature. High catalyst loading is needed to ensure that pyrolyzed vapor enters the pores of the HZSM-5 catalyst instead of adsorbing on the external surface of the catalyst where thermal decomposition produces coke and small oxygenates. High catalyst loading is especially necessary for the micro-pyrolzyer

due to limitations of mass and heat transfer in this instrument. With these findings, we used biomass-to-catalyst ratios of 20 for our subsequent tests.

As shown in Figure 2, temperature also affected carbon yields of other pyrolysis products. Carbon yields in the residue decreased dramatically from 63% to 24% in the temperature range of 400^{o}C to 800^{o}C, while yields of aromatics increased. This result suggests that the aromatic hydrocarbons and coke form in competing reaction pathways. CO and CO_2 are the main gaseous products. Carbon yields of CO increased from 6.4% to 17.2% as temperature increased from 400^{o}C to 800^{o}C. High temperature also favored the formation of CO_2, carbon yield of which increased from 18.2% to 30%. CO and CO_2 are generated by decarboxylation and decarbonylation reactions, both of which increase with temperature.[44]

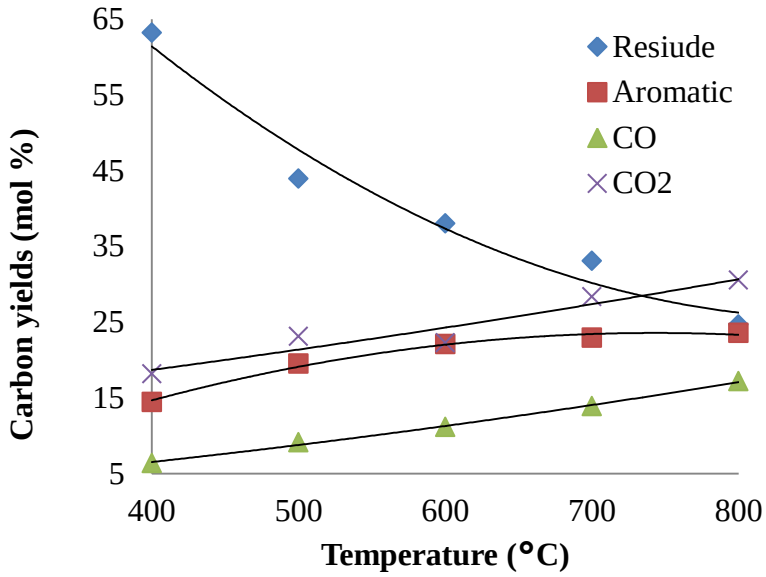

Figure 2. Effect of reaction temperature on carbon product distribution for catalytic fast pyrolysis of *C.vulgaris* using HZSM-5 (catalyst-to-biomass ratio of 20).

Since BTX compounds are important petrochemicals and more valuable than napthalenes and other polyaromatics, selectivity of BTX among aromatic hydrocarbons was examined here. As shown in Figure 3, increasing temperature had negligible effect on the

total aromatic selectivity of BTX, which increased from 70% to 74% as temperature increased from 400°C to 800°C. However, temperatures did have significant effect on the distribution of aromatic compounds. High temperature favored the formation of benzene. As the temperature increased from 400°C to 800°C, aromatic selectivity of benzene increased from 12% to 21%, while that of xylene decreased from 32% to 24%. The selectivity of toluene increased only slightly in the temperature range of 400°C to 600°C, with no significant change above that range. In conclusion, high temperature favors the formation of small aromatics.

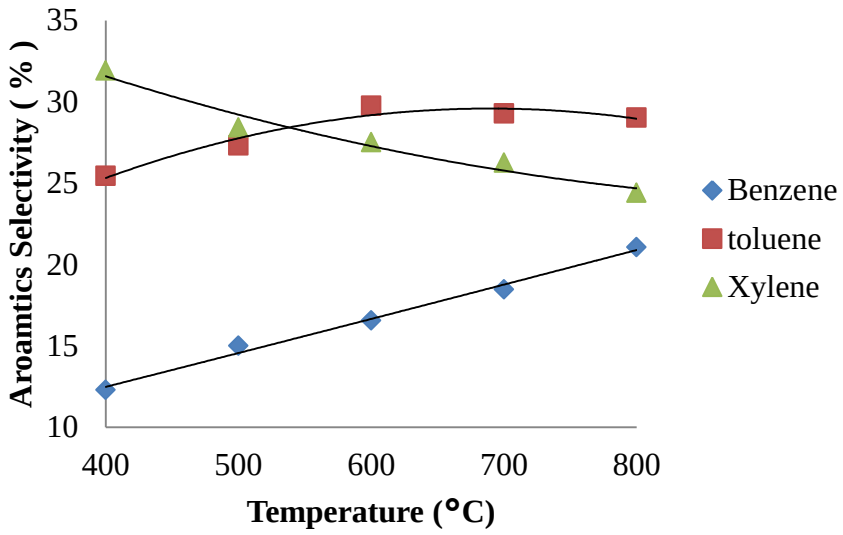

Figure 3. Effect of temperature on selectivity of BTX for the catalytic pyrolysis of *C.vulgaris* using HZSM-5 (catalyst-to-biomass ratio of 20).

Comparison with red oak pyrolysis

Catalytic pyrolysis of red oak was performed at the same reaction conditions used for C.vulgaris. As shown in Figure 4, aromatic yields for red oak are much lower than for C.vulgaris at every pyrolysis temperature. The aromatic yield for red oak was as low as 4% at 400oC, increasing to 16.7% at 800oC. C.vulgaris's aromatic yields, on the other hand, ranged

from 14% at 400oC to 24% at 800oC. Low aromatic yields from red oak may be due to its lignin content, which primarily converts to coke formation, especially at low reaction temperatures. The fact that fatty acid components in C.vulgaris are more readily upgraded to aromatics with HZSM-5 catalyst may also contribute to the higher aromatic yields from C.vulgaris.[96, 97]

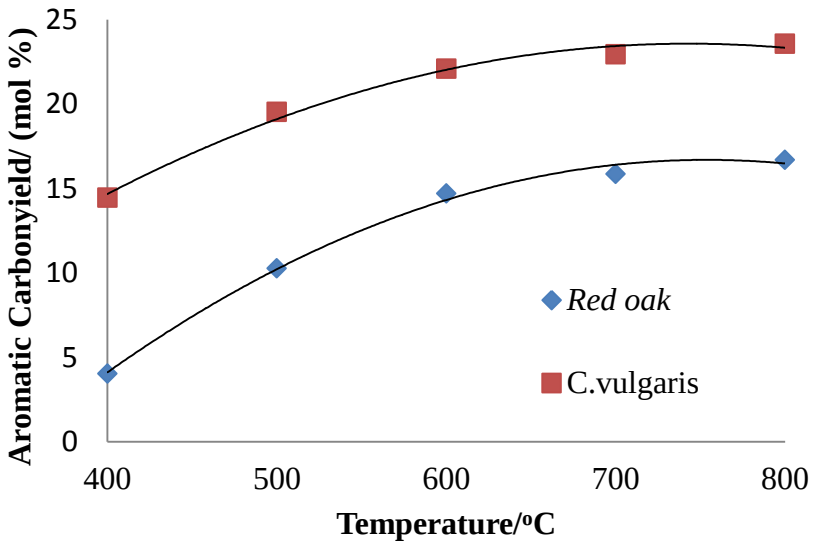

Figure 4. Aromatic yields from catalytic pyrolysis of red oak and *C.vulgaris* using HZSM-5 with varying reaction temperatures (catalyst-to-biomass ratio of 20).

The distribution of aromatic hydrocarbons from catalytic pyrolysis of red oak and *C.vulgaris* over HZSM-5 are shown in Figure 5. *C.vulgaris* showed higher selectivity toward smaller aromatic products such as benzene, toluene, and xylene. In contrast, red oak generated more napthalenes and other polyaromatics. Since BTX are more valuable than large aromatics such as napthalenes, *C.vulgaris* is a better feedstock for catalytic pyrolysis than red oak in terms of both aromatic yield and aromatics distribution.

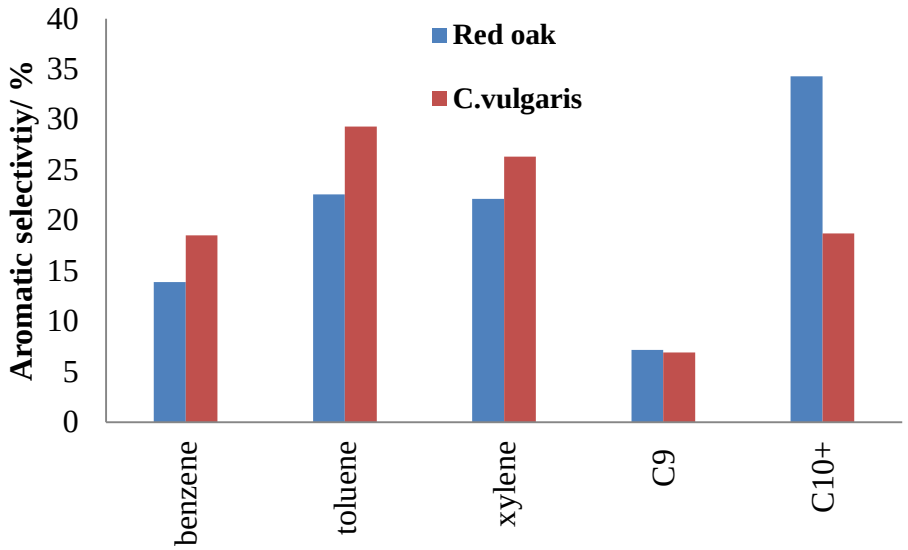

Figure 5. Aromatics Selectivities of from catalytic pyrolysis of red oak and *C.vulgaris* usingHZSM-5 (reaction temperatures: 700^{o}C; catalyst-to-biomass ratio: 20; C_9 includes indanes, indenes, and alkylbenzene; C_{10+} includes napthalenes and higher polyaromatics)

The fate of nitrogen

Figure 6 shows the nitrogen distribution in the products of catalytic pyrolysis of C.vulgaris as a function of pyrolysis temperature. At 400oC, only about 5% of the nitrogen was released as ammonia, while 92% was found in the carbonaceous residue of catalytic pyrolysis (char or coke). As temperature increased, however, the amount of nitrogen found in the residue dropped dramatically, decreasing to 50% at 500oC and to just 13% at 800oC. Correspondingly, the amount of nitrogen appearing as ammonia increased with temperature. At 800oC, ammonia accounted for 53% of the nitrogen in the products. This ammonia could be recycled as fertilizer for microalgae cultivation, thereby reducing the demand for new fertilizer, a situation that would lead to benefits in both production costs and greenhouse gas emissions.

However, a significant amount of the nitrogen appeared as hydrogen cyanide (HCN) accounting for 3% of the nitrogen yield at 400^{o}C and increasing to 13% at 800^{o}C. Since

HCN is extremely toxic, it must be mitigated during or after catalytic pyrolysis, possibly by passing the vapors through a basic solution or packed bed of metal hydroxide.

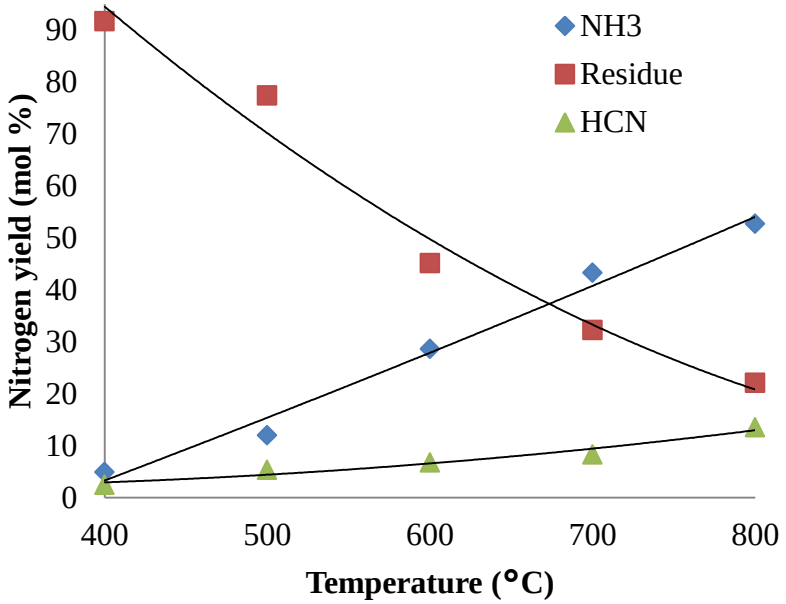

Figure 6. Effect of reaction temperature on nitrogen product distribution from the catalytic fast pyrolysis of *C.vulgaris* using HZSM-5 (catalyst-to-biomass ratio of 20).

Conclusion

We herein explored catalytic pyrolysis as a means to convert whole microalgae to biofuels and chemicals. Our research showed that catalytic pyrolysis of *C.vulgaris*, a lipid-lean microalgae, in the presence of HZSM-5 catalyst yielded aromatic hydrocarbons that removed both oxygen and nitrogen. The maximum carbon yield of aromatic hydrocarbons was 24%, mostly as BTX molecules, with total aromatic selectivity of 75%. Compared with red oak catalytic pyrolysis, *C.vulgaris* generated more aromatics and selectivity of BTX was higher. Nitrogen was distributed among carbonaceous residue, ammonia, and hydrogen cyanide. At low temperatures, most of the nitrogen appeared in the residue, but selectivity

shifted to ammonia as temperature increased. For reaction temperature of 800^{o}C, 53% of the nitrogen was released as ammonia, which suggests feasibility for recycling nitrogen as a nutrient for microalgae cultivation. In general, catalytic pyrolysis is attractive for upgrading microalgae because it converts all of the components of this high-nitrogen feedstock into fuels, chemicals, and nitrogen fertilizer. Additionally, energy-intensive lipid extraction process is eliminated in the process. The efficiency of such a system would greatly enhance the economy of the microalgae biorefinery.

Acknowledgement

The authors would like to acknowledge financial support from the Iowa Energy Center (Grant No.: 10-02). The authors are also grateful to Dr. Sukh S. Sidhu of University of Dayton Research Institute for providing the microalgae sample and to Dr. Tong Wang of Iowa State University for performing the total fatty acids analysis of the microalgae sample.

References

[1] Q. Hu, M. Sommerfeld, E. Jarvis, M. Ghirardi, M. Posewitz, M. Seibert, A. Darzins, Microalgal triacylglycerols as feedstocks for biofuel production: perspectives and advances, Plant J, 54 (2008) 621-639.

[2] DOE, National Algal Biofuels Technology Roadmap in, 2010.

[3] P.J.L. Williams, L.M.L. Laurens, Microalgae as biodiesel & biomass feedstocks: Review & analysis of the biochemistry, energetics & economics, Energy Environ Sci, 3 (2010) 554-590.

[4] T.M. Mata, A.A. Martins, N.S. Caetano, Microalgae for biodiesel production and other applications: A review, Renew Sust Energ Rev, 14 (2010) 217-232.

[5] M. Appl, Ammonia, in: Ullmann's Encyclopedia of Industrial Chemistry, Wiley-VCH Verlag GmbH & Co. KGaA, 2000.

[6] Y.-X. Huo, D.G. Wernick, J.C. Liao, Toward nitrogen neutral biofuel production, Curr Opin Biotechnol, 23 (2012) 406-413.

[7] K. Wang, R.C. Brown, S. Homsy, L. Martinez, S.S. Sidhu, Fast pyrolysis of microalgae remnants in a fluidized bed reactor for bio-oil and biochar production, Bioresource Technol, 127 (2013) 494-499.

[8] D. Mohan, C.U. Pittman, P.H. Steele, Pyrolysis of wood/biomass for bio-oil: A critical review, Energ Fuel, 20 (2006) 848-889.

[9] G. Chiavari, G.C. Galletti, Pyrolysis—gas chromatography/mass spectrometry of amino acids, J Anal Appl Pyrol, 24 (1992) 123-137.

[10] Y. Goldman, N. Garti, Y. Sasson, B.-Z. Ginzburg, M.R. Bloch, Conversion of halophilic algae into extractable oil. 2. Pyrolysis of proteins, Fuel, 60 (1981) 90-92.

[11] P. Pan, C. Hu, W. Yang, Y. Li, L. Dong, L. Zhu, D. Tong, R. Qing, Y. Fan, The direct pyrolysis and catalytic pyrolysis of Nannochloropsis sp. residue for renewable bio-oils, Bioresource Technol, 101 (2010) 4593-4599.

[12] X. Miao, Q. Wu, High yield bio-oil production from fast pyrolysis by metabolic controlling of Chlorella protothecoides, J Biotechnol, 110 (2004) 85-93.

[13] X. Miao, Q. Wu, C. Yang, Fast pyrolysis of microalgae to produce renewable fuels, J Anal Appl Pyrol, 71 (2004) 855-863.

[14] R. French, S. Czernik, Catalytic pyrolysis of biomass for biofuels production, Fuel Process Technol, 91 (2010) 25-32.

[15] T. Carlson, G. Tompsett, W. Conner, G. Huber, Aromatic Production from Catalytic Fast Pyrolysis of Biomass-Derived Feedstocks, Top Catal, 52 (2009) 241-252.

[16] A. Corma, G.W. Huber, L. Sauvanaud, P. O'Connor, Processing biomass-derived oxygenates in the oil refinery: Catalytic cracking (FCC) reaction pathways and role of catalyst, J Catal, 247 (2007) 307-327.

[17] T.R. Carlson, J. Jae, Y.-C. Lin, G.A. Tompsett, G.W. Huber, Catalytic fast pyrolysis of glucose with HZSM-5: The combined homogeneous and heterogeneous reactions, Journal of Catalysis, 270 (2010) 110-124.

[18] T.R. Carlson, Y.-T. Cheng, J. Jae, G.W. Huber, Production of green aromatics and olefins by catalytic fast pyrolysis of wood sawdust, Energy Environ Sci, 4 (2011) 145-161.

[19] J. Jae, G.A. Tompsett, A.J. Foster, K.D. Hammond, S.M. Auerbach, R.F. Lobo, G.W. Huber, Investigation into the shape selectivity of zeolite catalysts for biomass conversion, J Catal, 279 (2011) 257-268.

[20] T.A. Milne, R.J. Evans, N. Nagle, Catalytic conversion of microalgae and vegetable oils to premium gasoline, with shape-selective zeolites, Biomass, 21 (1990) 219-232.

[21] S. Thangalazhy-Gopakumar, S. Adhikari, S.A. Chattanathan, R.B. Gupta, Catalytic pyrolysis of green algae for hydrocarbon production using H+ZSM-5 catalyst, Bioresource Technol, 118 (2012) 150-157.

[22] AOAC, Official methods of analysis, Washington D.C, 1990.

[23] E.W. Becker, Micro-algae as a source of protein, Biotechnol Adv, 25 (2006) 207-210.

[24] V. Venugopal, Polysaccharides from Seaweed and Microalgae, in: Marine Polysaccharides, CRC Press, 2011, pp. 89-134.

[25] N. Kuzhiyil, D. Dalluge, X. Bai, K.H. Kim, R.C. Brown, Pyrolytic Sugars from Cellulosic Biomass, ChemSusChem, 5 (2012) 2228-2236.

[26] Ö. Tokuşoglu, M.K. üUnal, Biomass Nutrient Profiles of Three Microalgae: Spirulina platensis, Chlorella vulgaris, and Isochrisis galbana, J Food Sci, 68 (2003) 1144-1148.

[27] F.A. Twaiq, N.A.M. Zabidi, S. Bhatia, Catalytic conversion of palm oil to hydrocarbons: Performance of various zeolite catalysts, Ind Eng Chem Res, 38 (1999) 3230-3237.

[28] T.J. Benson, R. Hernandez, M.G. White, W.T. French, E.E. Alley, W.E. Holmes, B. Thompson, Heterogeneous Cracking of an Unsaturated Fatty Acid and Reaction Intermediates on H+ZSM-5 Catalyst, CLEAN – Soil, Air, Water, 36 (2008) 652-656.

CHAPTER 4 CATALYTIC PYROLYSIS OF INDIVIDUAL COMPONENTS OF LIGNOCELLULOSIC BIOMASS

A paper published by *Green Chemistry*

Kaige Wang, Kwang Ho Kim and Robert C. Brown

Abstract

We report on the catalytic pyrolysis of switchgrass and its three main components,(cellulose, hemicellulose and lignin) over H-ZSM5 catalyst. The yields of aromatic hydrocarbons for the three components decreased in the following order: cellulose > hemicellulose >> lignin. Moderately higher temperature favored formation of aromatics. The results indicate that H-ZSM5 catalyst did not remove oxygen in an optimal pathway for catalytic pyrolysis of biomass. Dehydration was the dominant oxygen removal mechanism for catalytic pyrolysis, while decarbonylation to CO was favored over decarboxylation to CO_2. This suggests that higher yields of aromatics might be achieved by catalyst improvements or reactor design that optimizes deoxygenation pathway. Our results indicate that thermal char contributed a large fraction of solid carbonaceous residue during catalytic pyrolysis. Product distribution from catalytic pyrolysis of switchgrass appeared to be the additive contribution of the three individual components, which indicates that there was no significant interaction among the biomass-derived products.

Introduction

Due to its large availability, the potential of lignocellulosic biomass as a feedstock for biofuel production has received wide interest.[1, 15] Several pathways to produce biofuels and bio-based chemicals from lignocellulosic biomass are under development, which can be broadly classified as either thermochemical or biochemical processes.[1] Among

thermochemical processes, catalytic pyrolysis is attractive for its ability to convert plant fibers into highly deoxygenated molecules in a single step.[44, 45, 91, 98] A number of catalysts have been evaluated for their function in catalytic pyrolysis including metal oxides, transition metals, and zeolites.[46, 92, 99]

Catalytic pyrolysis likely proceeds as two distinctive steps: thermal depolymerization and decomposition of plant polymers into volatile compounds that are subsequently deoxygenated to hydrocarbons.[44] The three main plant polymers of lignocellulosic biomass are cellulose, hemicellulose and lignin.[1] Cellulose is a glucose polymer constituting 40%-60% of lignocellulose.[1, 100] Hemicellulose, which accounts for about 20-35% of dry biomass, is a class of heterogeneous branched polysaccharides. In contrast to highly crystalline cellulose, hemicellulose has a random and amorphous structure that is cross-linked to cellulose and lignin.[51] Lignin, a highly branched phenol-based polymer, constitutes about 20-35% of lignocellulosic biomass.[101, 102] Extensive studies have shown that pyrolysis of these three main components of lignocellulose proceed at different temperature ranges and generates diverse products.[51, 101, 103, 104]

Catalytic pyrolysis of cellulose has been studied by several researchers.[44, 45, 105, 106] Fabbri et al.[106] found that H-ZSM5 zeolite mixed with pure cellulose substantially reduced the yield of anhydrosugars using an off-line micropyrolyzer. Carlos et al.[44, 45, 91] used a Py-GC/MS to study catalytic pyrolysis of both cellulose and glucose. They reported 30% yield of aromatics from glucose. Jae et al.[92] investigated the influence of zeolite pore size and shape selectivity on catalytic conversion of glucose to aromatics and found that H-ZSM5 zeolite has the highest aromatic yield and least amount of coke.

Guo et al.[107] investigated the pyrolysis of hemicellulose over zeolites using TG-FTIR and found that the catalyst decreased oxygenates yields and increased the formation of non-condensable gases. Mihacik[55] screened several catalysts for catalytic pyrolysis of hemicellulose and found that H-ZSM5 was the most effective at producing aromatic hydrocarbons from hemicellulose. Around 9 wt% aromatic yield was obtained from hemicellulose. Jeon[108] and co-workers studied catalytic pyrolysis of hemicellulose over mesoporous catalyst using Py-GC/MS. They found that deoxygenation performance of these mesoporous catalysts were limited compared with microporous zeolite.

Lignin is the most thermally resistant of the three main components of biomass. Pyrolysis of lignin produces acetic acid and monomeric phenolic compounds as the major condensable products along with large amounts of char.[101, 102, 104] Sharma and Bakhshi[109] and Jackson et al.[110] reported H-ZSM5 to be the most effective zeolite catalyst for the conversion of lignin into aromatic hydrocarbons. Ma et al.[111] pyrolyzed alkaline lignin in the presence of zeolite catalysts with various acidity and pore size using Py-GC/MS. They claimed 30% carbon yield of aromatic hydrocarbons for H-ZSM5 zeolite, which is the highest yield reported in the literature. In contrast, Mullen et al.[112] and Li et al. [113] also using Py-GC/MS for their experiments both reported only 5 wt% aromatic yield for the same ZSM5 zeolite catalyst.

These previous studies suggest very different behavior of the three principal components of lignocellulose under catalytic pyrolysis.[90, 114, 115] However, the results among different researchers are sometimes contradictory and experimental conditions have not been uniform for studies of the three components of lignocellulose. The current study investigates differences in the catalytic pyrolysis of cellulose, hemicellulose, and lignin under

similar pyrolysis conditions using the most promising zeolite catalyst, H-ZSM5. In addition, interactions among components for non-catalytic pyrolysis have been studied by many researchers.[116-119] However, no knowledge exists on interactions effects during catalytic pyrolysis. The current study also discusses interactions among the components.

For catalytic pyrolysis of biomass, large amounts of carbon in the biomass results in solid carbonaceous material, which is normally called coke.[15, 45, 91, 120] Coke formation is a major challenge to catalytic pyrolysis with zeolite. Generally, there are two types of coke for biomass catalytic pyrolysis, thermal coke and catalytic coke. Thermal coke, which is called char, is generated from both direct thermal decomposition of biomass and secondary-reaction of pyrolyzed biomass vapors. Char is normally located on the external surface of catalyst during catalytic pyrolysis. Catalytic coke is formed during catalytic reaction of biomass-derived oxygenates and deposited mainly within the internal pores or/and on the surface of catalyst. Char and coke formation not only decrease the conversion efficiency of catalytic pyrolysis, but also cause irreversible deactivation of catalyst. However, all previous studies discussed the solid carbonaceous material formation in catalytic pyrolysis as a whole, without distinguishing its thermal and catalytic origin. This study investigates the char and coke formation comparatively during catalytic pyrolysis from biomass components.

Like carbonaceous solid residue, carbon oxides (CO_x), consisting of CO and CO_2, formed during catalytic pyrolysis can arise from either of two mechanisms. First, thermal decomposition of carboxylic and carbonyl functional groups or abscission of C-O bonds can generate CO_x along with condensable oxygenates. Second, acid-catalyzed reactions of biomass-derived oxygenates result in oligomerization, decarboxylation and decarbonylation with the net effect of removing oxygen in the form of CO_x and H_2O.[44] To our knowledge,

little research has focused on how oxygen is removed in this process. The current study quantitatively investigates the deoxygenation by decarboxylation, decarbonylation or dehydration.

Experimental

Materials

Cellulose, in the form of microcrystalline powder, was purchased from Sigma Aldrich. Xylan, purchased from Sigma Aldrich, was used as the proxy of hemicellulose in this study. However, this beechwood-extracted xylan contains significant quantities of ash, which is known to strongly influence pyrolysis.[50, 51] Dialysis was employed to remove the inorganic impurities from the xylan before pyrolysis following the method described by Patwardhan et al.[51] Milled wood lignin (MWL) was the source of lignin for these experiments since it shows minimal structural and chemical modification compared with other extracted lignins, such as Klason lignin and alkali lignin.[102] Milled wood lignin was prepared according to the procedures recommended by Björkman.[121] To investigate potential interactions of cellulose, hemicellulose, and lignin, catalytic pyrolysis of switchgrass, purchased from Wood Residual Solutions, LLC of Montello, Wisconsin, was also studied. To eliminate interference by inorganic minerals the switchgrass was washed with 0.1N HNO_3 by the method described by Patwardhan et al.[11] To eliminate interference from resins and waxes, the acid-washed switchgrass was extracted using ethanol and toluene mixture (V/V=1:1). Component analysis of the switchgrass was determined by methods described in the literature.[122] All the samples were ground and screened to less than 200 meshes.

Effective hydrogen-to carbon ratio (H/C_{eff}) as defined by Chen et al. [105] is an important parameter in catalytic pyrolysis for comparing different feedstock. H/C_{eff} is defined in equation (1), where H, C and O are the moles of hydrogen, carbon and oxygen, respectively.

$$H/C_{eff} = (H - 2(O))/C \quad (1)$$

Results for the elemental and compositional analyses of the feedstock as well as their H/C_{eff} ratios are listed in Table 1. Ash and moisture contents of feedstock are summarized in Table S1. Mineral content of feedstocks is also given in Table S1. We chose commercially-available ZSM5 catalyst (CBV2314 with SiO_2/Al_2O_3 ratio of 23, Zeolyst, USA) for this study. The catalyst was calcined at 550^oC (5^oC /min) for 5 hours in a muffle furnace to activate it prior to use. Calcined catalyst and biomass were combined in a catalyst-to-biomass weight ratio of 20 in all catalytic pyrolysis experiments. Approximately 5mg biomass/catalyst mixture and 0.5mg biomass were used in a typical test for catalytic pyrolysis and non-catalytic pyrolysis respectively.

Table 1. Elemental and composition analysis of feedstock (as received basis)

Feedstock	Elemental analysis (wt.%)				H/C_{eff}	Composition analysis (wt.%)		
	C	H	N	O		Cellulose fraction	Hemicellulose fraction	Lignin fraction
Cellulose	42.8	5.48	0	50.5	0	93.8	0	0
Hemicellulose	39.2	6.57	0	51.9	0	0	93.2	0
Lignin	58.3	6.0	0	35.0	0.3	0	0	94.3
Switchgrass	47.6	6.1	0.4	42.9	0.2	39.6	31.6	19.5

Pyrolysis experiment and products analysis

Pyrolysis experiments were conducted in a micro-furnace pyrolyzer (PY-2020iS, Frontier Laboratories, Japan) equipped with an auto-shot sampler (AS-1020E, Frontier

Laboratories, Japan). The micro-pyrolyzer can be temperature controlled in the range of 40-800^{o}C. The interface between the pyrolyzer and GC can be heated to 100-400^{o}C. Samples were loaded in deactivated stainless steel sample cups, which were automatically lowered into the preheated furnace. Helium carrier gas was used to sweep pyrolysis vapor into the GC (Varian CP3800, USA). The aromatic hydrocarbons that were condensable were separated in a capillary column (Ultra Alloy-5, Frontier Laboratories, Japan) with stationary phase consisting of 5% diphenyl and 95% dimethylpolysiloxane (30 m x 0.250 mm and 0.250 μm film thickness). Helium was employed as the carrier gas at a flow rate of 1ml/min. The GC oven was programmed for a 3-minute hold at 40^{o}C followed by heating (10^{o}C/min) to 250^{o}C, after which temperature was held constant for 9 minutes. The injector temperature was 260^{o}C and the injector split ratio was set to 100:1. Separated pyrolysis vapors were analyzed either by a mass spectrometer (MS) or a Flame Ionization Detector (FID). The MS (Saturn 2200, Varian, USA) was used for molecular identification. After the peaks were identified, standards were prepared to quantify the results using FID.

Measurement of non-condensable gas (NCG) products (CO, CO_2, CH_4, C_2H_4, C_2H_6, C_3H_6, C_3H_8, and C_4H_8) required replication of experiments substituting a Porous Layer Open Tubular (PLOT) column (60 m x 0.320 mm) (GS-GasPro, Agilent, USA) in the GC. For NCG analysis, the GC oven was programmed for a 3-minute hold at 30^{o}C then ramped at 10^{o}C/min to 250^{o}C, after which temperature was held constant for 4 minutes. Mass spectroscopy (Saturn 2200, Varian, USA) was used to identify chemical species. A standard gas mixture consisting of CO, CO_2, CH_4, C_2H_4, C_2H_6, C_3H_6, C_3H_8, and C_4H_8 in helium (Praxair, USA) was used to calibrate the yield of NCG. Olefins and alkenes $\geq C_5$ were either not detected or negligible in this study.

Pyrolysis residue from both non-catalytic and catalytic pyrolysis experiment was recovered from the sample cups to determine its carbon content. This was quantified by combustion elemental analysis using a vario MICRO cube elemental analyzer (Elementar, USA).

Biomass and catalyst mixed together and pyrolyzed, making it impossible to distinguish whether solid carbonaceous residue was thermally derived char or catalytically derived coke. Similarly, it was impossible to determine the origin of CO_x. To estimate the amount of carbonaceous solid carbon and CO_x from each source, it was assumed that thermally derived product yields were not influenced by the proximate occurrence of catalytic reactions generating similar products. Thus, catalytically derived coke could be calculated by subtracting from the total yield of carbonaceous solid residue obtained from catalytic pyrolysis the char yield obtained from non-catalytic pyrolysis of the same amount of biomass under otherwise similar reaction condition. Similarly, CO_x yields derived from catalytic reactions (as opposed to thermal reactions) were calculated as the differences in CO_x yields for pyrolysis of biomass with and without catalyst present.

All measurements including aromatics, NCG and carbonaceous residue, were performed at least in duplicate to check the reproducibility of the data. Final product distribution was reported as molar carbon yield, which was defined as the molar ratio of carbon in a specific product to the carbon in the feedstock.

Results and Discussion

Effect of temperature on aromatic yields

Aromatic yields from cellulose, hemicellulose and lignin over different temperatures are shown in Fig. 1. The aromatic yields varied significantly among the three components.

Cellulose had the highest aromatic yields across the temperature range, with a low of 15% at 400°C and peaking at 30% at 700°C. Hemicellulose had the next highest aromatic yields peaking at 20% at 700°C. Lignin generated only 2% aromatics at 400°C increasing to 9% at 800°C.

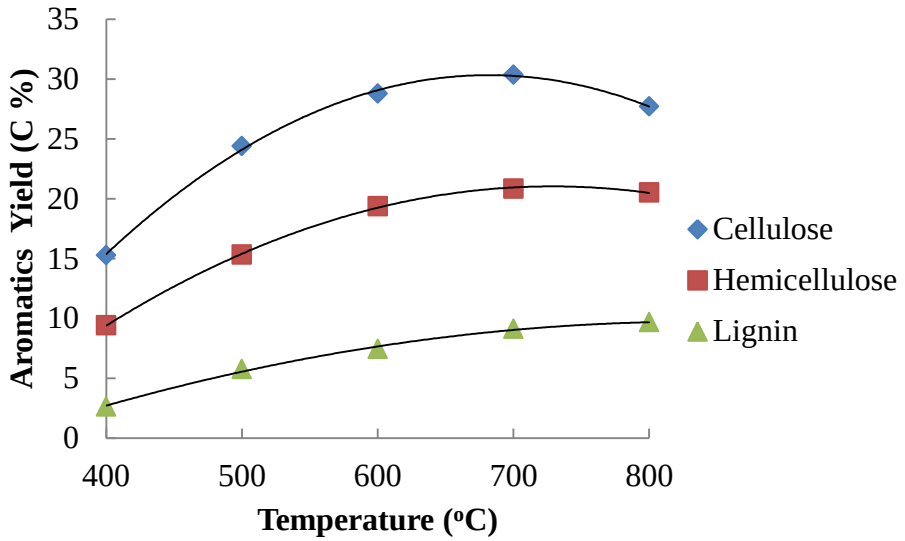

Figure 1. Effect of reaction temperature on aromatic hydrocarbon yields for the catalytic pyrolysis of cellulose, hemicellulose and lignin using HZSM-5 (catalyst to biomass ratio of 20).

In contrast, non-catalytic pyrolysis is well known to produce maximum yields of organic products in the temperature range of 400 - 500°C.[51, 101, 103] Pyrolysis at elevated temperatures promotes decomposition of biomass to smaller molecules. Carbohydrates yield more formic acid and aldehydes and less anhydrosugars.[101] Lignin yields more acetic acid and aldehyde.[101, 123] These small molecular compounds are easier to enter into the pores of the H-ZSM5 catalyst, compared to anhydrosugars and phenolic compounds, molecules of which are bigger than catalyst pore.[92]

There are several possible explanations for the extremely low aromatic yield from lignin. Non-catalytic pyrolysis of lignin produces large amounts of "thermal" char,[101, 102] possibly from both primary and secondary reactions. Lignin generates few volatile products

that can diffuse into the pores of the zeolite catalyst.[101] Considering the highly reactive nature of many lignin-derived molecules, any volatile products may oligomerize and dehydrate on the external surface of the zeolites to form "catalytic coke" before they can diffuse into the catalyst pores. Finally, it may be possible that phenolic monomers produced from lignin are not reactive toward zeolite catalysts. Major volatile products from non-catalytic pyrolysis of lignin include phenol, 4-vinylphenol and 2,6-dimethoxyl phenol.[101] As observed by other researchers, phenolic compounds have extremely low reactivity on H-ZSM5 compared to other oxygenates from biomass pyrolysis such as ketones, aldehydes, and acids.[124-126]

Effect of temperature on char/coke formation

Carbon yields for solid carbonaceous residue (char/coke) from catalytic pyrolysis of the three components of lignocellulose are illustrated in Fig. 2. We do not distinguish between carbonaceous residue generated thermally (char) and catalytically (coke). As with aromatic yields, char/coke yields varied significantly among the three components. Char/coke yield from cellulose decreased dramatically from 62% to 19% in the temperature range of 400-800°C, while that from hemicellulose decreased from 60% to 25%. Compared to carbohydrates, lignin generated the highest char/coke yield across the whole temperature range. Char/coke yield was 79% at 400^{o}C for catalytic pyrolysis of lignin. This number decreased slightly with increasing temperature; however the change after 600^{o}C was negligible. The coke yield was as high as 55% even at 800^{o}C.

The thermally resistant structure of lignin and low reactivity of lignin-derived phenolic compounds over zeolite catalyst can explain the extremely high coke yield for catalytic pyrolysis of lignin. As discussed in the previous section, high temperatures favor the

formation of low molecular weight species from lignin that readily diffuse into catalyst pores. Thus, total char/coke yield decreases with increasing temperature for the three components. Another reason may be that coke precursors desorb more quickly into the gas phase with increasing temperature.

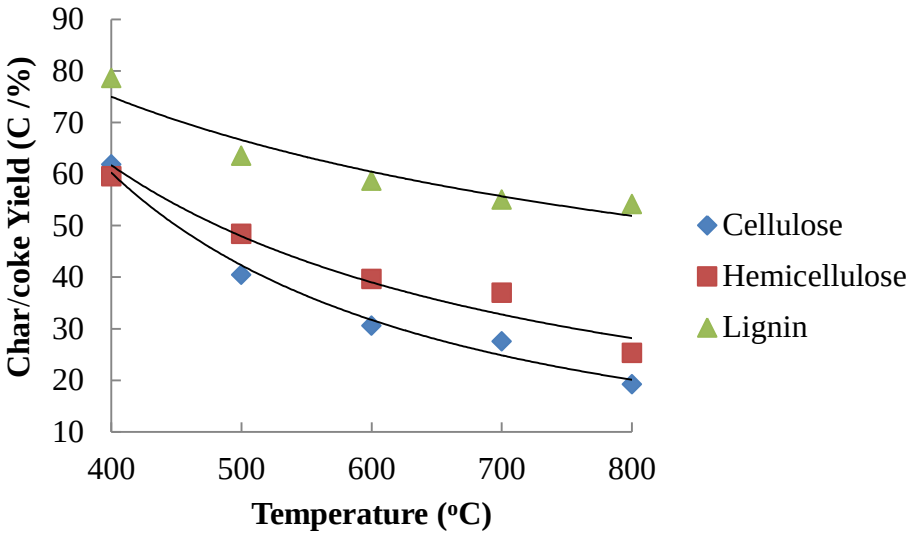

Figure 2. Effect of reaction temperature on char/coke yields for catalytic pyrolysis of cellulose, hemicellulose and lignin using HZSM-5 (catalyst to biomass ratio of 20).

In agreement with previous studies, we find that excessive char/coke formation is a major challenge to catalytic pyrolysis of lignocellulose.[44, 45, 91, 127] Moreover, lignin is the largest contributors to char/coke formation among the three components during catalytic pyrolysis.

Product distribution from catalytic pyrolysis

Based on the discussion above, we investigate product distribution from catalytic pyrolysis with reaction temperature of 600°C. Table 2 summarizes complete products from catalytic pyrolysis of the three components. Aromatics selectivity given here is defined as

moles of carbon in a specific aromatic hydrocarbon to total moles of carbon in the aromatic products. Selectivity of C_1-C_4 light hydrocarbons is also defined accordingly.

Table 2. Distribution of catalytic pyrolysis products from cellulose, hemicellulose and lignin (reaction temperatures: 600^{o}C; catalyst-to-biomass ratio: 20).

Sample	Cellulose	Hemicellulose	Lignin
Overall yield (C %)			
CO	16.4±0.10	13.9±0.63	7.9±0.25
CO_2	6.4±0.35	11.1±0.19	4.0±0.08
Char/coke	30.6±0.35	39.6±0.39	58.9±0.29
Aromatic Hydrocarbons	28.8±0.72	19.4±0.39	7.4±0.53
C_1-C_4 Hydrocarbons	4.5±0.18	8.3±0.29	5.2±0.14
Total	86.8±1.72	92.3±2.17	83.5±1.31
Aromatics selectivity (%)			
Benzene	14.4±0.11	13.3±0.31	9.5±0.13
Toluene	23.9±0.07	25.7±0.17	17.3±0.18
Xylene	15.2±0.26	23.7±0.03	24.3±0.17
C_9 aromatics[a]	7.8±0.16	8.9±0.26	8.0±0.15
C_{10+} aromatics[b]	38.8±0.21	25.0±0.86	40.8±0.02
C_1-C_4 selectivity (%)			
Methane	6.2±0.46	4.7±1.73	16.9±0.04
Ethane	2.2±0.00	3.2±0.18	4.4±0.03
Ethylene	58.4±0.62	54.4±0.26	49.6±0.58
Propane	7.0±0.13	6.5±0.24	7.3±0.00
Propene	23.6±0.16	28.5±1.90	19.6±0.33
2-Butene	2.5±0.14	2.8±0.04	2.2±0.23

[a] C_9 aromatics include indanes, indenes, and alkylbenzene; [b] C_{10+} aromatics include naphthalenes and higher polyaromatics

Aromatic hydrocarbons distribution

Aromatic hydrocarbons are the major target products from catalytic pyrolysis. Carbon yield of aromatics from cellulose, hemicellulose and lignin were 28.8%, 19.4 and 7.4%,

respectively. Aromatic selectivity from the three components is also listed in Table 2. Benzene and toluene selectivity for cellulose and hemicellulose were similar, while selectivity of naphthalenes and higher polyaromatics from cellulose (38.79%) was much higher than that from hemicellulose (24.95%). The dominant product from cellulose pyrolysis is levoglucosan, yield of which was as high as 60wt%.[103] With a molecule size of 0.67nm, which is larger than the maximum pore size of H-ZSM5 (0.63nm), levoglucosan cannot readily diffuse into the zeolite pores.[92] Levoglucosan may undergo dehydration reaction to form furan compounds, which subsequently either diffuse into the catalyst pore or polymerize to catalytic coke on the external surface of catalyst. These external coke may hinder the diffusion of monocyclic aromatics, which further react with oxygenates or other reaction intermediates to produce polyaromatics.[44] In contrast, anhydrosugar product (dianhydro xylose) from hemicellulose pyrolysis has a kinetic diameter of 5.98nm, thus can easily diffuse into zeolite pores without further dehydration reactions on catalyst surface. The molecular size difference between oxygenates from cellulose and hemicellulose may explain the variance of aromatics selectivity from the two carbohydrates.

Lignin had a trend to generate even more polyaromatics, compared with carbohydrates. This can also be explained by the low activity of phenolic compound over zeolite catalyst and resulting large amounts of catalytic coke. This observation is consistent with reports about catalytic conversion of phenolic compounds over H-ZSM5 zeolite and FCC catalyst.[114, 126, 128, 129]

CO and CO_2 formation

Carbon oxides (CO_x), consisting of CO and CO_2, are the major non-condensable gas products. Catalytic pyrolysis of hemicellulose generated the highest CO_2 yield (11.1%),

compared with CO_2 yield of 6.4% and 4.0% from cellulose and lignin respectively. This may contribute to the abundant CO_2 generation by cracking and abscission of C-C and C-O bonds connected the main branch of hemicellulose during thermal decomposition. This is in agreement with previous studies that showed that CO_2 is the most abundance product from hemicellulose pyrolysis.[51, 104] CO yield from catalytic pyrolysis of hemicellulose was 13.9%, which is comparable to that from cellulose (16.4%). Lignin generated the lowest CO yield, which was 7.9%.

Using the method described in the experimental section, Thermally-derived and catalytically-derived CO_x from catalytic pyrolysis of the three components was calculated and the results were given in Table 3. The fraction of CO and CO_2 from catalytic pyrolysis of lignin was lower than thermal-derived fraction, which indicates the low conversion of phenolic compounds over zeolite catalyst, as discussed in the previous section. In contrast, yields of catalytically-derived CO_x were much higher than for thermally-derived CO_x from catalytic pyrolysis of cellulose and hemicellulose, which indicates overwhelming acid-catalyzed reactions of carbohydrates-derived oxygenates over H-ZSM5. This trend was especially clear in comparing the thermally and catalytically-derived fractions of CO. The carbon yields of thermally-derived CO from catalytic pyrolysis of cellulose and hemicellulose were only 3.0% and 4.0%, respectively, while carbon yields of catalytically-derived CO were 13.4% and 9.6%, respectively.

Table 3. Thermal and catalytic fractions of CO_x and char/coke yield from catalytic pyrolysis of cellulose, hemicellulose and lignin (reaction temperatures: 600^oC; catalyst-to-biomass ratio: 20).

Feedstock	Cellulose		Hemicellulose		Lignin	
origin	Thermal	Catalytic	Thermal	Catalytic	Thermal	Catalytic
CO yield (C %)	3.0±0.06	13.4±0.17	4.1±0.16	9.8±0.80	4.0±0.17	3.9±0.43
CO_2 yield (C %)	2.5±0.08	3.9±0.43	7.1±0.05	4.0±0.25	2.8±0.08	1.2±0.16
Char/coke yield (C %)	n.d.[a]	30.6±0.36	18.4±0.64	23.1±1.03	33.1±2.02	25.8±2.31

[a] non-detectable

The strong acid sites in H-ZSM5 catalyst have been proven to be more active for decarbonylation to produce CO than decarboxylation to CO_2 from oxygenates during catalytic process.[90, 115, 129] [130] The study by Foster et al.[131] of catalytic pyrolysis of cellulose over H-ZSM5 with different alumina content also indicated that maximum CO generation correlated with maximum aromatic hydrocarbons generation. It is reasonable to speculate that there is a relationship between formation of CO by catalyzed decarbonylation and formation of aromatics. Fig. 3 shows the relationship between carbon yields of catalytic-derived CO and aromatic from catalytic pyrolysis of the three components of lignocellulose. Exact linear relations can be found between the yield of aromatics and catalytic CO. This indicates thermally-produced oxygenates primarily went through decarbonylation other than decarboxylation to form reaction intermediates which subsequently were converted into aromatics over zeolite catalyst. Catalytic CO yield can be seen as an index of aromatic formation for catalytic pyrolysis of biomass.

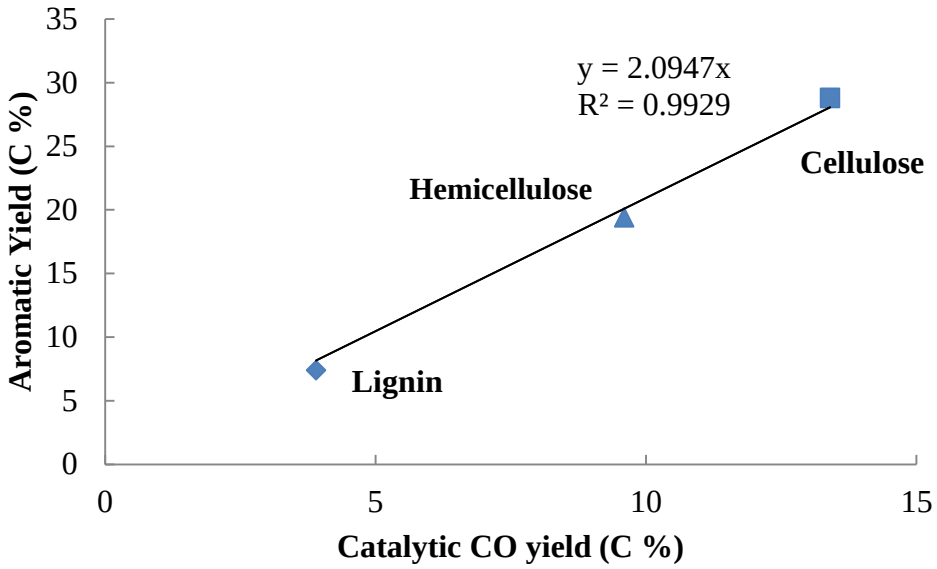

Figure 3. Correlation between carbon yields of aromatic hydrocarbons and catalytic-derived CO from catalytic pyrolysis of cellulose, hemicellulose and lignin (reaction temperatures: 600^{o}C; catalyst-to-biomass ratio: 20)

Char and coke distribution

Total carbon yields for carbonaceous solid residue (char/coke) from cellulose, hemicellulose and lignin were 30.6%, 39.6% and 58.7%, respectively. Using the method described in the experimental section, thermally-derived char and catalytically-derived coke during catalytic pyrolysis were distinguished as given in Table 3. Thermally derived char from catalytic pyrolysis of cellulose was negligible; while carbon yields of thermal char from hemicellulose and lignin were 18.4% and 33.1%, respectively. Catalytically-derived coke yields from cellulose, hemicellulose and lignin were 30.6%, 23.1% and 25.8%, respectively. This indicates that the solid residue formation was mainly attributed to the catalytic conversion step for catalytic pyrolysis of cellulose and hemicellulose. In contrast, thermal char formation was the primary pathway for catalytic pyrolysis of lignin. In general, to

increase the carbon conversion efficiency for catalytic pyrolysis, less thermal char and catalytic coke formation should be encouraged synergistically.

Light hydrocarbons distribution

Non-catalytic pyrolysis of biomass components produced a small amount of light hydrocarbons. Light hydrocarbon yields from all the three components were less than 1.5%. Due to its branched amorphous structure and low degree of polymerization, pyrolysis of hemicellulose produced more C_1- C_4 hydrocarbons compared with cellulose. Methane was the dominant light hydrocarbon product from non-catalytic pyrolysis of lignin. It was formed by thermal demethylation of abundant methoxyl groups in the lignin structure, which was investigated by other researchers.[101, 102]

In contrast, olefins were the most abundant light hydrocarbon products from catalytic pyrolysis of biomass components. These olefins may be formed through decarbonylation of oxygenated intermediates or formed from alkyl aromatics.[90] Ethylene is the dominant olefin, with C_1- C_4 selectivity from cellulose, hemicellulose and lignin was all around 50%. Propene selectivity was 23.6%, 28.5% and 19.6%, respectively, for the three components. Selectivity for butene from all three components was less than 3%. Alkanes such as methane, ethane and propane were also detected. However, amounts of these alkanes were much lower, compared with olefins. Selectivity of methane from lignin was higher than that from cellulose and hemicellulose. This can be explained by the fact that non-catalytic pyrolysis of lignin produces large amounts of methane, while methane from pyrolysis of cellulose and hemicellulose were negligible. Some of the thermally-derived methane may be released from the reactor to be analyzed by the GC without further aromatization reaction to form large molecules.

Deoxygenation products from catalytic pyrolysis

Aromatic hydrocarbons are produced through a series of acid-catalyzed decarboxylation, decarbonylation, dehydration and oligomerization reactions of oxygenates, while oxygen is removed by the formation of H_2O, CO or CO_2 in this process. [44, 90] To calculate theoretical yield of aromatics, we use glucose and toluene as representative of the biomass reactants and aromatic products, respectively, for catalytic pyrolysis. Assuming that oxygen in glucose is removed as combination of CO_x and H_2O, the overall stoichiometry for the conversions are given by Eqs. 2-4.

$$C_6H_{12}O_6 \rightarrow (2/3)\ C_7H_8 + (4/3)\ CO_2 + (10/3)\ H_2O \quad (2)$$

$$C_6H_{12}O_6 \rightarrow (6/11)\ C_7H_8 + (24/11)\ CO + (42/11)\ H_2O \quad (3)$$

$$C_6H_{12}O_6 \rightarrow (0)\ C_7H_8 + (6)\ C + (6)\ H_2O \quad (4)$$

According to Eq. 2, if oxygen is removed as CO_2 and H_2O, the maximum theoretical carbon yield of toluene is 66.7%. If oxygen is removed in the form of CO and H_2O, as shown in Eq. 3, then the maximum theoretical carbon yield of toluene is 54.5%. If all the oxygen in glucose is removed as H_2O by dehydration (Eq. 4), then no hydrogen is available to produce toluene and only coke is formed. Theoretically, to increase the aromatic yield from the catalytic pyrolysis, oxygen in biomass-derived oxygenates should be removed as a combination of decarbonylation to CO_2 and dehydration to H_2O.

To discuss quantitatively these three deoxygenation pathways during catalytic pyrolysis, deoxygenation product (H_2O, CO and CO_2) distributions from catalytic pyrolysis were calculated (Table 4), using data from Table 1 and 3. Oxygen yield given here was defined as the mole ratio of oxygen in H_2O or CO_x to the oxygen in the feedstock. It should be noted that H_2O data was calculated based on H_2O yield from Patwardhan et al.[50, 51,

101], who conducted non-catalytic pyrolysis experiments on the three biomass components using the same instrument but performed at a lower temperature (500^{o}C). This may give some variation to the dehydration data in this study.

Total thermal oxygen removal efficiencies (CO_x+H_2O) from cellulose, hemicellulose and lignin were 14.8%, 43.7% and 37.8%, respectively, while catalytic deoxygenation efficiencies were 85.2%, 56.3% and 62.2%. This indicates that that thermal decomposition only removed a small portion of oxygen, while most of the oxygen was removed by catalytic deoxygenation during catalytic pyrolysis. Among these deoxygenation pathways, dehydration was the primary one for both thermal decomposition and catalytic conversion during catalytic pyrolysis. The total oxygen yields of H_2O from the three components were 70.7%, 63.9% and 74.0%, respectively.

For thermal deoxygenation, the mechanism of decarboxylation to remove oxygen in biomass as CO_2 is favored, with that of decarbonylation to give CO is less favored. This is in contrast with the deoxygenation pathways during catalytic conversion. As discussed in the last section, decarbonylation to CO is overwhelmed compared with decarboxylation during catalytic transformation. The strong acidity of H-ZSM5 catalyst may explain the difference.

Table 4. Deoxygenation products from catalytic pyrolysis of cellulose, hemicellulose, and lignin (reaction temperatures: 600^{o}C; catalyst-to-biomass ratio: 20).

Sample	Cellulose		Hemicellulose		Lignin	
origin	Thermal	Catalytic	Thermal	Catalytic	Thermal	Catalytic
CO / O %	3.0±0.06	13.4±0.17	4.0±0.16	9.8±0.80	8.72±0.17	8.5±0.43
CO_2 / O %	5.1±0.08	7.8±0.43	14.2 ±0.05	8.0±0.25	6.1±0.08	2.7±0.16
H_2O / O %	6.67[a]	64.1[b]	25.2[a]	38.7[b]	23.0[a]	60.0[b]
Total	14.8	85.2	43.7	56.3	37.8	62.2

[a]Thermal H_2O data calculated based on H_2O yield from pyrolysis of cellulose, hemicellulose and lignin in literature[50, 51, 101]; [b]Catalytic H_2O data calculated from the equation: 100-

thermal H_2O-thermal CO_x-catalytic CO_x, assuming that oxygen was fully removed as H_2O and CO_x.

As illustrated in Eq.2, maximum theoretical yield of aromatics (66.7%) is reached when oxygen is removed by CO_2 and H_2O, oxygen yields of which were 44.4% and 55.56%, respectively. However, experimental results in Table 4 show that oxygen yield of CO_2 and H_2O from catalytic pyrolysis of cellulose were 12.86% and 70.72%, respectively. Meanwhile, a large amount of coke (carbon yield of 30.56%) was formed by dehydration during catalytic pyrolysis of cellulose. Excessive dehydration removed large amounts of hydrogen, which left a deficient hydrogen source for aromatic formation. This suggests the H-ZSM5 zeolite catalyst did not remove the oxygen by the optimal pathway. Further improvements of aromatic yields from catalytic pyrolysis can be made. Catalysts and reactors maybe improved to maximize CO_2 production by increasing the decarboxylation reaction and minimizing dehydration reactions.

Components interactions during catalytic pyrolysis

A study by Jing et al.[116] demonstrated that interaction effects among biomass components during thermal pyrolysis of lignocellulosic biomass was negligible. Assuming there are no interactions between different biomass-derived oxygenates during catalytic conversion over H-ZSM5, theoretical product yields for catalytic pyrolysis of switchgrass were calculated using composition data of switchgrass shown in Table 1 and product yields from individual components shown in Table 2. Calculated results are given in Table 5. Experimental product yields from catalytic pyrolysis of switchgrass are also shown in Table 5 for comparison.

It can be seen that the calculated result is highly consistent with the experimental result. Experimental CO and CO_2 yield were 12.4% and 5.7%, respectively, while the calculated values were 11.5% and 6.3%. Experimental coke yield was 32.9%, which is also consistent with the calculated one (33.3%). Experimental yields of aromatics and C_1-C_4 hydrocarbons also appeared to be the combination of the yields from individual components. This suggests that no significant interaction existed between the thermally derived oxygenates during catalytic transformation. A previous study of oxygenate mixtures with different functional groups on H-ZSM5 also showed that the product distribution only depended on the H/C_{eff} ratio. No interaction effects were found between oxygenates during catalytic conversion.[132]

Table 5. Experimental and calculated product distribution from catalytic pyrolysis of switchgrass (reaction temperatures: 600^{o}C; catalyst-to-biomass ratio: 20).

Product yields / C %	Experimental	Calculated
CO	12.4±0.36	11.5±0.29
CO_2	5.7±0.10	6.3±0.22
Char/coke	32.9±0.00	33.3±0.32
Aromatic hydrocarbons	21.1±0.22	19.9±0.46
C_1-C_4 Hydrocarbons	5.7±0.10	5.2±0.19

Reactions network of catalytic pyrolysis of lignocellulosic biomass

Generally, catalytic pyrolysis goes through a series of pyrolysis reactions followed by catalytic conversion of biomass-derived oxygenates with effect of catalysts. [44] In this study, we quantified the catalytic pyrolysis products distribution and revealed deoxygenation pathways for cellulose, hemicellulose, and lignin. Based on the results and discussion, the

reactions network of catalytic pyrolysis of lignocellulosic biomass is summarized and shown in the Fig.4.

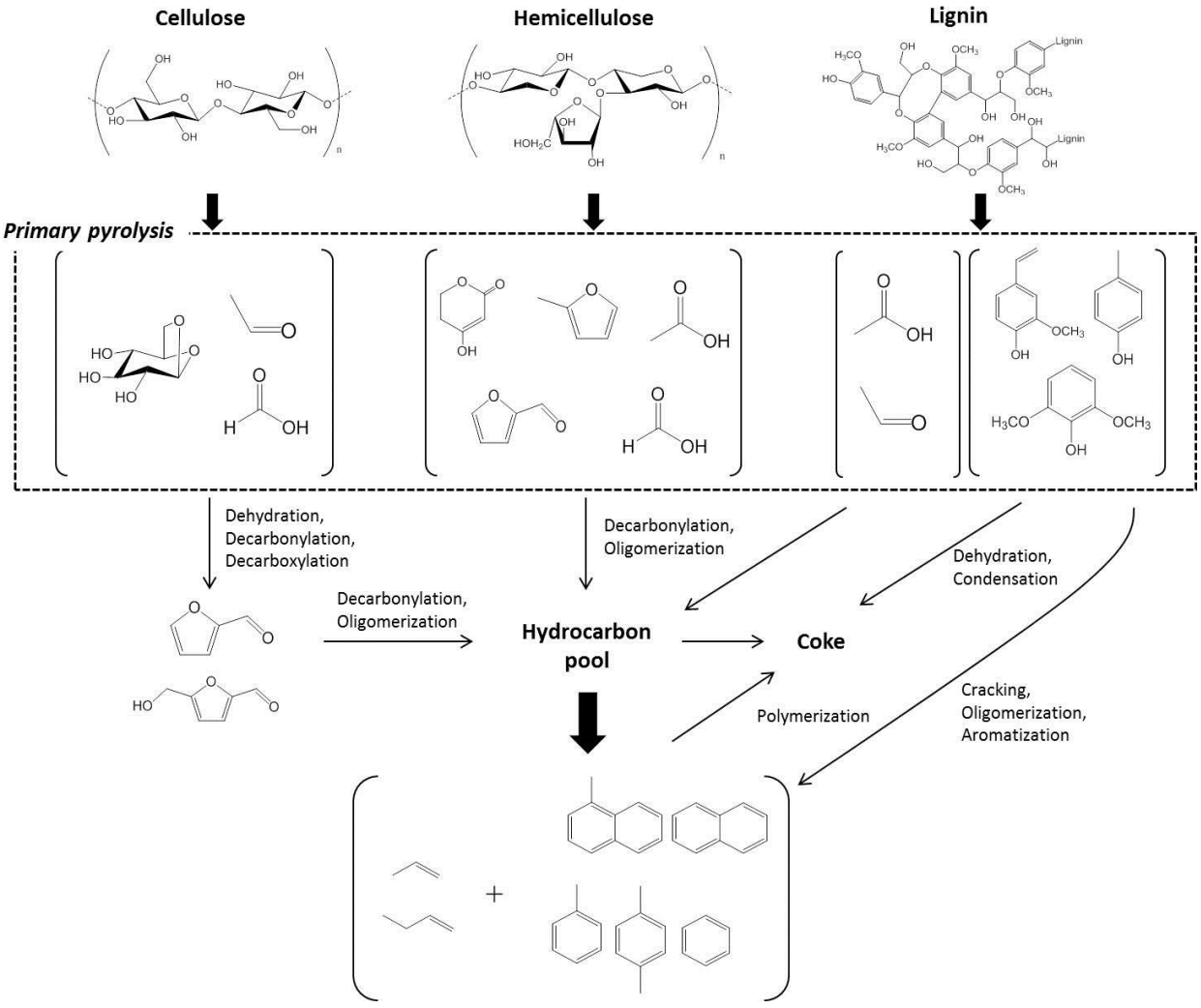

Figure 4. Reaction pathways for catalytic pyrolysis of lignocellulosic biomass with HZSM-5

There are no significant interaction effects between the three components during both thermal pyrolysis and catalytic conversion stages. During catalytic pyrolysis, levoglucosan, the predominant product from pyrolysis of cellulose will undergo dehydration, decarbonylation or decarboxylation reactions to form smaller furanic compounds with effects of catalyst. These furans then undergo a series of acid-catalyzed decarbonylation and

oligomerization reactions inside the pores of zeolite to form aromatics and olefins. Being distinct from pyrolysis of cellulose, the major product from pyrolysis of hemicellulose is double-hydrated xylose, which can diffuse into zeolite pores without further reactions along with other low molecular weight compounds such as formic acid, acetic acid, acetol and furaldehyde. Pyrolysis of lignin primarily generates monomeric phenolic compounds, which have very low reactivity on HZSM-5 catalyst. Predominant acid-dehydration of phenols leads to large amounts of coke formation, while cracking of phenols produce aromatics at times. Olefins produced from cracking of alkyl-phenols maybe another intermediate to production of aromatics.

Conclusion

We have investigated the catalytic fast pyrolysis of cellulose, hemicellulose and lignin over H-ZSM5 catalyst. Characteristics of the three main components in catalytic pyrolysis were distinct from each other. The yield of aromatic hydrocarbons decreased in the following order: cellulose > hemicellulose >> lignin. Higher aromatic yields and lower coke yields were observed at moderately higher temperatures for all three components due to the formation of more low molecular weight oxygenates and higher desorption of coke precursors. Among the three components, lignin has the most complicated structure and phenolic compounds generated from lignin thermal decomposition are prone to coke/char formation, which reduce the carbon conversion efficiency for catalytic pyrolysis of biomass. Dehydration was the primary deoxygenation pathway for catalytic pyrolysis. Meanwhile, the mechanism of decarbonylation to CO is favored, with that of decarboxylation to give CO_2 is less favored. This indicates that dehydrated oxygenates primarily went through

decarbonylation to form reaction intermediates which subsequently be converted into aromatics over zeolite catalyst. CO yield can be seen as an index of aromatic formation for catalytic pyrolysis of biomass. Results from catalytic pyrolysis of switchgrass show that there were no significant interactions between the thermal-derived products. Product distribution from catalytic pyrolysis of lignocellulosic biomass highly depends on its compositions.

Acknowledgements

The authors would like to acknowledge the financial support of the Iowa Energy Center (Grant No.: 10-02). The authors are also grateful to Patrick Johnston of the Center for Sustainable Environmental Technologies for product analysis.

References

[1] G.W. Huber, S. Iborra, A. Corma, Synthesis of transportation fuels from biomass: chemistry, catalysts, and engineering, Chem. Rev., 106 (2006) 4044-4098.

[2] R.C. Brown, Biorenewable Resources: Engineering New Products from Agriculture, Ames,IA, 2003.

[3] T.R. Carlson, G. Tompsett, W. Conner, G. Huber, Aromatic Production from Catalytic Fast Pyrolysis of Biomass-Derived Feedstocks, Topics in Catalysis, 52 (2009) 241-252.

[4] T.R. Carlson, Y.-T. Cheng, J. Jae, G.W. Huber, Production of green aromatics and olefins by catalytic fast pyrolysis of wood sawdust, Energy Environ Sci, 4 (2011) 145-161.

[5] T.R. Carlson, J. Jae, Y.-C. Lin, G.A. Tompsett, G.W. Huber, Catalytic fast pyrolysis of glucose with HZSM-5: The combined homogeneous and heterogeneous reactions, Journal of Catalysis, 270 (2010) 110-124.

[6] H. Zhang, Y.-T. Cheng, T.P. Vispute, R. Xiao, G.W. Huber, Catalytic conversion of biomass-derived feedstocks into olefins and aromatics with ZSM-5: the hydrogen to carbon effective ratio, Energy Environ Sci, 4 (2011) 2297-2307.

[7] A.A. Lappas, K.G. Kalogiannis, E.F. Iliopoulou, K.S. Triantafyllidis, S.D. Stefanidis, Catalytic pyrolysis of biomass for transportation fuels, Wiley Interdisciplinary Reviews: Energy and Environment, 1 (2012) 285-297.

[8] C. Zhou, X. Xia, C. Lin, D. Tong, J. Beltramini, Catalytic conversion of lignocellulosic biomass to fine chemicals and fuels, Chem Soc Rev, 40 (2011) 5588-5617.

[9] J. Jae, G.A. Tompsett, A.J. Foster, K.D. Hammond, S.M. Auerbach, R.F. Lobo, G.W. Huber, Investigation into the shape selectivity of zeolite catalysts for biomass conversion, J Catal, 279 (2011) 257-268.

[10] X. Guo, S. Wang, K. Wang, Q. Liu, Z. Luo, Influence of extractives on mechanism of biomass pyrolysis, Journal of Fuel Chemistry and Technology, 38 (2010) 42-46.

[11] P.R. Patwardhan, R.C. Brown, B.H. Shanks, Product Distribution from the Fast Pyrolysis of Hemicellulose, ChemSusChem, 4 (2011) 636-643.

[12] P.R. Patwardhan, R.C. Brown, B.H. Shanks, Understanding the fast pyrolysis of lignin, ChemSusChem, 4 (2011) 1629-1636.

[13] S. Wang, K. Wang, Q. Liu, Y. Gu, Z. Luo, K. Cen, T. Fransson, Comparison of the pyrolysis behavior of lignins from different tree species, Biotechnol Adv, 27 (2009) 562-567.

[14] P.R. Patwardhan, J.A. Satrio, R.C. Brown, B.H. Shanks, Product distribution from fast pyrolysis of glucose-based carbohydrates, J Anal Appl Pyrol, 86 (2009) 323-330.

[15] H. Yang, R. Yan, H. Chen, D.H. Lee, C. Zheng, Characteristics of hemicellulose, cellulose and lignin pyrolysis, Fuel, 86 (2007) 1781-1788.

[16] N.Y. Chen, T.F. Degnan, L.R. Koenig, LIQUID FUEL FROM CARBOHYDRATES, Chemtech, 16 (1986) 506-511.

[17] D. Fabbri, C. Torri, V. Baravelli, Effect of zeolites and nanopowder metal oxides on the distribution of chiral anhydrosugars evolved from pyrolysis of cellulose: An analytical study, J Anal Appl Pyrol, 80 (2007) 24-29.

[18] X. Guo, S. Wang, Y. Zhou, Z. Luo, Catalytic pyrolysis of xylan-based hemicellulose over zeolites, in: Proceedings of the 6th IASME/WSEAS international conference on Energy, World Scientific and Engineering Academy and Society (WSEAS), Cambridge, UK, 2011, pp. 137-142.

[19] D.J. Mihalcik, C.A. Mullen, A.A. Boateng, Screening acidic zeolites for catalytic fast pyrolysis of biomass and its components, Journal of Analytical and Applied Pyrolysis, 92 (2011) 224-232.

[20] M.-J. Jeon, J.-K. Jeon, D.J. Suh, S.H. Park, Y.J. Sa, S.H. Joo, Y.-K. Park, Catalytic pyrolysis of biomass components over mesoporous catalysts using Py-GC/MS, Catal Today, 204 (2013) 170-178.

[21] R.K. Sharma, N.N. Bakhshi, Catalytic upgrading of pyrolysis oil, Energ Fuel, 7 (1993) 306-314.

[22] M.A. Jackson, D.L. Compton, A.A. Boateng, Screening heterogeneous catalysts for the pyrolysis of lignin, J Anal Appl Pyrol, 85 (2009) 226-230.

[23] Z. Ma, E. Troussard, J.A. van Bokhoven, Controlling the selectivity to chemicals from lignin via catalytic fast pyrolysis, Appl Catal A-Gen, 423–424 (2012) 130-136.

[24] C.A. Mullen, A.A. Boateng, Catalytic pyrolysis-GC/MS of lignin from several sources, Fuel Process Technol, 91 (2010) 1446-1458.

[25] X. Li, L. Su, Y. Wang, Y. Yu, C. Wang, X. Li, Z. Wang, Catalytic fast pyrolysis of Kraft lignin with HZSM-5 zeolite for producing aromatic hydrocarbons, Frontiers of Environmental Science & Engineering, 6 (2012) 295-303.

[26] P.D. Chantal, S. Kaliaguine, J.L. Grandmaison, Reactions of phenolic compounds over HZSM-5, Applied Catalysis, 18 (1985) 133-145.

[27] A. Corma, G.W. Huber, L. Sauvanaud, P. O'Connor, Processing biomass-derived oxygenates in the oil refinery: Catalytic cracking (FCC) reaction pathways and role of catalyst, J Catal, 247 (2007) 307-327.

[28] H. Dao Le, M. Haniff, A. Houle, D. Lamothe, Reactions of Model Compounds of Biomass Pyrolysis Oils over ZSM5 Zeolite Catalysts, in: Pyrolysis Oils from Biomass, American Chemical Society, 1988, pp. 328-341.

[29] J. Zhang, Y.S. Choi, C.G. Yoo, T.H. Kim, R.C. Brown, B.H. Shanks, Cellulose-hemicellulose, cellulose-lignin interactions during fast pyrolysis, Green Chem, (Submitted).

[30] S. Wang, X. Guo, K. Wang, Z. Luo, Influence of the interaction of components on the pyrolysis behavior of biomass, J Anal Appl Pyrol, 91 (2011) 183-189.

[31] K. Wang, S. Wang, X. Guo, Z. Luo, T. Fransson, Comparison of Pyrolysis Characteristics of degreased and synthesized Mongolian Pine, AIP Conference Proceedings, 1251 (2010) 221-224.

[32] Q. Liu, Z. Zhong, S. Wang, Z. Luo, Interactions of biomass components during pyrolysis: A TG-FTIR study, J Anal Appl Pyrol, 90 (2011) 213-218.

[33] K. Wang, R.C. Brown, Catalytic pyrolysis of microalgae for production of aromatics and ammonia, Green Chem, 15 (2013) 675-681.

[34] P.R. Patwardhan, J.A. Satrio, R.C. Brown, B.H. Shanks, Influence of inorganic salts on the primary pyrolysis products of cellulose, Bioresource Technol, 101 (2010) 4646-4655.

[35] A. Björkman, Studies on finely divided wood. Part 1. Extraction of lignin with neutral solvents, Svensk Papperstidning, 59 (1956) 477-485.

[36] A. Sluiter, B. Hames, R. Ruiz, C. Scarlata, J. Sluiter, D. Templeton, D. Crocker, Determination of Structural Carbohydrates and Lignin in Biomass, in, 2011.

[37] M.R. Rover, P.A. Johnston, L.E. Whitmera, R.G. Smith, R.C. Brown, The Effect of Pyrolysis Temperature on Recovery of Bio-Oil as Distinctive Stage Fractions J Anal Appl Pyrol, (Submitted).

[38] A.G. Gayubo, A.T. Aguayo, A. Atutxa, R. Aguado, M. Olazar, J. Bilbao, Transformation of Oxygenate Components of Biomass Pyrolysis Oil on a HZSM-5 Zeolite. II. Aldehydes, Ketones, and Acids, Ind Eng Chem Res, 43 (2004) 2619-2626.

[39] A.G. Gayubo, A.T. Aguayo, A. Atutxa, R. Aguado, J. Bilbao, Transformation of Oxygenate Components of Biomass Pyrolysis Oil on a HZSM-5 Zeolite. I. Alcohols and Phenols, Ind Eng Chem Res, 43 (2004) 2610-2618.

[40] J.D. Adjaye, N.N. Bakhshi, Catalytic conversion of a biomass-derived oil to fuels and chemicals I: Model compound studies and reaction pathways, Biomass Bioenergy, 8 (1995) 131-149.

[41] D.M. Alonso, J.Q. Bond, J.A. Dumesic, Catalytic conversion of biomass to biofuels, Green Chem, 12 (2010) 1493-1513.

[42] M. Bertero, U. Sedran, Upgrading of bio-oils over equilibrium FCC catalysts. Contribution from alcohols, phenols and aromatic ethers, Catal Today, (2013).

[43] P.A. Horne, P.T. Williams, Reaction of oxygenated biomass pyrolysis model compounds over a ZSM-5 catalyst, Renewable Energy, 7 (1996) 131-144.

[44] Y.-T. Cheng, G.W. Huber, Chemistry of Furan Conversion into Aromatics and Olefins over HZSM-5: A Model Biomass Conversion Reaction, ACS Catalysis, 1 (2011) 611-628.

[45] A.J. Foster, J. Jae, Y.-T. Cheng, G.W. Huber, R.F. Lobo, Optimizing the aromatic yield and distribution from catalytic fast pyrolysis of biomass over ZSM-5, Applied Catalysis A: General, 423–424 (2012) 154-161.

[46] J. Fuhse, F. Bandermann, Conversion of organic oxygen compounds and their mixtures on H-ZSM-5, Chem Eng Technol, 10 (1987) 323-329.

CHAPTER 5 CATALYTIC PYROLYSIS OF CORN DRY DISTILLERS GRAINS WITH SOLUBLES TO PRODUCE HYDROCARBONS

A paper submitted to *ACS Sustainable chemistry and Engineering*

Kaige Wang, and Robert C. Brown

Abstract

This paper explores distillers dried grains with solubles (DDGS) from corn ethanol production as a potential feedstock for production of hydrocarbons from catalytic pyrolysis. We found substantially higher yield of aromatics and olefins from DDGS compared with lignocelluosic biomass for pyrolysis over HZSM-5. Experiments on individual components of DDGS showed that protein and lipid account for these enhanced yields. We also found that lipids had a positive synergistic effect with other components in the DDGS, enhancing the yield of aromatics. Product distributions for HZSM-5 catalysts with different SiO_2/Al_2O_3 ratios were evaluated. The highest carbon yields of aromatics and olefins (44.5% and 12.3%, respectively) occurred for a SiO_2/Al_2O_3 ratio of 30 for *in-situ* catalytic pyrolysis at 600^{o}C. *Ex-situ* catalytic pyrolysis using the same HZSM-5 catalyst produced lower overall yields of hydrocarbons, but the relative yields of aromatics and olefins were reversed (17.6% and 24.5% respectively) compared to *in-situ* catalytic pyrolysis.

KEYWORD: catalytic pyrolysis, pyrolysis, DDGS, HZSM-5, green aromatics, green olefins

Introduction

Production of ethanol from corn has become a major industry in the United States over the past decade, during which corn ethanol production increased eight fold between 2000 and 2012. [34, 35, 133] With nearly 14 billion gallons of production in 2012, corn

ethanol in now 10% percent of fuel supply and 25% of all the transportation fuel produced from domestic resources in the United States.[133] The production of corn ethanol utilizes the starch present in corn, leaving behind protein, crude fat and fibers as a by-product, which is called dry distillers grains with solubles (DDGS). For every gallon of ethanol produced, approximately 2.6 kg of DDGS are produced. [7] The US ethanol industry produced 36 million metric tons of DDGS in 2012, which is an increase of nearly 32 million metric tons over the past decade.[7, 34]

Currently, DDGS is primarily used as feed supplement for livestock.[134] As the corn ethanol industry grows, however, the increasing supply of DDGS may saturate or eventually surpass the demand of livestock feed market. The demand for DDGS by the livestock industry may also be constrained by deleterious effects associated with overfeeding DDGS to cattle, including growth depression and undesirable meat quality.[134] Studies have also shown that feeding DDGS to beef cattle results in net increase in greenhouse gas emissions.[11]

Various process technologies have been explored to convert DDGS into value-added bio-products including energy, biofuel or bio-based chemicals.[7] DDGS has relatively high energy content, making it a potential feedstock heat and power production. For example, several researchers have investigated gasification of DDGS. [17-19] They found that the resulting syngas was produced at higher yield with higher heating value than syngas from lignocellulosic biomass. Davies et al. [19] also demonstrated electricity generation by burning the syngas in a steam power cycle. Pyrolysis has also been well explored as a potential route for converting DDGS into biofuels or bio-based materials.[32] Wood et al. [34, 35] showed that yield of bio-oil produced from DDGS was comparable to that from

lignocellulosic biomass. GC/MS analysis indicated that the bio-oil from microwave pyrolysis of DDGS contained both aliphatic and aromatic hydrocarbons.[36] Boateng's group [37, 38] pyrolyzed barley-derived DDGS, pennycress press cake and other proteinaceous biomass in a fluidized bed reactor and reported relatively higher yield of bio-oil with high-energy content compared with bio-oil from lignocellulosic biomass. They also found that bio-oil from high-protein biomass exhibited better thermal stability than bio-oil from low-protein biomass. In spite of these appealing advantages, bio-oil from proteinaceous DDGS contains substantial high content of nitrogen, which can poison catalysts during bio-oil upgrading and produce unacceptable nitrogen oxide emissions during combustion.[34, 36, 42, 43, 135] A means to eliminated nitrogen from bio-oil must be devised if transportation fuels are the final products from DDGS.

Catalytic pyrolysis has been investigated to improve quality of bio-oil and zeolite catalyst has been intensively investigated due to their ability to form gasoline-range hydrocarbons. [44-46, 55] While many catalytic pyrolysis studies have been conducted using lignocellulosic biomass, there are few that have explored catalytic pyrolysis of protein-rich biomass. We have demonstrated that catalytic pyrolysis of microalgal biomass yields pure hydrocarbons while most of the nitrogen in the biomass is rejected as ammonia.[43] A recent study by Liu et al. [136] explored catalytic pyrolysis of DDGS using nickel-based catalyst in a fixed bed reactor. Bio-oil with high-energy content was obtained and hydrogen concentration in the gaseous products reached to 55.6 vol.% using Ni-Pd-γ-Al_2O_3 as a catalyst.

The goal of this research is to explore the potential of catalytic pyrolysis of DDGS using zeolite catalyst. Catalytic pyrolysis of individual components, namely protein, lipid,

and carbohydrates were also performed to investigate to contribution of each component and the interactions among the components. Different methods including adjusting the SiO_2/Al_2O_3 ratio (SAR) of the HZSM-5 catalyst and changing the contacting method of catalyst and biomass were explored to improve the product yield and distribution from catalytic pyrolysis of DDGS.

Experiential

Materials

DDGS samples were obtained from a local corn ethanol plant (Lincolnway Energy LLC, Nevada, IA). Oven-dried DDGS samples were grounded in a ball miller and sieved down to 200 meshes before analysis. Composition of the DDGS sample were determined and summarized in Table 1. The main components of the DDGS samples were carbohydrates, protein and crude fat, contents of which were 37.3 wt.%, 33.5 wt.%, and 11.3 wt.%. The DDGS also contained 10.4 wt.% lignin. The elemental analysis shows that DDGS contained 48.8 wt.% C, 6.63 wt.% H, and 5.36 wt.% N. Protein extracted from maize and palmitic acid purchased from Sigma Aldrich were used as model compounds for protein and lipid in DDGS. Zeolite catalysts were purchased from Zeolyst with SAR of 23, 30, and 80. Zeolite catalysts were calcined under air at 550^{o}C for 5 hours before use.

Table 1. Characterization of DDGS

Feedstock	Elemental analysis / wt.%				Biochemical analysis / wt.%			
	C	H	N	O	Protein	Carbohydrates	lignin	Lignin
DDGS	48.8	6.6	5.4	34.1	37.3	33.5	11.3	10.4

Pyrolysis experiments

Pyrolysis experiment was performed in a Tandem micro-scale reactor system from Frontier Laboratories (Rx-3050 TR). The detailed description of the reactor can be found in a previous study.[137] Except where otherwise indicated, all experiments were *in-situ* catalytic pyrolysis (that is, the zeolite was mixed directly with the catalyst). Catalyst was mixed with DDGS samples in a ratio of 20:1 for these tests. Although no catalysts were used in the quartz tube of the second furnace of the tandem system, the temperature of the interface and second reactor were maintained at 350^{o}C to prevent condensation of pyrolysis products. For *ex-situ* catalytic pyrolysis, approximately 0.5mg biomass sample was pyrolyzed in the first reactor and the pyrolysis vapors transported to the second reactor, which contained 10 mg of catalyst particles. These were obtained by pelletizing the zeolite power and sieving to 50-70 mesh. Pyrolysis products were identified by GC/MS and quantified by GC/FID/TCD. Final product distribution was reported as molar carbon yield, defined as the molar ratio of carbon in a specific product to the carbon in the feedstock. All measurements were performed at least in duplicate to check the reproducibility of the data. Average data were reported with standard derivation.

Results and discussion

Effect of reaction temperature for catalytic pyrolysis of DDGS

Temperatures of 400^{o}C, 500^{o}C, 600^{o}C, and 700^{o}C were tested to investigate the influence of reaction temperature on product distributions for catalytic pyrolysis of DDGS. HZSM-5 catalyst with SAR of 23 was used for this series of experiments. Carbon yields of

aromatic, gaseous products and carbonaceous residues under these reaction temperatures are compared in Fig.1.

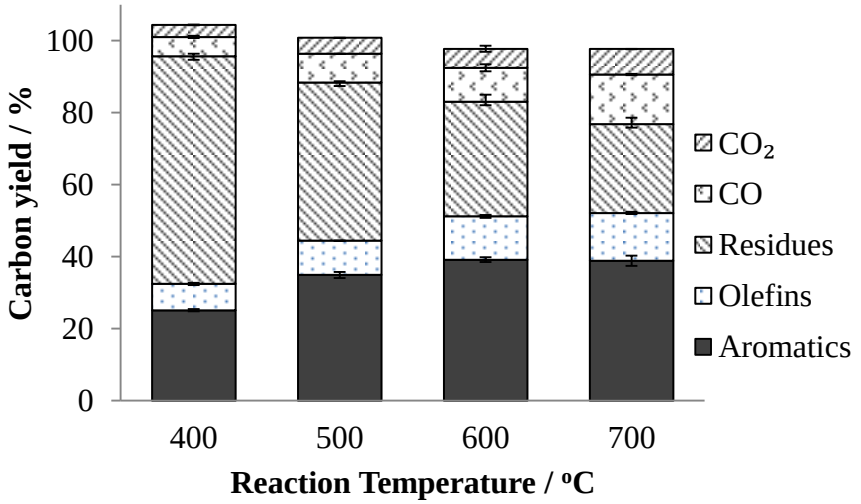

Figure 1. Product distribution from catalytic pyrolysis of DDGS using HZSM-5 under different reaction temperatures (*in-situ* catalysis; SiO_2/Al_2O_3 ratio = 23; catalyst to biomass ratio = 20).

Aromatics and olefins were the two major hydrocarbon products from catalytic pyrolysis of DDGS. For the reaction conditions used, aromatic hydrocarbons prevailed over olefins. Aromatic yield was 25.1% at 400^{o}C, increasing to 38.8% at 700^{o}C. Olefin yield increased from 7.3% to 13.2% as temperature increased from 400^{o}C to 700^{o}C. However, no further significant changes occurred above 600^{o}C. At 600^{o}C, yield of olefins and aromatics were 39.2% and 12.1%, respectively. Increasing reaction temperature increased yields of both hydrocarbon products, which may be due to faster approach to thermodynamic equilibrium as a result of higher diffusion rates with increasing temperature.[138] Compared to lignocellulosic biomass, DDGS produced substantially higher yield of aromatics and olefins. With identical reaction conditions, yield of aromatics and olefins from switchgrass at 600^{o}C were only 21.1% and 5.7%, respectively.[139] Much of the difference in hydrocarbon yields for these two feedstocks is due to the much larger fraction of lignin in the

lignocellulosic feedstock, which primarily produces solid carbonaceous residues, including char and coke, during catalytic pyrolysis.[139] The relatively low lignin content and higher content of fat and protein in the DDGS is expected to produce higher yields of aromatics and olefins. As subsequently described, catalytic pyrolysis of individual components found in DDGS confirm this hypothesis.

High temperature also enhanced decarbonylation and decarboxylation of biomass components to form CO and CO_2, the yields of which doubled in increasing temperature from 400^{o}C to 700^{o}C. Carbonaceous residues decreased dramatically over this same temperature range. Alkanes such as methane, ethane and propane were also detected although the yields were very low.

Catalytic pyrolysis of individual components

The major components of DDGS are protein, lipid, and carbohydrates, while those for lignocellulosic biomass are cellulose, hemicellulose, and lignin. Structures of these components are shown in Table 2. H/C_{eff} ratios of these feedstocks are also listed in Table 2. In a previous study we showed that product distributions from catalytic pyrolysis of lignocellulosic biomass depends on the composition of the biomass.[139] Previous studies suggest that, with the exception of lignin, feedstocks with higher H/C_{eff} ratios will produce higher yields of hydrocarbons. Thus, DDGS with its high contents of lipid and and protein, should yield relatively more hydrocarbons during catalytic pyrolysis.

To investigate the contribution of protein and lipid to hydrocarbon yields from DDGS, *in-situ* catalytic pyrolysis was performed on corn protein and palmitic acid as model compounds. Product distributions and aromatic selectivity are summarized in Fig. 2 and Fig.

3, respectively, along with results obtained in a previous study for cellulose, hemicellulose, and lignin pyrolyzed under identical reaction conditions [139].

As shown in Fig. 2, yields of aromatics and olefins from catalytic pyrolysis of palimitc acid were 38.2% and 28.9%, respectively. High yields of olefin and aromatic products obtained from palmitic acids in this study are in accordance with previous studies. [97, 140, 141] Compared with other components of biomass, triglyceride or fatty acid in biomass has much less oxygen content and more effective hydrogen content available to form hydrocarbon fuel over zeolite catalyst. Among all the components, catalytic pyrolysis of palmitic acid produced the lowest carbonaceous residues yield, which was less than 10%.

Catalytic pyrolysis of protein produced a very high carbon yield of olefin: 12.4% compared with 4.5%, 8.3%, and 5.2% for pyrolysis of cellulose, hemicellulose, and lignin, respectively. The difference can be explained by the unique composition of proteins compared to the other components. Proteins are macromolecules composed of various amino acids. Pyrolysis of some aliphatic protein amino acids, such as valine and isoleucine, generate substantial amounts of olefins.[142-144] In this study, we also performed non-catalytic pyrolysis of those individual components at 600^{o}C. Carbon yield of olefins from non-catalytic pyrolysis of corn protein was 3.4%. In comparison, olefin yields from non-catalytic pyrolysis of cellulose, hemicellulose, and lignin were 0.34%, 0.45%, and 0.24%, respectively, under identical reaction conditions. The large amounts of thermally-derived olefins from corn protein may also contribute to the total olefins from catalytic pyrolysis. Moreover, compared to the components of lignocellulose, corn protein and amino acids have relatively high H/C_{eff} ratio, which is an index of the relative abundance of hydrogen in feedstocks.[131, 145, 146] The H/C_{eff} ratio for corn protein and its major amino acids,

leucine and valine, are 0.23, 1.17, and 0.80, respectively, while it is zero for both cellulose and xylan. The high H/C_{eff} ratio for corn protein and its amino acids may also account for the high yields of aromatics and olefins.

Table 2. Structures of individual components of biomass

Components	H/C_{eff}[a]	Structure
Cellulose	0	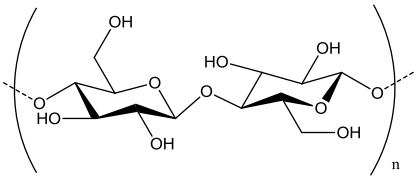
Xylan	0	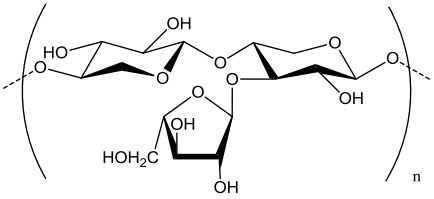
Lignin	0.3	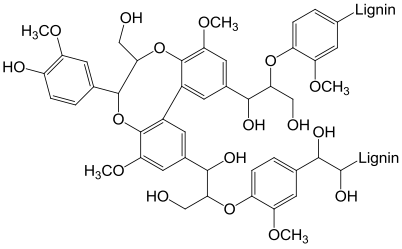
Corn protein	0.23	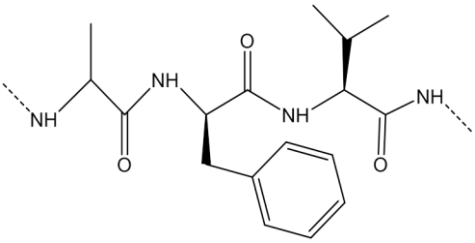
Palmitic acid	1.75	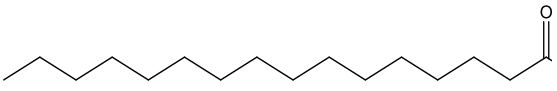

[a] $H/C_{eff} = (H-2O-3N-2S)/C$

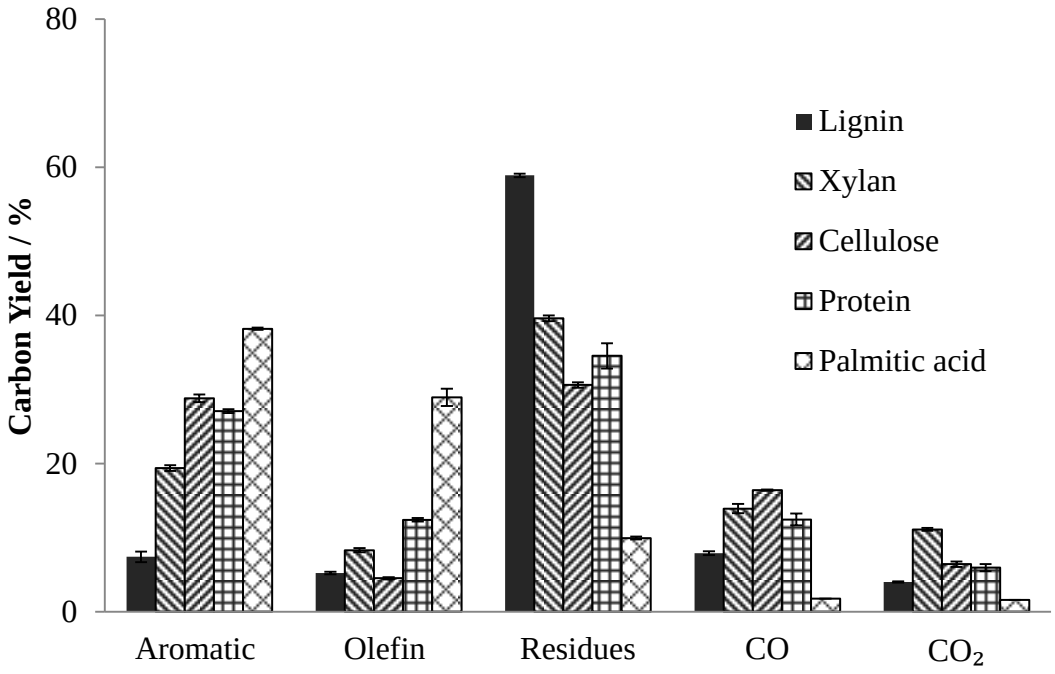

Figure 2. Product distributions for catalytic pyrolysis of individual components using HZSM-5 catalyst (*in-situ* catalysis; reaction temperature: 600^{o}C; SiO_2/Al_2O_3 ratio = 23; catalyst to biomass ratio = 20).

The yield of aromatics from catalytic pyrolysis of protein was 27.1%, which was comparable to the yield from cellulose. The high yield of aromatics from protein can also be explained by the structure of protein as previously described. In addition, corn protein contains large amounts of aromatic amino acids, from which non-catalytic pyrolysis can produce substantial amounts of toluene, styrene, and other aromatic hydrocarbons.[7, 144] These thermally derived aromatic hydrocarbons may also contribute to the aromatics from catalytic pyrolysis of protein.

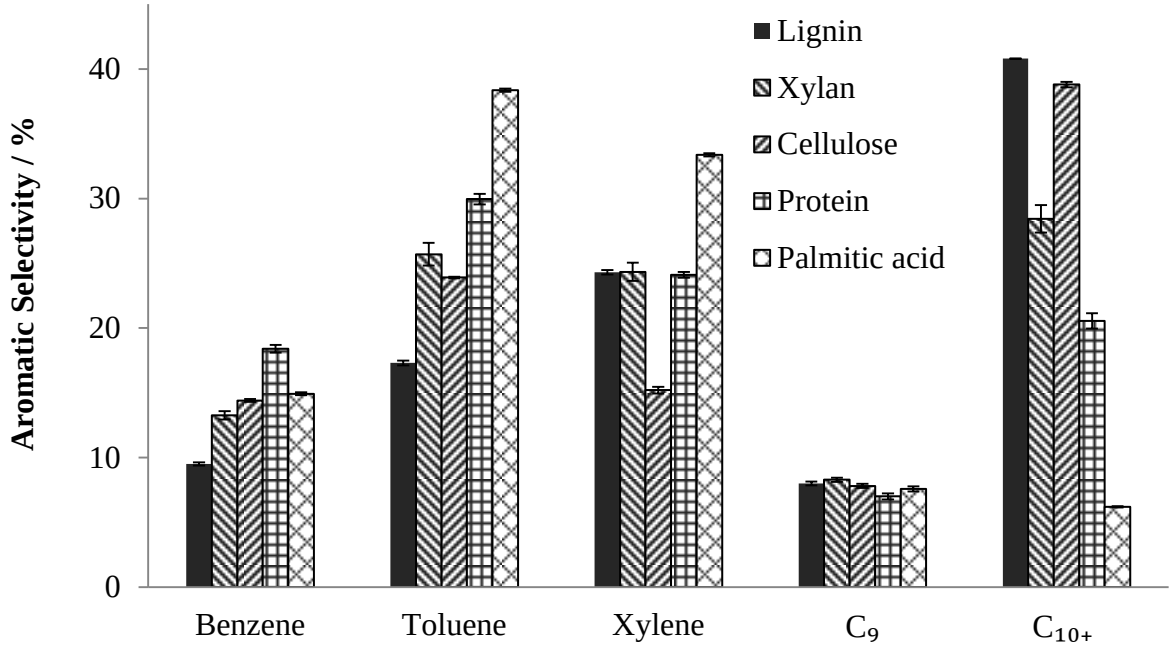

Figure 3. Aromatic selectivity for catalytic pyrolysis of individual components using HZSM-5 (*in-situ* catalysis; reaction temperatures: 600 °C; SiO_2/Al_2O_3 ratio = 23; catalyst to biomass ratio= 20; C_9 includes indanes, indenes, and alkylbenzene; C_{10+} includes naphthalenes and higher polyaromatics).

As indicated in Fig. 3, the distribution of aromatic hydrocarbons from catalytic pyrolysis of individual components also varied dramatically. DDGS components, especially lipid, showed the highest selectivity toward lower molecular weight aromatic products such as benzene, toluene, and xylene (BTX). The total selectivity for BTX was 72.5% and 86.7% for corn protein and palmitic acid, respectively, while that for cellulose, hemicellulose, and lignin was 53.5%, 63.2%, and 51.1%, respectively. In contrast, lignocellulosic components, especially lignin, were more selective toward larger aromatic compounds including naphthalenes and higher polyaromatic hydrocarbons. The selectivity difference may also be explained by the higher H/C_{eff} ratio for protein and lipid.

Synergetic effect among components during catalytic pyrolysis

Previous studies on catalytic pyrolysis indicate that a positive synergetic effect occurred when co-feeding biomass and plastics.[54, 147, 148] Presence of hydrogen-rich plastics enhanced the yield of aromatics, which may be attributed to the interactions of abundant olefins produced from plastics and biomass-derived oxygen compounds over zeolite catalyst.[147] Synergistic yield benefits were also obtained from catalytic pyrolysis when biomass was co-processed with alcohol of high H/C_{eff} ratio. [52, 149] Since plastics and fatty acids both contain long chain hydrocarbons and higher H/C_{eff} ratios, lipid compounds in DDGS might also have a positive synergetic effect on catalytic pyrolysis. To test this hypothesis, the observed carbon yields of gaseous products and aromatic hydrocarbons from DDGS were compared with calculated yields obtained from the weighted sum of yields for the individual components of DDGS, which assumes no interactions between lipid and other components during catalytic pyrolysis

As shown in Fig. 4 (a), the observed yield of aromatic hydrocarbons from DDGS was 52.1% higher than the calculated yield. The enhanced aromatic yield indicates a prominent synergistic effect among the components of DDGS. Observed yields of benzene, toluene, and xylene from DDGS were 36-65% higher than the calculated yields. The observed yield of C10+ aromatics was only 10.9% higher than the predicted yield, suggesting that the synergistic effect among components favors light aromatics (BTX). These results are

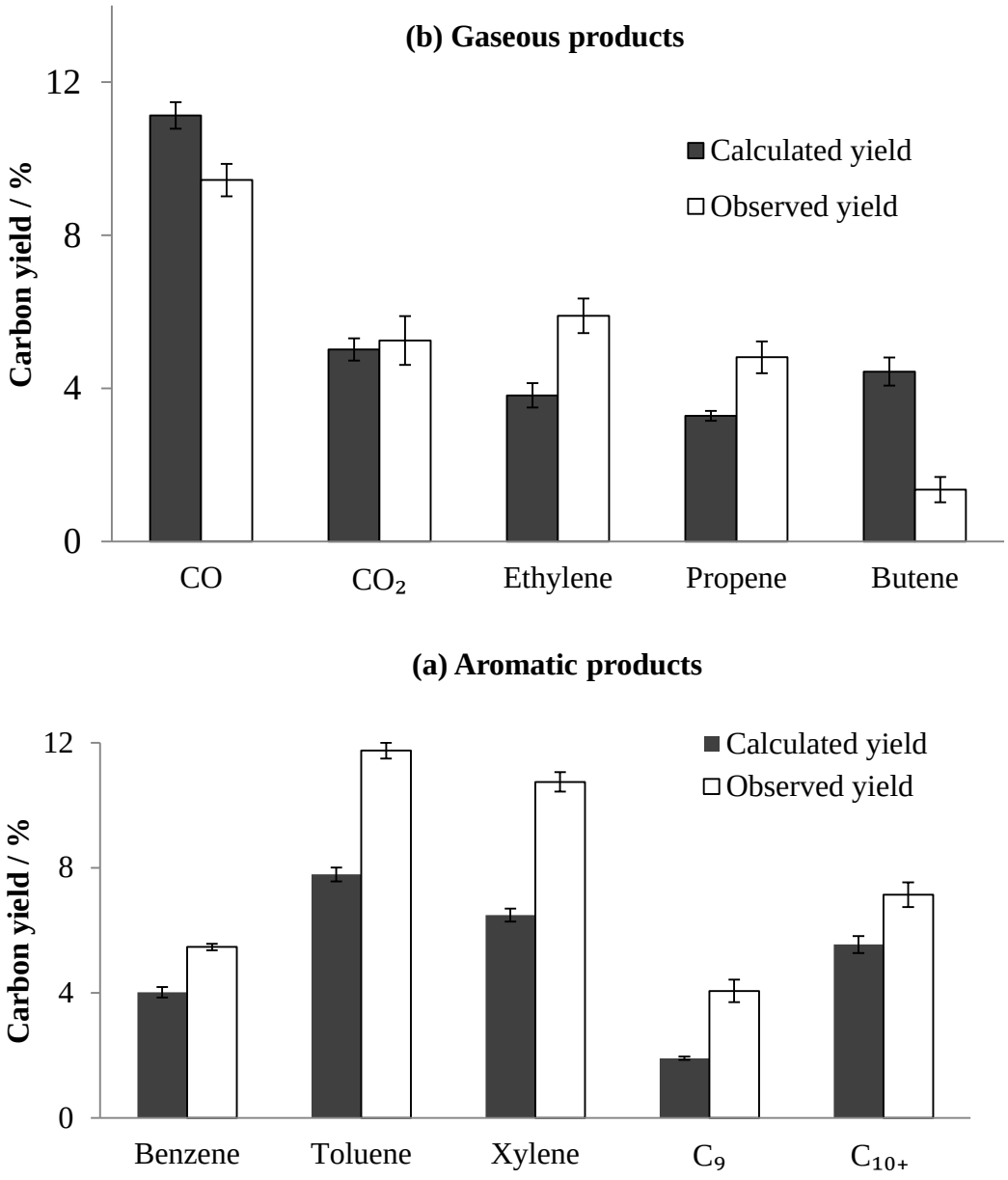

Figure 4. Comparison of observed and calculated yields of (a) aromatic hydrocarbons and (b) gaseous products from catalytic pyrolysis of DDGS using HZSM-5 (*in-situ* catalysis; reaction temperatures: 600 °C; SiO_2/Al_2O_3 ratio = 23; catalyst to biomass ratio = 20; C_9 includes indanes, indenes, and alkylbenzene; C_{10+} includes naphthalenes and higher polyaromatics; calculated yields assume no interactions among components of DDGS).

consistent with the recent study by Li et al. and Dorado et al. [54, 147] who have shown that co-feeding polyethylene (PE) with lignocellulosic biomass improved aromatic production

from catalytic pyrolysis. A recent study showed that co-feeding hydrogen-rich propylene or higher olefins with furanic compounds over HZSM-5 increased the rate of toluene and xylene production through Diels-Alder reactions.[145] The abundant olefins produced from lipids in DDGS are expected to account for much of the enhanced selectivity toward toluene and xylene.

As shown in Fig. 4 (b), observed and calculated yields of CO were 9.4% and 11.1% respectively. The slight decrease is expected because lipid-derived olefins increase the rate of Diels-Alder reactions, thus shifting deoxygenation from carbon monoxide-producing decarbonylation reactions to water-producing dehydration reactions.[145] Only a small difference between observed and calculated CO_2 yield was found. Observed yield of total olefins from DDGS was 12.1%, which was similar with the calculated yield 11.5%. However, the olefins yield varied between the observed and calculated values. Observed yields of ethylene and propene were higher than the calculated yields while the observed yield of butene was lower than the calculated yield.

Effect of SiO_2/Al_2O_3 ratio of zeolite

Changing the SiO_2/Al_2O_3 ratio (SAR) of zeolite catalyst will impact the strength of acid sites as well as the density of Brønsted acid sites. An optimum SAR of zeolite catalyst may exist for catalytic pyrolysis. Experiments were conducted using HZSM-5 with three different SAR (i.e. 23, 30, and 80) to study its effect on catalytic pyrolysis of DDGS. The product distributions for the products of the three samples are summarized in Fig. 5.

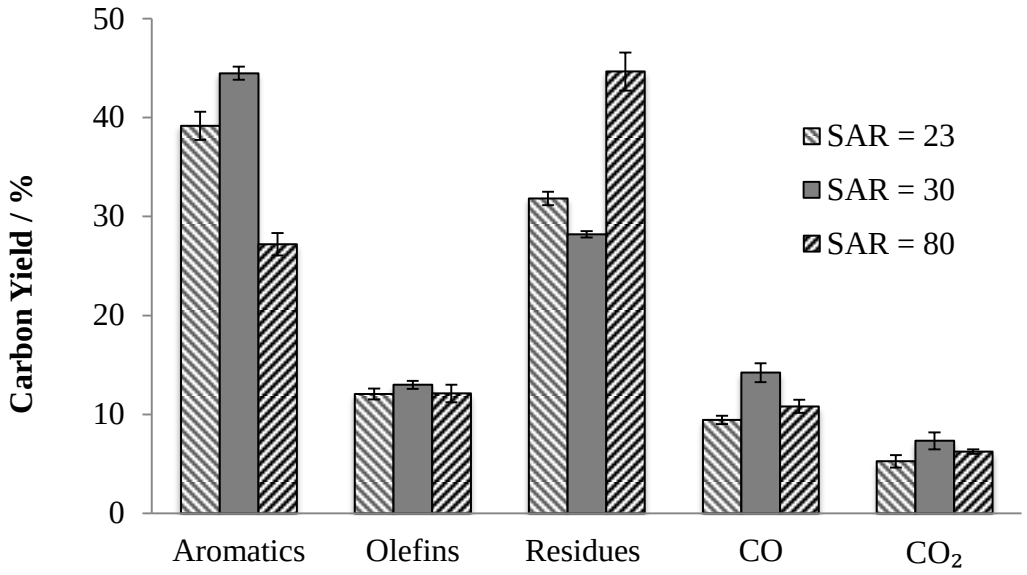

Figure 5. Product distribution from catalytic pyrolysis of DDGS using HZSM-5 with varying SAR (*in-situ* catalysis; reaction temperatures: 600 °C; catalyst to biomass ratio = 20).

The maximum yield of aromatics occurred at SAR of 30, while no significant changes were observed for the yield of olefins for different SARs. The lowest yield of residues was also obtained for SAR of 30. A previous study of catalytic pyrolysis of glucose over HZSM-5 also showed that SAR of 30 produced the highest aromatic yield.[131] With increasing SAR, the density of Brønsted acid sites in the HZSM-5 crystal decreases, whereas the strength of the individual acid sites will increase. A methanol-to-olefins study showed that increased Brønsted acid site density facilitates the formation of larger coke species and enhances their rate of formation.[138] The incorporation of excessive Brønsted acid sites may promote secondary reactions responsible for converting aromatic species to coke within the microspores of zeolite. SAR of 30 may represents an optimal Brønsted acidity, providing maximum availability of acid site and simultaneously minimizing coke formation. The amount of CO produced is at maximum for the sample of SAR of 30. This agrees with our

previous study of catalytic pyrolysis in which the formation of aromatic and olefins correlated with the formation of CO by decarbonylation.[139]

Comparison of in-situ and ex-situ catalytic pyrolysis

Depending upon the method of contacting catalyst and pyrolysis vapors, catalytic pyrolysis is classified as either *in-situ* or *ex-situ*. In a previous study on catalytic pyrolysis of lignocellulosic biomass we showed that *ex-situ* catalytic pyrolysis has the potential to produce predominantely olefins while *in-situ* catalytic pyrolysis produces predominately aromatics.[137] A comparison of *in-situ* and *ex-situ* catalytic pyrolysis of DDGS as feedstock is shown in Table 3 using HZSM-5 with SiO_2/Al_2O_3 ratio of 30.

As shown in Table 3, the yield of aromatics by the *in-situ* method was 44.5%, which was much higher than the17.6% yield using *ex-situ* catalytic pyrolysis. In comparison, the yield of olefins by the *ex-situ* method was 24.5%, which was substantially higher than for the *in-situ* method. Distribution of aromatic hydrocarbons showed differences between the *in-situ* and *ex-situ* methods. Selectivities of benzene and toluene for the *ex-situ* method were 20.6% and 38.2%, respectively, compared with 13.2% and 28% for the *in-situ* method. The olefin selectivity also varied for these two methods. Ethylene was the predominate olefin product for *in-situ* catalytic pyrolysis while propene was the predominate olefin for the *ex-situ* method. Differences in heat and mass transfer for the two methods may explain the differences in product distributions. [137] The results suggest some flexibility in controlling product yields by changing reactor configurations.

Table 3. Distribution of products for *ex-situ* and *in-situ* catalytic pyrolysis (CP) of DDGS (Pyrolysis temperature: 600°C; HZSM-5 SiO_2/Al_2O_3 ratio = 30; catalyst bed temperature for *ex-situ* method: 600°C; catalyst-to-biomass ratio = 20; total carbonaceous residues is sum of pyrolysis char and catalytic coke; C_9 includes indanes, indenes, and alkylbenzene; C_{10+} includes naphthalenes and higher polyaromatics)

Methods	*In-situ* CP	*Ex-situ* CP
Overall yield /C %		
CO	14.2±0.95	9.05±0.13
CO_2	7.33±0.86	9.74±0.75
Pyrolysis char	n.d.	27.1±0.87
Catalytic coke	n.d.	15.1±1.32
Total Carbonaceous residues	28.2±0.33	42.2±2.19
Aromatic Hydrocarbons	44.5±0.66	17.6±0.39
Olefins	12.3±0.41	24.5±0.65
Carbon atom efficiency	56.8±1.07	42.1±1.04
Total carbon balance	107.2±3.20	103.1±4.11
Aromatic selectivity/%		
Benzene	13.2±0.14	20.6±0.31
Toluene	28±0.62	38.2±0.46
Xylene	30±0.11	16.1±0.18
C_9 aromatics	13.3±0.71	11.3±0.46
C_{10+} aromatics	15.7±0.15	14.1±0.14
Olefin selectivity		
Ethylene	48.1±0.64	36.6±1.28
Propene	39.6±0.82	45.8±0.55
Butene	12.3±0.18	17.6±1.84

Conclusion

This study found that DDGS is an attractive feedstock for producing aromatic and olefin hydrocarbons via catalytic pyrolysis, producing significantly higher yields and selectivity of

desired products compared to lignocellulosic biomass. Both the protein and lipid content of DDGS contribute to this advantage, especially compared to lignin. The observed synergistic effect among the components of DDGS is likely due to the lipid content, which produces significantly higher yields of hydrogen-rich olefins compared to the other components. The optimum SiO_2/Al_2O_3 ratio for the zeolite catalyst for hydrocarbon production appears to be about 30. Olefins have previously been observed to enhance yields of hydrocarbons during co-pyrolysis of biomass and plastics. Both *ex-situ* and *in-situ* catalytic pyrolysis were explored, with the former producing predominately olefins and the latter producing predominately aromatics.

Currently DDGS has a market value of around $270 per metric ton while olefins and aromatics have market values of around $1500 per metric ton. Although the selling price for DDGS is more than twice that for lignocellulosic feedstocks, the hydrocarbon yields from protein and lipid in DDGS is several fold higher than from the lignin in lignocellulose and the olefin yield from the lipid is several fold higher than from even the carbohydrates. Moreover, the price of DDGS has more variability than for petrochemicals such as olefins and aromatics, which makes conversion of DDGS to hydrocarbons potentially attractive to the corn ethanol industry. Whether these trade-offs result in a profitable route to hydrocarbon production from DDGS requires a detailed techno-economic analysis, the subject of a future study.

Acknowledgement

The authors greatly acknowledge financial support from Iowa Energy Center (Grant No.10-02). The authors are also grateful to Lincolnway Energy for providing DDGS sample and Dr. Zhiyou Wen of Iowa State University for performing fatty acid analysis.

Reference

[1] C. Wood, K. Muthukumarappan, K.A. Rosentrater, Pyrolysis of Distillers Grains, in: Agricultural and Biosystems Engineering Presentations and Posters, 2012.

[2] C. Wood, K. Muthukumarappan, K.A. Rosentrater, Optimization of the Pyrolysis of Distillers Dried Grains with Solubles, in: Agricultural and Biosystems Engineering Presentations and Posters, 2013.

[3] R.F. Association, 2013 Ethanol Industry Outlook, in, 2013.

[4] T.M. Lammens, M.C.R. Franssen, E.L. Scott, J.P.M. Sanders, Availability of protein-derived amino acids as feedstock for the production of bio-based chemicals, Biomass and Bioenergy, 44 (2012) 168-181.

[5] R. Song, Lipid peroxidation in corn dried distillers grains with solubles (DDGS) and effects of feeding a highly oxidized DDGS source to swine, in, The University of Minnesota, 2013.

[6] M. Hünerberg, S.M. Little, K.A. Beauchemin, S.M. McGinn, D. O'Connor, E.K. Okine, O.M. Harstad, R. Kröbel, T.A. McAllister, Feeding high concentrations of corn dried distillers' grains decreases methane, but increases nitrous oxide emissions from beef cattle production, Agricultural Systems, (2014).

[7] A. Kumar, K. Eskridge, D.D. Jones, M.A. Hanna, Steam–air fluidized bed gasification of distillers grains: Effects of steam to biomass ratio, equivalence ratio and gasification temperature, Bioresour. Technol., 100 (2009) 2062-2068.

[8] A. Tavasoli, M.G. Ahangari, C. Soni, A.K. Dalai, Production of hydrogen and syngas via gasification of the corn and wheat dry distiller grains (DDGS) in a fixed-bed micro reactor, Fuel Processing Technology, 90 (2009) 472-482.

[9] A. Davies, R. Soheilian, C. Zhuo, Y.A. Levendis, Pyrolytic Conversion of Biomass Residues to Gaseous Fuels for Electricity Generation, Journal of Energy Resources Technology, 136 (2013) 021101-021101.

[10] D. Mohan, C.U. Pittman, P.H. Steele, Pyrolysis of Wood/Biomass for Bio-oil: A Critical Review, Energy & Fuels, 20 (2006) 848-889.

[11] H.W. Lei, S.J. Ren, L. Wang, Q. Bu, J. Julson, J. Holladay, R. Ruan, Microwave pyrolysis of distillers dried grain with solubles (DDGS) for biofuel production, Bioresour. Technol., 102 (2011) 6208-6213.

[12] A.A. Boateng, C.A. Mullen, N.M. Goldberg, Producing Stable Pyrolysis Liquids from the Oil-Seed Presscakes of Mustard Family Plants: Pennycress (Thlaspi arvense L.) and Camelina (Camelina sativa)†, Energy & Fuels, 24 (2010) 6624-6632.

[13] C. Mullen, A. Boateng, Production and Analysis of Fast Pyrolysis Oils from Proteinaceous Biomass, Bioenerg. Res., 4 (2011) 303-311.

[14] C.A. Mullen, A.A. Boateng, K.B. Hicks, N.M. Goldberg, R.A. Moreau, Analysis and Comparison of Bio-Oil Produced by Fast Pyrolysis from Three Barley Biomass/Byproduct Streams, Energy & Fuels, 24 (2010) 699-706.

[15] K. Wang, R.C. Brown, Catalytic pyrolysis of microalgae for production of aromatics and ammonia, Green Chemistry, (2013).

[16] K. Wang, R.C. Brown, S. Homsy, L. Martinez, S.S. Sidhu, Fast pyrolysis of microalgae remnants in a fluidized bed reactor for bio-oil and biochar production, Bioresour. Technol., 127 (2013) 494-499.

[17] T.R. Carlson, J. Jae, Y.-C. Lin, G.A. Tompsett, G.W. Huber, Catalytic fast pyrolysis of glucose with HZSM-5: The combined homogeneous and heterogeneous reactions, Journal of Catalysis, 270 (2010) 110-124.

[18] T.R. Carlson, G. Tompsett, W. Conner, G. Huber, Aromatic Production from Catalytic Fast Pyrolysis of Biomass-Derived Feedstocks, Topics in Catalysis, 52 (2009) 241-252.

[19] A.A. Lappas, K.G. Kalogiannis, E.F. Iliopoulou, K.S. Triantafyllidis, S.D. Stefanidis, Catalytic pyrolysis of biomass for transportation fuels, Wiley Interdisciplinary Reviews: Energy and Environment, 1 (2012) 285-297.

[20] D.J. Mihalcik, C.A. Mullen, A.A. Boateng, Screening acidic zeolites for catalytic fast pyrolysis of biomass and its components, Journal of Analytical and Applied Pyrolysis, 92 (2011) 224-232.

[21] W.-w. Liu, X.-p. Wang, C.-w. Hu, D.-m. Tong, L.-f. Zhu, G.-y. Li, Catalytic pyrolysis of distillers dried grain with solubles: An attempt towards obtaining value-added products, International Journal of Hydrogen Energy, 39 (2014) 6371-6383.

[22] K. Wang, P.A. Johnston, R.C. Brown, Comparison of *in-situ* and *ex-situ* catalytic pyrolysis in a micro-reactor system, in, 2014.

[23] D. Mores, J. Kornatowski , U. Olsbye, B.M. Weckhuysen, Coke Formation during the Methanol-to-Olefin Conversion: In Situ Microspectroscopy on Individual H-ZSM-5 Crystals with Different Brønsted Acidity, Chemistry – A European Journal, 17 (2011) 2874-2884.

[24] K. Wang, K.H. Kim, R.C. Brown, Catalytic pyrolysis of individual components of lignocellulosic biomass, Green Chemistry, 16 (2014) 727-735.

[25] T.J. Benson, R. Hernandez, M.G. White, W.T. French, E.E. Alley, W.E. Holmes, B. Thompson, Heterogeneous Cracking of an Unsaturated Fatty Acid and Reaction Intermediates on H+ZSM-5 Catalyst, CLEAN – Soil, Air, Water, 36 (2008) 652-656.

[26] S. Lestari , P. Mäki-Arvela, J. Beltramini, G.Q.M. Lu, D.Y. Murzin, Transforming Triglycerides and Fatty Acids into Biofuels, ChemSusChem, 2 (2009) 1109-1119.

[27] P.B. WEISZ, W.O. HAAG, P.G. RODEWALD, Catalytic Production of High-Grade Fuel (Gasoline) from Biomass Compounds by Shape-Selective Catalysis, Science, 206 (1979) 57-58.

[28] P.G. Simmonds, E.E. Medley, M.A. Ratcliff, G.P. Shulman, Thermal decomposition of aliphatic monoaminomonocarboxylic acids, Analytical Chemistry, 44 (1972) 2060-2066.

[29] M.A. Ratcliff, E.E. Medley, P.G. Simmonds, Pyrolysis of amino acids. Mechanistic considerations, The Journal of Organic Chemistry, 39 (1974) 1481-1490.

[30] S. Tsuge, H. Matsubara, High-resolution pyrolysis-gas chromatography of proteins and related materials, Journal of Analytical and Applied Pyrolysis, 8 (1985) 49-64.

[31] Y.-T. Cheng, G.W. Huber, Production of targeted aromatics by using Diels-Alder classes of reactions with furans and olefins over ZSM-5, Green Chemistry, 14 (2012) 3114-3125.

[32] Y.-T. Cheng, J. Jae, J. Shi, W. Fan, G.W. Huber, Production of Renewable Aromatic Compounds by Catalytic Fast Pyrolysis of Lignocellulosic Biomass with Bifunctional Ga/ZSM-5 Catalysts, Angewandte Chemie, 124 (2012) 1416-1419.

[33] A.J. Foster, J. Jae, Y.-T. Cheng, G.W. Huber, R.F. Lobo, Optimizing the aromatic yield and distribution from catalytic fast pyrolysis of biomass over ZSM-5, Applied Catalysis A: General, 423–424 (2012) 154-161.

[34] C. Dorado, C.A. Mullen, A.A. Boateng, H-ZSM5 Catalyzed Co-Pyrolysis of Biomass and Plastics, ACS Sustainable Chemistry & Engineering, 2 (2013) 301-311.

[35] X. Li, H. Zhang, J. Li, L. Su, J. Zuo, S. Komarneni, Y. Wang, Improving the aromatic production in catalytic fast pyrolysis of cellulose by co-feeding low-density polyethylene, Applied Catalysis A: General, 455 (2013) 114-121.

[36] H. Zhang, J. Nie, R. Xiao, B. Jin, C. Dong, G. Xiao, Catalytic co-pyrolysis of biomass and different plastics (PE, PP, PS) to improve hydrocarbon yield in a fluidized bed reactor, Energy & Fuels, (2014).

[37] H. Zhang, T.R. Carlson, R. Xiao, G.W. Huber, Catalytic fast pyrolysis of wood and alcohol mixtures in a fluidized bed reactor, Green Chemistry, 14 (2012) 98-110.

[38] N. Chen, D. Walsh, L. Koenig, Fluidized-bed upgrading of wood pyrolysis liquids and related compounds, in: Pyrolysis Oils from Biomass, American Chemical Society, 1988, pp. 277-289.

CHAPTER 6 COMPARISON OF *IN-SITU* AND *EX-SITU* CATALYTIC PYROLYSIS IN A MICRO-REACTOR SYSTEM

A paper submitted to *RSC Advances*

Kaige Wang, Patrick A. Johnston and Robert C. Brown

Abstract

In this study, we compared *ex-situ* catalytic pyrolysis (CP) and *in-situ* CP of hybrid poplar in a micro-reactor system. When both pyrolysis and catalysis were performed at 700^{o}C, the carbon yield of olefins was greater for *ex-situ* CP than for *in-situ* CP (17.4 % vs. 5.4 %). On the other hand, *in-situ* CP produced more aromatic hydrocarbons than *ex-situ* CP (26.1% vs. 18.9 %). The remarkably high yield of olefins from *ex-situ* CP indicates the potential of exploiting the process to preferentially produce olefins as a primary product from biomass, with aromatics being the secondary products. The carbon yield of carbonaceous residues from *ex-situ* CP was 18.6 % compared to 31.3 % for *in-situ* CP. Substantial carbon was deposited as char during *ex-situ* CP, which could be easily recovered as by-product, simplifying catalyst regeneration. The effects of catalyst loading, pyrolysis temperature and catalysis temperature on product distributions for *ex-situ* CP were also investigated. Our results showed that catalyst temperature strongly affected product distribution. While high catalyst temperature enhanced both olefin and aromatic production, yield of olefin increased to a greater extent than did aromatics. Neither pyrolysis temperature nor catalyst loadings had significant effect on product distribution for *ex-situ* CP.

Introduction

Fast pyrolysis has emerged as a promising technology for the production of biofuels and biobased products. The resulting bio-oil is a complex mixture of oxygenated compounds, including carboxylic acids, aldehydes, ketones, sugars, furans and phenolic compounds [1-4]. The high oxygen content and instability during storage of bio-oil impedes commercial deployment of pyrolysis technology. Catalytic pyrolysis has emerged as a means for improving the quality of liquid products from pyrolysis [5-10]. Although alkali in biomass can catalytically react with solid biomass [11, 12], most heterogeneous catalysts appear to react with the vapor products released from pyrolyzing biomass [5, 6, 13-16].

Depending upon the method of contacting catalyst and pyrolysis vapors, the process is classified as either *in-situ* or *ex-situ* catalytic pyrolysis. For *in-situ* catalytic pyrolysis (*in-situ* CP), the catalyst is mixed with the biomass to be pyrolyzed. For *ex-situ* catalytic pyrolysis (*ex-situ* CP), biomass is separately pyrolyzed and the resulting vapor products are transported to a catalytst bed downstream of the pyrolyzer. Catalytic pyrolysis can be performed in the presence of transition metal or precious metal catalysts and gaseous hydrogen to promote hydrodeoxygenation, in which case the process is referred to as hydropyrolysis [9, 10]. Otherwise, zeolite catalysts such as HZSM-5 are used to deoxygenate pyrolysis vapors through decarbonylation, decarboxylation and dehydration to produce aromatics and olefins [6, 13, 14]. Catalytic pyrolysis with zeolites is attractive for several reasons. Zeolites are relatively inexpensive and robust compared to transition metal and precious metal catalysts. They can be readily regenerated to remove deposits of coke. They do not require hydrogen or other reactive agents and can be used at atmospheric pressure. Thus, zeolites are very attractive for both *in-situ* and *ex-situ* catalytic conversion of pyrolysis

vapors into partially or fully deoxygenated molecules suitable as blendstocks for refining to hydrocarbon transportation fuels

In-situ CP using zeolites has been conducted in both continuous and batch reactors. Aho et al. [17] investigated catalytic pyrolysis in a fluidized bed reactor with zeolite catalyst as bed materials. Their result found that HZSM-5 zeolite gave the highest yield of organic fraction in bio-oil compared with other types of zeolites. The organic fraction was not fully deoxygenated and contained aldehydes, acids, ketones, phenols and other oxygenates. More recently, Huber's group reported *in-situ* CP in a fluidized bed reactor using HZSM5 catalyst to produce aromatic hydrocarbons [13, 18, 19]. Carbon yield of aromatic hydrocarbons was 23.2 % when gallium was added to H-ZSM5 and pyrolyzed in continuous fluidized bed reactor [19]. Other researchers have reported partial deoxygenation rather than complete deoxygenation for *in-situ* CP experiments in fluidized bed reactors [8, 17, 20, 21] . Zhang et al. [20] performed catalytic pyrolysis of corncobs in a fluidized bed reactor in the presence of HZSM-5 zeolite and found the oxygen content of the bio-oil to decrease. Recently, Py-GC/MS, which closely couples an analytical pyrolyzer to a GC/MS, has been widely used to investigate catalytic pyrolysis because it makes possible rapid on-line characterization of pyrolysis products. Extensive studies of *in-situ* CP have been conducted on this type of microgram-scale reactor to explore the complex reaction mechanism of CP [5, 6, 15, 16, 22].

Although Py-GC/MS is a powerful analytical tool for non-catalytic and *in-situ* CP research, it does not lend itself to studies of *ex-situ* CP because of the absence of second furnace to contain the catalyst bed. *Ex-situ* CP in the past was mostly conducted using bench-scale continuous reactors. Diebold and Scahill [23] reported 10 wt.% yield of gasoline range hydrocarbons using a pilot plant vortex reactor followed by a fixed-bed catalytic cracker.

French and Czernik [24] screened metal-modified zeolite catalysts for catalytic pyrolysis in a system consisting of a tubular pyrolysis reactor and a fixed catalyst bed. Hydrocarbon yield of 16 wt. % was achieved using nickel-substituted HZSM-5. Adam et al. [25] examined several mesoporous catalysts in a lab-scale fixed bed reactor with similar arrangements of pyrolyzer and catalyst bed as. Increased yields of hydrocarbon and phenol in the organic phase were reported. Williams and Nugranad [21] pyrolyzed rice husks in a fluidized bed reactor with catalytic conversion of pyrolysis vapors in a downstream HZSM-5 catalyst bed. They found aromatic hydrocarbons increased with increasing catalyst temperature, while bio-oil yield markedly decreased.

To date, no direct comparisons between *in-situ* and *ex-situ* CP have been reported. Such comparisons might help understand the reaction mechanisms for catalytic pyrolysis and improve the design of catalytic pyrolysis systems. The present study conducts experiments on both *in-situ* and *ex-situ* CP using a micro-scale reactor system that consists of two reactors in series that are housed in separate furnaces with independent temperature control. For *in-situ* CP, biomass and catalyst were mixed together in the first (pyrolysis) reactor with the second reactor empty. For *ex-situ* experiments, biomass was loaded in the first (pyrolysis) reactor and zeolite catalyst loaded in the second reactor. Product distributions for the two kinds of CP were compared. The effect of pyrolysis temperature, catalysis temperature, and catalyst loading for *ex-situ* CP were investigated to determine their influence on the yield and composition of aromatics, olefins and other non-condensable gases.

Experimental

Materials

Hybrid poplar wood with a particle range of approximately 0.2 to 3 mm was purchased from Wood Residual Solutions (USA). To eliminate interferences by naturally occurring alkali and alkaline earth metals in the biomass, the wood was washed with acid solution using the method described by Patwardhan et al. [11]. The acid-washed poplar sample was ground using a ball mill to obtain particle size below 200 mesh. Cellulose, in the form of microcrystalline powder, was purchased from Sigma Aldrich. Milled wood lignin prepared according to the procedures recommended by Björkman [26] was used in this study. Results for elemental and compositional analyses of the feedstocks are listed in Table 1.

Table 1. Elemental and compositional analyses of feedstocks

Feedstock	Elemental analysis (wt%)				Composition analysis (wt%)		
	C	H	N	O	Cellulose fraction	Hemicellulose fraction	Lignin fraction
Hybrid Poplar	50.0	6.2	0.1	43.0	45.3	18.2	30.0
Cellulose	44.0	6.7	0.0	53.3	100.0	-	-
Lignin	58.3	6.0	0.1	35.6	-	-	100.0

Pyrolysis equipment and analytical instrumentation

A Tandem micro-reactor system (Rx-3050 TR, Frontier Laboratories, Japan) was used for the catalytic pyrolysis experiments. A schematic diagram of the system is shown in Fig.1. It consists of two reactors arranged in tandem, both of which can be independently controlled in the temperature range of 40-900^{o}C. The interface between the furnace and gas chromatograph (GC) can be independently heated to 100-400^{o}C. Helium gas was used as carrier gas to sweep the reaction products into a GC for detailed compositional analysis.

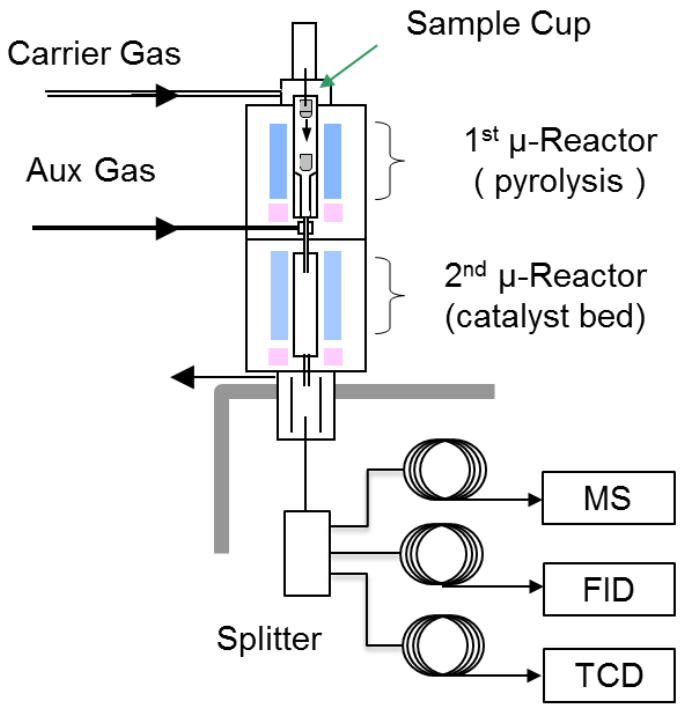

Figure 1. Schematic diagram of Tandem Micro-Reactor system in this study

We chose commercially available HZSM-5 catalyst (CBV2314 with SiO_2/Al_2O_3 ratio of 23, Zeolyst, USA) for this study. The catalyst was calcined at 550 °C (5 °C/min) for 5 hours in a muffle furnace to activate it prior to use. For *ex-situ* CP, approximately 0.5 mg biomass sample was pyrolyzed in the first reactor and the pyrolysis vapors transported to the second reactor containing catalyst particles of 50-70 mesh size, which was prepared by pelletizing and sieving. Quartz wool was used to support the catalyst particles and prevent solids from exiting the catalyst bed. The temperatures of the pyrolysis and catalysis reactors were controlled independently during *ex-situ* CP experiments. The interface temperature was set to 350^{o}C to minimize condensation of products. For *in-situ* CP, catalyst was prepared as described above and directly mixed with biomass particles sized to less than 200 mesh using a catalyst-to-biomass weight ratio of 20. Approximately 5 mg of biomass/catalyst mixture

was pyrolyzed in the first reactor at the desired pyrolysis temperature. The reactor in the second furnace was empty for these *in-situ* catalytic experiments, with the temperature of the second furnace and the interface held at 350^{o}C to prevent product condensation. A microbalance (PX6, Mettler Toledo, Swaziland) with sensitivity of 0.001 mg was used to determine the sample weight in this study.

The products were analyzed by a gas chromatograph (GC) (7890A, Agilent Technologies, USA) installed with a three-way splitter that directed the gas stream to three GC columns,. The GC oven was programmed for a 3-minute hold at 40^{o}C then ramped at 10^{o}C/min to 250^{o}C, after which temperature was held constant for 6 minutes. The injector temperature was 250 °C and the total helium flow passing through the reactor was 90ml/min. Two identical capillary columns, Phenomenex ZB 1701 (60 m × 0.250 mm and 0.250 μm film thickness) were used to separate condensable aromatic hydrocarbons. One 1701 column was connected to a mass spectrometer (MS) (5975C, Agilent Technologies, USA) for compound identification while the other one was connected to a flame ionization detector (FID) for product quantification by calibration with standards. A Porous Layer Open Tubular (PLOT) column (60 m x 0.320 mm) (GS-GasPro, Agilent, USA) connected to a thermal conductivity detector (TCD) was used to measure non-condensable gas (NCG) products (CO, CO_2, CH_4, C_2H_4, C_2H_6, C_3H_6, C_3H_8, and C_4H_8). A standard gas mixture consisting of these NCG compounds in helium (Praxair, USA) was used to calibrate the yield of NCG. Olefins and alkenes $\geq C_5$ were either not detected or negligible in this study.

For *ex-situ* CP, the yield of pyrolysis char generated in the first reactor and catalytic coke deposited on the catalyst in the second reactor were analyzed separately. Carbon in the char product and coke were quantified by combustion analysis using an elemental analyzer

(vario MICRO cube, Elementar, USA). Because the biomass and catalyst were mixed together for *in-situ* CP, distinguishing between pyrolysis-derived char and catalysis-derived coke was not possible. Thus, yields of total carbonaceous residues in the mixture after reaction, quantified by combustion analysis, were determined.

All measurements including aromatics, NCG, and carbonaceous residues, were performed at least in duplicate to verify the reproducibility of the data. Final product distribution was reported as molar carbon yield, defined as the molar ratio of carbon in a specific product to the carbon in the feedstock. Carbon atom efficiency in producing desired products (aromatics and olefins) was calculated as moles of carbon atoms in these products divided by the moles of carbon atoms in the biomass. Selectivity for aromatics in this study was defined as moles of carbon in a specific aromatic hydrocarbon to total moles of carbon in the aromatic products. Selectivity of olefins was similarly defined. The overall carbon balance was performed for each run, which closed at over 90% in most cases. The unaccounted fraction included large molecular weight compounds unidentified by GC and/or unrecovered char/coke deposited on the walls of the reactors.

Results and Discussion

Effect of catalyst loading on ex-situ CP

Because zeolite catalysts can rapidly deactivate due to the build-up of coke on the surface of the catalyst, tests were conducted to determine the appropriate catalyst-to-biomass ratio for *ex-situ* CP experiments without needing to replace catalyst between replicated tests. Catalyst loadings of 10 mg, 20 mg and 40 mg in the second reactor were tested for three replications of *ex-situ* CP, each using 0.5 mg biomass in the first (pyrolysis) reactor. These

represented initial catalyst-to-biomass ratios of 20, 40, and 80, respectively. Such high catalyst loadings were chosen with the intention of substantially deoxygenating the pyrolysis vapors to aromatic compounds and olefins. Reaction temperatures for both reactors were kept at 500^{o}C.

Products distribution from these three catalyst loadings are summarized in Fig.2. It can be seen that no significant differences in product distributions were observed. Carbon yield of aromatics and olefins were around 15% and 8%, respectively, for all catalyst loadings. Yield of CO, CO_2 and carbonaceous residues were consistently measured around 15%, 7%, and 45%, respectively, for all catalyst loadings. Coke formation in the catalyst bed was consistently at the entrance of the bed, indicating substantial capacity to catalytically convert the vapors for three to four successive replications of ex-situ catalysis trials. For subsequent experiments of *ex-situ* CP, catalyst loadings of 10 mg were deemed adequate to obtain reproducible results.

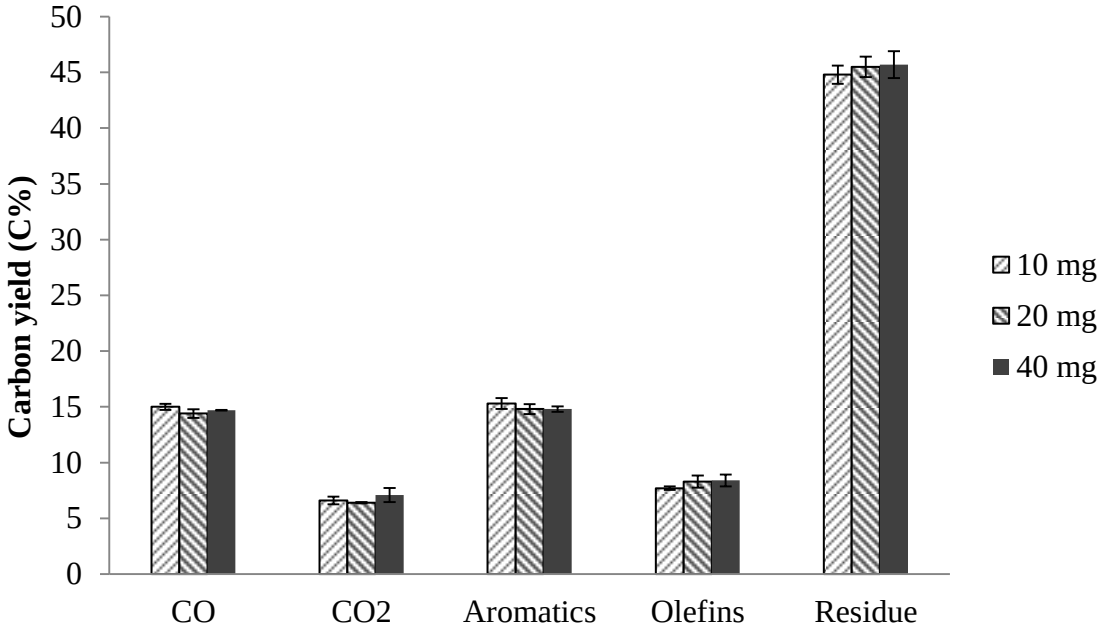

Figure 2. Effect of catalyst loading on distribution of products for *ex-situ* CP of hybrid poplar (biomass loading: 0.5 mg; pyrolysis temperature: 500^{o}C; catalysis temperature: 500^{o}C).

Effect of pyrolysis temperature on ex-situ CP

To investigate the effect of pyrolysis temperature on *ex-situ* CP, catalyst temperature was kept at 500^{o}C while the pyrolysis temperature was varied between 400-700^{o}C. The resulting product distributions are summarized in Table 2.

Table 2. Effect of pyrolysis temperature on distribution of products for *ex-situ* CP of hybrid poplar (catalysis temperature: 500^{o}C; biomass loading: 0.5 mg; catalyst loading: 10mg).

Pyrolysis temperature/^{o}C	400	500	600	700
Overall yield /C %				
CO	13.3±0.06	15.0±0.27	15.5±0.02	19.8±0.10
CO_2	5.90±0.05	6.60±0.35	6.6±0.25	6.90±0.34
Pyrolysis char	26.5±0.40	18.3±0.09	16.4±0.11	11.1±0.29
Catalytic coke	25.8±1.02	26.5±0.73	23.8±0.48	18.8±0.58
Total Carbonaceous residues [a]	52.3±1.42	44.8±0.82	40.2±0.59	29.9±0.87
Aromatic Hydrocarbons	14.1±0.55	15.3±0.50	14.1±0.59	14.6±0.23
Olefins	7.10±0.16	7.70±0.16	8.0±0.30	9.90±0.16
Carbon atom efficiency	21.2±0.71	23.0±0.66	23.6±0.53	24.5±0.39
Total carbon balance	93.7±2.24	89.4±2.10	86.9±1.42	85.4±1.72
Aromatic selectivity/%				
Benzene	12.4±0.63	11.7±0.07	12.4±0.10	12.9±0.22
Toluene	41.6±0.81	33.7±0.37	29.5±0.05	29.2±0.46
Xylene	13.3±0.05	19.2±0.69	21.1±0.70	21.6±0.23
C_9 aromatics [b]	10.7±0.45	9.9±0.71	10.0±0.74	9.70±0.42
C_{10+} aromatics [c]	22.2±1.03	25.8±0.29	27.2±0.19	26.8±0.48
Olefin selectivity				
Ethylene	41.5±0.16	50.5±0.20	52.1±0.92	52.6±0.21
Propene	50.9±0.29	43.7±0.07	41.3±0.36	41.4±0.33
Butene	7.70±0.44	5.90±0.13	6.70±0.56	6.20±0.54

[a]Sum of pyrolysis char and catalytic coke; [b]C_9 aromatics include indanes, indenes, and alkylbenzene; [c] C_{10+} aromatics include naphthalenes and higher polyaromatics ($\leq C_{15}$)

As shown in Table 2, the carbon yield of olefins for *ex-situ* CP changed only slightly as pyrolysis temperature increased from 400^{o}C to 700^{o}C, increasing from 7.1% to 9.9%. Non-catalytic pyrolysis of hybrid poplar at the same four temperatures as shown in Table 2 produced olefin yields of 0.1%, 0.2%, 0.7% and 2.6%. Thus, much of the increase in olefin yields in this temperature range could be ascribed to thermal rather than catalytic effects.

Aromatic yield did not change significantly with increasing pyrolysis temperature. Carbon yields of aromatic hydrocarbons were 14.1%, 15.3%, 14.1% and 14.6% for pyrolysis temperatures of 400^{o}, 500^{o}, 600^{o} and 700^{o}C, respectively. The distribution of aromatic hydrocarbons also remained unchanged at pyrolysis temperatures in the temperature range of 500-700^{o}C.

The reason for the small pyrolysis temperature effect on aromatic yield may be the result of two counteracting processes during CP. Previous studies have shown that increasing pyrolysis temperature favors formation of light oxygenates, which because of their small size are more readily able to enter the pores of zeolite catalyst to form desirable hydrocarbons [12, 27]. On the other hand, increasing pyrolysis temperature is well known to increase the yield of carbon oxides, especially CO as the temperature becomes very high. Non-catalytic pyrolysis of hybrid poplar was performed at temperature of 400^{o}C, 500^{o}C, 600^{o}C and 700^{o}C. Carbon yield of CO at these temperatures was 1.2%, 2.2%, 5.1% and 11.1%, respectively. Carbon yield of CO_2 over the same temperature range was smaller, but still almost doubled from 3.3% at 400^{o}C to 6.1% at 700^{o}C. This large increase in permanent gases as temperature increased would dramatically decrease the concentration of organic vapors, which would be expected to decrease production of hydrocarbons over the zeolite catalyst bed. The simultaneous increase in small organic molecules and non-condensable gases with increasing pyrolysis temperature, however, would mitigate against change in aromatic yield.

As expected, char yield decreased with increasing pyrolysis temperature, which enhanced the decomposition of biomass in the pyrolysis reactor. Carbon yield of pyrolysis char decreased rapidly from 26.5% to 11.1% as the pyrolysis temperature increased from

400°C to 700°C. As shown in Table 2, the amount of coke deposited on the catalyst bed was not significantly influenced by pyrolysis temperature. Yields of catalytic coke were around 24% at pyrolysis temperature over the range of 400°C-600°C. Changes in CO and CO_2 were also insignificant in the pyrolysis temperature range of 400-700°C, with the exception that CO increased from 15.5% to 19.8% as temperature increased from 600°C to 700°C. It is more likely that the increase is ascribed to thermal decomposition in the pyrolysis reactor, as described above.

Effect of catalysis temperature on *ex-situ* CP

To investigate the effect of catalyst temperature, hybrid poplar was pyrolyzed at 500°C, while increasing the catalyst temperature from 400°C to 700°C. Product distributions are summarized in Table 3.

Table 3. Effect of catalyst temperature on product distributions for *ex-situ* CP of hybrid poplar (pyrolysis temperature: 500°C, biomass loading: 0.5 mg; catalyst loading: 10mg).

Catalyst temperature/°C	400	500	600	700
Overall yield /C %				
CO	10.0±0.05	15.0±0.27	16.1±0.08	21.3±0.09
CO_2	5.80±0.27	6.60±0.35	7.30±0.24	8.30±0.50
Pyrolysis char	18.3±0.09	18.3±0.09	18.3±0.09	18.3±0.09
Catalytic coke	37.1±0.33	26.5±0.73	17.9±0.62	13.8±0.48
Total carbonaceous residues [a]	55.4±0.42	44.8±0.82	36.2±0.71	32.1±0.57
Aromatic hydrocarbons	7.10±0.34	15.3±0.50	19.5±0.09	19.4±0.29
Olefins	2.60±0.23	7.70±0.16	13.6±0.24	17.3±1.04
Carbon atom efficiency/%	9.70±0.57	23.0±0.66	33.1±0.33	36.7±1.33
Total carbon balance	80.9±1.31	89.4±2.10	95.2±1.47	103±2.51
Aromatic selectivity/%				
Benzene	5.90±0.18	11.7±0.07	22.1±0.08	36.8±0.57

Table 3 (continued)

Toluene	32.9±1.51	33.7±0.37	37.2±0.29	32.3±0.21
Xylene	20.3±2.84	19.2±0.69	12.7±0.09	8.60±0.01
C_9 aromatics [b]	13.8±1.56	9.90±0.71	8.70±0.1	7.10±0.53
C_{10+} aromatics [c]	27.6±3.24	25.8±0.29	19.6±0.36	15.4±1.29
Olefin selectivity				
Ethylene	28.8±0.56	50.5±0.20	52.8±0.48	56.8±0.44
Propene	58.3±1.17	43.7±0.07	43.1±0.10	38.2±0.79
Butene	13.0±0.61	5.90±0.13	4.30±0.57	5.20±0.36

[a]Sum of pyrolysis char and catalytic coke; [b]C_9 aromatics include indanes, indenes, and alkylbenzene; [c] C_{10+} aromatics include naphthalenes and higher polyaromatics ($\leq C_{15}$)

As shown in Table 3, the yield of CO_2 increased slightly from 5.8% to 8.3% as temperature increased. Yield of CO increased from 10% at 400^{o}C to 21.3% at 700^{o}C. This is in accordance with our previous study of CP, which showed that decarbonylation to CO is favored over decarboxylation to CO_2 for catalytic pyrolysis of biomass.[14] Increasing CO yield correspond to an increase in aromatics and olefins with increasing temperature, which also indicated that catalytic CO generation is mechanistically related to the production aromatics and olefins.[14, 22] Yield of catalyst coke fell from 37.2% to 13.8% as catalyst temperature increased from 400^{o}C to 700^{o}C. Thus, increasing catalyst temperature improves yields of desired products while reducing coke formation.

Catalyst temperature affected yield of both aromatic and olefins. Total yield of which increased from 9.7% to 36.7% in increasing the catalyst temperature from 400^{o}C to 700^{o}C. However, the influence of catalyst temperature was different for the two products. At 400^{o}C, yield of aromatics was 7.1%, which increased to 15.3% at 500^{o}C, but remained relatively constant with further increase in temperature. Selectivity for specific aromatic hydrocarbons varied dramatically with temperature. High temperature favored the formation of small

aromatics especially benzene. Aromatic selectivity for benzene was only 5.9% at 400^{o}C increasing to 36.8% at 700^{o}C. Aromatic selectivity for toluene remained approximately constant at 33%, while selectivity for xylene and higher aromatics decreased significantly. Aromatic selectivity for xylene decreased from 20.3% to 8.6% as temperature increased from 400^{o}C to 700^{o}C. Aromatic selectivity for C_{10+} aromatics decreased from 27.6% to 15.4% over the same temperature range. One possible reason is that higher temperatures favor desorption of products from zeolite before further reaction can form larger aromatics. Additionally, high temperatures enhanced the dealkylation of alkylbenzenes, which may also account for the selectivity toward smaller aromatics especially benzene.[28]

Compared with aromatics, yield of olefins was more highly influenced by catalyst temperature. Yield of olefins at 400^{o}C was only 2.6% but increased almost five-fold to 17.3% as temperature increased to 700^{o}C. Olefin yield increased monotonously from 13.6% to 17.3% as catalyst temperature increased from 600^{o}C to 700^{o}C in contrast to the constancy for aromatic yield. Selectivity of olefins was also affected by catalyst temperature. This temperature behavior is similar to that observed by Cheng and Huber [29] who also saw a shift in selectivity from aromatics to olefins as catalyst temperature increased in a study on furan conversion over HZSM-5. The different yield responses of olefins and aromatics to changes in catalyst temperature suggests different reaction pathways for these two products. Also notable was a shift in olefin selectivity from propene to ethylene as catalyst temperature increased, with ethylene selectivity increasing from 28.8% to 56.8% as temperature increased from 400^{o}C to 700^{o}C.

The theory of indirect hydrocarbon pools in zeolites, originally formulated to explain the methanol to gasoline process via zeolite catalysts, has also found application in

explaining catalytic pyrolysis of biomass [30]. However, previous studies of catalytic pyrolysis focused on production of aromatics, overlooking the significant production of olefins. Recent studies on the hydrocarbon pool mechanism have led to the concept of dual catalytic cycles [31-33], which helps explain the different effect of temperature on aromatics and olefins production observed in the present work. The dual-cycle mechanism is introduced for biomass catalytic pyrolysis and depicted in Fig.3. During pyrolysis biomass is thermally decomposed into vaporous oxygenates including furanic compounds, acids, and phenols. As these biomass-derived oxygenates diffuse into pores of zeolite, two catalytic cycles operate in competition with each other: the olefin cycle involving methylation/cracking of olefins and the aromatics-based cycle involving methylation/dealkylation of polymethylbenzenes. [31, 32, 34]

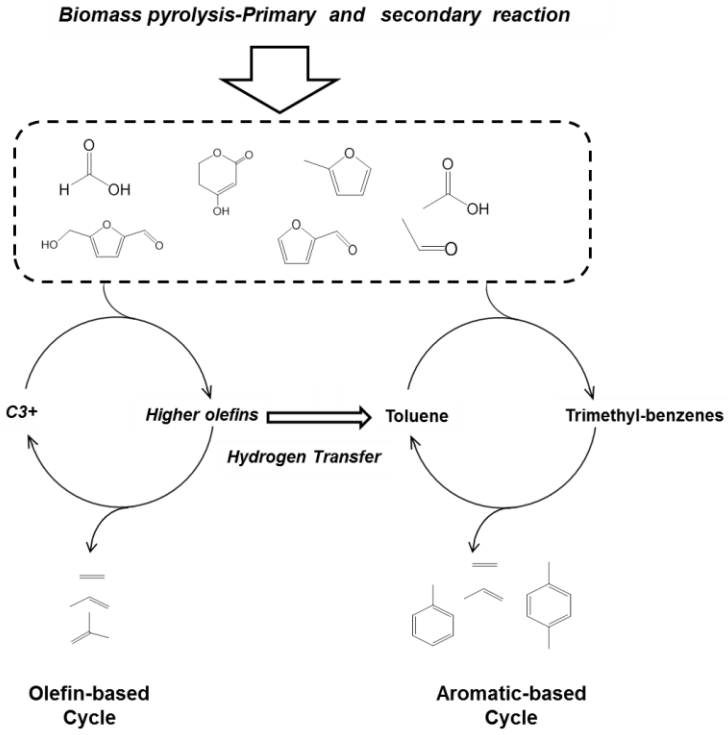

Figure 3. Dual olefin-based and aromatic-based cycles for catalytic pyrolysis of biomass over HZSM-5.

A previous study on methanol to olefin (MTO) reported the activation energy for olefin formation was 93 kJ/mol, while that for hydrogen transfer to aromatics formation was only 9 kJ/mol.[34] Increasing reaction temperature would significantly enhance the rate of olefin formation compared to aromatics. At low temperatures, the aromatic carbon pool would dominate while the olefin carbon pool would dominate at high temperatures. This is consistent with the observations of this study, which found that increasing catalyst temperature had a greater effect on yields of olefins than aromatics.

Notice that both the aromatic-based and olefin-based cycles in the dual cycle mechanism contribute to olefin production, with the aromatic-based cycle more selective for ethylene production. [33, 34] Increasing temperature enhances dealkylation reactions to form ethylene in the aromatic based cycle. Although the olefin-based cycle is less selective for ethylene formation, selectivity for ethylene, which is thermodynamically favored, increased with increasing temperature.[34]

Comparison of ex-situ and in-situ catalytic pyrolysis

To compare *in-situ* and *ex-situ* CP, both kinds of CP were performed in the tandem reactor system. The first (pyrolysis) reactor was held at 700°C for both kinds of CP while the second reactor was held at 700°C when loaded with catalyst for *ex situ* CP and at 350°C when empty for *in situ* CP (to prevent product condensation). Product distributions for both kinds of pyrolysis are summarized in Fig.3. *In-situ* CP generated strikingly more aromatic hydrocarbons than did *ex-situ CP*. At 700^{o}C, carbon yield of aromatics for *in-situ* CP was 26.1% compared to only 18.5% for *ex-situ* CP. In comparison, olefin yield from *ex-situ* CP was as high as 17.4%, which was three times higher than for *in-situ* CP at 700^{o}C. Thus, for *ex-situ* CP olefins are preferentially produced compared to aromatics. *In-situ* and *ex-situ* CP

experiments were also performed with milled wood lignin and cellulose, product distributions from which are summarized in Table S1. It also showed that *ex-situ* CP produced significantly more olefins and less aromatic compounds. A recent study by Carlson et al. [18] on the conversion of furan over HZSM-5 showed that higher yield of aromatics were obtained for *in-situ* catalysis using with a pyroprobe instrument compared to *ex-situ* pyrolysis in a fixed bed reactor.

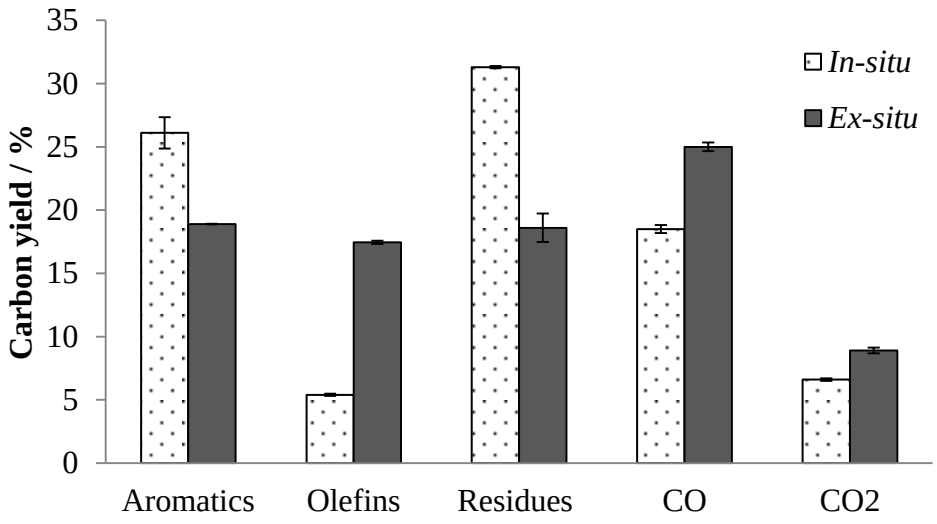

Figure 4. Distribution of products for *ex-situ* and *in-situ* CP of hybrid poplar (Pyrolysis temperature: 700^{o}C; catalyst temperature for *ex-situ CP*: 700^{o}C; catalyst-to biomass ratio = 20; residues: sum of pyrolysis char and catalytic coke)

Since aromatics and olefins are two important products from catalytic pyrolysis, detailed distributions of these two types of products are summarized in Fig 5 (a) and (b). Aromatic selectivity was distinct for these two types of pyrolysis. Selectivity of monocyclic aromatics such as benzene and toluene for *ex-situ* CP was higher than for *in-situ* CP, while *in-situ* CP generated more naphthalenes and higher polyaromatics. At 700^{o}C, aromatic selectivity of benzene and toluene were 34% and 31.9%, respectively, for *ex-situ* CP

compared to 14.3% and 24.4%, respectively, for *in-situ* CP. More rapid desorption of aromatic hydrocarbon products from the acid sites of the zeolite catalyst during *ex-situ* CP might explain the lower yields of polyaromatics compared to *in-situ* CP. Olefins formed from both types of catalytic pyrolysis were predominantly ethylene and propene. Selectivity of propene for *ex-situ* CP was higher than for *in-situ* CP.

Fig. 5 a) Aromatic Selectivity

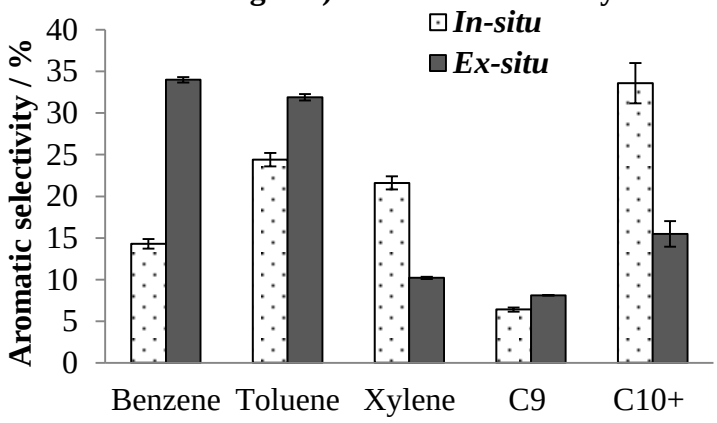

Fig. 5 b) Olefins Selectivity

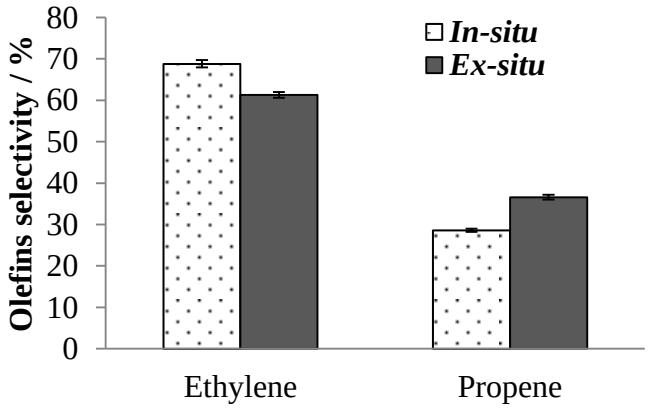

Figure 5 Product selectivity for in-situ and ex-situ CP of hybrid poplar **(a)**: Aromatic selectivity **(b)**: Olefin selectivity (Pyrolysis temperature: 700^{o}C; Catalyst temperature for *ex-situ CP*: 700^{o}C; catalyst-to-biomass ratio = 20; C_9 aromatics include indanes, indenes, and alkylbenzene; C_{10+} aromatics include naphthalenes and higher polyaromatics).

Differences in yields of olefins and aromatics for *in-situ* and *ex-situ* CP are statistically significant. A possible explanation is differences in gas flow for the two arrangements of catalysts. For *in-situ* CP, biomass was directly mixed with the catalyst; thus, the catalyst was exposed to a concentrated stream of pyrolysis vapors. For *ex-situ* CP, the vapors released from the pyrolyzing biomass were mixed with sweep gas before being transported through the catalyst bed; thus, the pyrolysis vapors were diluted and had a shorter contact time with the catalyst compared to *in-situ* CP. Accordingly, *in-situ* CP provided more opportunity for small olefins to oligomerize to larger aromatic compounds at acid sites within the zeolite pores. Moreover, the resulting monocyclic aromatics may more readily methylate and oligomerize to larger aromatics during *in-situ* CP as a result of suppressed mass transfer [33, 34]. Since the aromatic-based cycle is more selective for ethylene production [31, 33], ethylene selectivity for *in-situ* CP would be expected to be higher than for *ex-situ* CP, as observed in this study.

It should be noted that the large mass of catalyst mixed with biomass for *in-situ* CP would substantially slow the heating rate of biomass during pyrolysis, likely suppressing olefin-based cycle, as discussed in section 3.3. In contrast, *ex-situ* CP occurred at constant set-point temperature because the catalyst is preheated in a separate reactor from pyrolysis, favoring olefin formation.

The yield of carbonaceous residues for *ex-situ* CP was 18.6%, which was much lower than the 31.3% observed for *in-situ* CP. For *in-situ* CP, lower mass transfer rates as previously described would enhance coke-forming reactions, which would explain the higher yield of residue. For *ex-situ* CP, large amounts of carbon were deposited as pyrolysis char. At

pyrolysis temperature of 700^{o}C, thermal char yield and catalytic coke yield were 11.1% and 7.5% respectively. This suggests that *ex-situ* CP has the potential to reduce the rate of catalyst regeneration. Furthermore, pyrolysis char can be separated as a by-product, which has potential as carbon sequestration agent and soil amendment. [35]

Conclusions

The effect of catalyst loading, pyrolysis temperature, and catalyst temperature on production of aromatics and olefins for *ex-situ* CP of hybrid poplar were investigated. The results indicate that pyrolysis temperature had negligible effect on catalytic pyrolysis despite the fact that more small oxygenates are formed at high pyrolysis temperature. On the other hand, product distribution highly depended on catalyst temperature. Product selectivity shifted from aromatics to olefins as catalyst temperature increased. A dual catalytic reaction cycle mechanism was introduced to explain these differences. *In-situ* and *ex-situ* CP were compared using identical reaction conditions. The carbon atom efficiency obtained from *ex-situ* CP was 35.9% when both pyrolysis and catalyst temperatures were 700^{o}C. Yields of olefins and aromatics for *ex-situ* CP of hybrid poplar were 17.4% and 18.5%, respectively. In comparison, *in-situ* CP produced significantly more aromatics and less olefins with yields of 26.1% and 5.4%, respectively. Selectivity of monocyclic aromatics such as benzene and toluene for *ex-situ* CP was higher than for *in-situ* CP, while *in-situ* CP generated more naphthalenes and other polyaromatics. Differences yields of aromatics and olefins for *in-situ* and *ex-situ* CP are explained by differences in gas flow and heat transfer for the two kinds of CP. The remarkably high olefin yield from *ex-situ* CP suggests the possibility of exploiting the process to preferentially obtain olefins from biomass.

Acknowledgements

The authors would like to acknowledge the financial support of the Iowa Energy Center (Grant No. 13-01).

References

[1] A.V. Bridgwater, Review of fast pyrolysis of biomass and product upgrading, Biomass and Bioenergy, 38 (2012) 68-94.

[2] R.C. Brown, Biorenewable Resources: Engineering New Products from Agriculture, Ames,IA, 2003.

[3] G.W. Huber, A. Corma, Synergies between Bio- and Oil Refineries for the Production of Fuels from Biomass, Angewandte Chemie International Edition, 46 (2007) 7184-7201.

[4] G.W. Huber, S. Iborra, A. Corma, Synthesis of transportation fuels from biomass: chemistry, catalysts, and engineering, Chemical Reviews, 106 (2006) 4044-4098.

[5] T.R. Carlson, J. Jae, Y.-C. Lin, G.A. Tompsett, G.W. Huber, Catalytic fast pyrolysis of glucose with HZSM-5: The combined homogeneous and heterogeneous reactions, Journal of Catalysis, 270 (2010) 110-124.

[6] T.R. Carlson, G. Tompsett, W. Conner, G. Huber, Aromatic Production from Catalytic Fast Pyrolysis of Biomass-Derived Feedstocks, Topics in Catalysis, 52 (2009) 241-252.

[7] A.A. Lappas, K.G. Kalogiannis, E.F. Iliopoulou, K.S. Triantafyllidis, S.D. Stefanidis, Catalytic pyrolysis of biomass for transportation fuels, Wiley Interdisciplinary Reviews: Energy and Environment, 1 (2012) 285-297.

[8] E.F. Iliopoulou, S. Stefanidis, K. Kalogiannis, A.C. Psarras, A. Delimitis, K.S. Triantafyllidis, A.A. Lappas, Pilot-scale validation of Co-ZSM-5 catalyst performance in the catalytic upgrading of biomass pyrolysis vapours, Green Chemistry, (2013).

[9] T.L. Marker, L.G. Felix, M.B. Linck, M.J. Roberts, Integrated hydropyrolysis and hydroconversion (IH2) for the direct production of gasoline and diesel fuels or blending components from biomass, part 1: Proof of principle testing, Environmental Progress & Sustainable Energy, 31 (2012) 191-199.

[10] V.K. Venkatakrishnan, J.C. Degenstein, A.D. Smeltz, W.N. Delgass, R. Agrawal, F.H. Ribeiro, High-pressure fast-pyrolysis, fast-hydropyrolysis and catalytic hydrodeoxygenation of cellulose: production of liquid fuel from biomass, Green Chemistry, (2013).

[11] P.R. Patwardhan, J.A. Satrio, R.C. Brown, B.H. Shanks, Influence of inorganic salts on the primary pyrolysis products of cellulose, Bioresource Technology, 101 (2010) 4646-4655.

[12] P.R. Patwardhan, R.C. Brown, B.H. Shanks, Product Distribution from the Fast Pyrolysis of Hemicellulose, ChemSusChem, 4 (2011) 636-643.

[13] H. Zhang, T.R. Carlson, R. Xiao, G.W. Huber, Catalytic fast pyrolysis of wood and alcohol mixtures in a fluidized bed reactor, Green Chemistry, 14 (2012) 98-110.

[14] K. Wang, K.H. Kim, R.C. Brown, Catalytic pyrolysis of individual components of lignocellulosic biomass, Green Chemistry, (2013).

[15] K. Wang, R.C. Brown, Catalytic pyrolysis of microalgae for production of aromatics and ammonia, Green Chemistry, 15 (2013) 675-681.

[16] D.J. Mihalcik, C.A. Mullen, A.A. Boateng, Screening acidic zeolites for catalytic fast pyrolysis of biomass and its components, Journal of Analytical and Applied Pyrolysis, 92 (2011) 224-232.

[17] A. Aho, N. Kumar, K. Eränen, T. Salmi, M. Hupa, D.Y. Murzin, Catalytic pyrolysis of woody biomass in a fluidized bed reactor: Influence of the zeolite structure, Fuel, 87 (2008) 2493-2501.

[18] T.R. Carlson, Y.-T. Cheng, J. Jae, G.W. Huber, Production of green aromatics and olefins by catalytic fast pyrolysis of wood sawdust, Energy & Environmental Science, 4 (2011) 145-161.

[19] Y.-T. Cheng, J. Jae, J. Shi, W. Fan, G.W. Huber, Production of Renewable Aromatic Compounds by Catalytic Fast Pyrolysis of Lignocellulosic Biomass with Bifunctional Ga/ZSM-5 Catalysts, Angewandte Chemie, 124 (2012) 1416-1419.

[20] H. Zhang, R. Xiao, H. Huang, G. Xiao, Comparison of non-catalytic and catalytic fast pyrolysis of corncob in a fluidized bed reactor, Bioresource Technology, 100 (2009) 1428-1434.

[21] P.T. Williams, N. Nugranad, Comparison of products from the pyrolysis and catalytic pyrolysis of rice husks, Energy, 25 (2000) 493-513.

[22] A.J. Foster, J. Jae, Y.-T. Cheng, G.W. Huber, R.F. Lobo, Optimizing the aromatic yield and distribution from catalytic fast pyrolysis of biomass over ZSM-5, Applied Catalysis A: General, 423–424 (2012) 154-161.

[23] J. Evans Robert, T. Milne, Molecular-Beam, Mass-Spectrometric Studies of Wood Vapor and Model Compounds over an HZSM?5 Catalyst, in: Pyrolysis Oils from Biomass, American Chemical Society, 1988, pp. 311-327.

[24] R. French, S. Czernik, Catalytic pyrolysis of biomass for biofuels production, Fuel Processing Technology, 91 (2010) 25-32.

[25] J. Adam, E. Antonakou, A. Lappas, M. Stöcker, M.H. Nilsen, A. Bouzga, J.E. Hustad, G. Øye, In situ catalytic upgrading of biomass derived fast pyrolysis vapours in a fixed bed reactor using mesoporous materials, Microporous and Mesoporous Materials, 96 (2006) 93-101.

[26] A. Björkman, Studies on finely divided wood. Part 1. Extraction of lignin with neutral solvents, Svensk Papperstidning, 59 (1956) 477-485.

[27] J. Jae, G.A. Tompsett, A.J. Foster, K.D. Hammond, S.M. Auerbach, R.F. Lobo, G.W. Huber, Investigation into the shape selectivity of zeolite catalysts for biomass conversion, J Catal, 279 (2011) 257-268.

[28] S. Al-Khattaf, Catalytic Transformation of Toluene over a High-Acidity Y-Zeolite Based Catalyst, Energy & Fuels, 20 (2006) 946-954.

[29] Y.-T. Cheng, G.W. Huber, Chemistry of furan conversion into aromatics and olefins over HZSM-5: a model biomass conversion reaction, ACS Catalysis, 1 (2011) 611-628.

[30] I.M. Dahl, S. Kolboe, On the Reaction Mechanism for Hydrocarbon Formation from Methanol over SAPO-34: I. Isotopic Labeling Studies of the Co-Reaction of Ethene and Methanol, Journal of Catalysis, 149 (1994) 458-464.

[31] S. Ilias, A. Bhan, Mechanism of the Catalytic Conversion of Methanol to Hydrocarbons, ACS Catalysis, 3 (2012) 18-31.

[32] M. Bjørgen, S. Svelle, F. Joensen, J. Nerlov, S. Kolboe, F. Bonino, L. Palumbo, S. Bordiga, U. Olsbye, Conversion of methanol to hydrocarbons over zeolite H-ZSM-5: On the origin of the olefinic species, Journal of Catalysis, 249 (2007) 195-207.

[33] S. Ilias, A. Bhan, Tuning the selectivity of methanol-to-hydrocarbons conversion on H-ZSM-5 by co-processing olefin or aromatic compounds, Journal of Catalysis, 290 (2012) 186-192.

[34] X. Sun, Catalytic Conversion of Methanol to Olefins over HZSM-5 Catalysts, in, München, Technische Universität München, Diss., 2013, 2013.

[35] C.E. Brewer, K. Schmidt-Rohr, J.A. Satrio, R.C. Brown, Characterization of biochar from fast pyrolysis and gasification systems, Environmental Progress & Sustainable Energy, 28 (2009) 386-396.

CHAPTER 7 BEYOND ETHANOL: A TECHNO-ECONOMIC ANALYSIS OF AN INTEGRATED CORN BIOREFINERY TO PRODUCE HYDROCARBON FUELS AND CHEMICALS

A manuscript submitted to *Biofuel, Bioproducts and Biorefinery*

Kaige Wang, Longwen Ou, Tristan Brown, Robert C. Brown

Abstract

Dried Distillers grains with solubles (DDGS) are potential feedstocks for the production of hydrocarbon fuels and chemicals from catalytic pyrolysis. This study evaluates the economic feasibility of a 2000-metric-ton-corn-per-day integrated biorefinery with an add-on facility processing corn DDGS to hydrocarbons. In addition to ethanol, a wide range of hydrocarbons, including aromatics, olefins, and synthetic gasoline and diesel, are produced from the integrated facility. The hydrocarbon products command a substantially higher market value than could be realized by selling the pre-processed DDGS: $109 million per year vs. $78 million per year. The add-on DDGS conversion facility contributes an extra $148 million of capital investment compared with the stand-alone corn ethanol production scenario. The operating costs for the integrated scenario are also higher than for the stand-alone scenario, mainly due to the increase in utilities, labor costs, and capital depreciation. The minimum fuel selling price (MFSP) for the integrated scenario is $2.27/gallon, which is comparable to the MFSP of $2.18/gallon for stand-alone scenario. Sensitivity analysis shows that the feedstock cost, hydrocarbon yield, and fixed capital investment have the greatest impacts on the MFSP. Combined with the benefit of products diversity, the proposed integrated corn biorefinery may be competitive with conventional stand-alone ethanol production.

Keywords: catalytic pyrolysis, DDGS, corn ethanol, integrated biorefinery, green aromatics, green olefins

Introduction

Grain ethanol is by far the most widely used biofuel for transportation worldwide and the United States accounts for nearly half of global ethanol production. [1-3] The U.S. corn ethanol production volume increased eight-fold between 2000 and 2012. [1, 4] The production of corn ethanol utilizes only the starch present in the corn, leaving protein, crude fat, and fibers as by-products that are known, when combined, as dried distillers grains and solubles (DDGS). With every gallon of ethanol produced, approximately 2.6 kg of DDGS are produced. [5] Approximately 210 corn ethanol plants operating in the United States produced nearly 15 billion gallons ethanol along with 36 million metric tons of DDGS in 2012. [1]

Currently, DDGS is primarily used as enriched feed for livestock, the price of which considerably improves the economic viability of corn ethanol production.[5, 6] The price of DDGS has exhibited volatility in the past decade, varying in price from $70-$330/ton, which makes the economic feasibility of the corn ethanol industry vulnerable. [1, 7] As the biofuel industry grows, the increasing supply of DDGS may saturate or eventually surpass the demand of the livestock feed market. Moreover, concerns about the negative effects of feeding DDGS to animals may constrain the demand from the livestock industry.[8] All of these factors may have negative influences on the DDGS market price, which could in turn impair the economic performance of corn ethanol production.[6]

To increase the financial profitability of the corn ethanol industry, it is necessary to expand the application and improve the value of DDGS. Various process routes have been

explored to convert DDGS into value-added by-products, including energy, biofuel, or bio-based chemicals.[5, 9, 10] DDGS has inherently high energy content, making it suitable for gasification for syngas production. The potential of DDGS as a feedstock for gasification was explored by various researchers.[9, 11] However, the cost of the fuel generated from this gasification pathway was predicted to be two times the price of conventional gasoline due to high capital costs.[12, 13] Pyrolysis has also been explored to convert DDGS to bio-oil, which may then be upgraded into transportation biofuel.[14-16] Although the bio-oil from DDGS exhibited some advantages compared with bio-oil from lignocellulosic biomass, the high nitrogen content in DDGS bio-oil can deactivate catalysts during bio-oil upgrading, leading to additional upgrading challenges.[10, 15-19]

Catalytic pyrolysis using zeolite catalyst to produce aromatic and olefin hydrocarbons from lignocellulosic biomass has been investigated extensively.[20-23] Techno-economic analysis indicates catalytic pyrolysis is a promising pathway to produce transportation fuels from lignocellulosic biomass.[24] Under this background, DDGS was explored as a potential feedstock for production of hydrocarbons from catalytic pyrolysis.[25] Substantially higher yields of aromatics and olefins were observed with DDGS compared with yields from lignocellulosic biomass. Benzene, toluene, and xylene (BTX) were the predominant aromatic hydrocarbons while ethylene and propylene were the predominant olefin hydrocarbons.[25] BTX with high octane number could be blended with gasoline. However, with regulation on gasoline content of aromatics, benzene especially becomes restricted, and currently the usage of BTX as a gasoline octane booster is less popular.[26] BTX, along with ethylene and propylene, are mainly used as elementary petrochemicals with higher market value than gasoline. Benzene is used mainly as an intermediate to make other chemicals such as

polymers, plastics, and resins.[26, 27] Toluene and xylene are common solvents in many applications. Para-xylene is the principal precursor to terephthalic acid and dimethyl terephthalate, which are used in the production of plastic bottles and polyester clothing.[26] Ethylene and propylene are also widely used in the chemical industry to produce polymers.[26]

Currently DDGS has an average market value of $242 per metric ton as an animal feed supplement over last 12 months, while BTX, ethylene, and propylene have a tremendously higher market value of around $1300 per metric ton at the same period. This benefit may make hydrocarbon production from DDGS appealing to corn ethanol producers. Moreover, DDGS pricing has more variability than the pricing for petrochemicals. As shown in Figure 1, The price for DDGS has varied dramatically in the past decade from $70-$330 per metric ton, while the petrochemical index was relatively stable at the same period.[7, 28] Additionally, the fuel and petrochemical market is much larger compared with the animal feed market. To maximize the efficiency of the corn biorefinery and to achieve significant market penetration, it may be economically more feasible to convert DDGS to hydrocarbons instead of selling it as animal feed supplement.

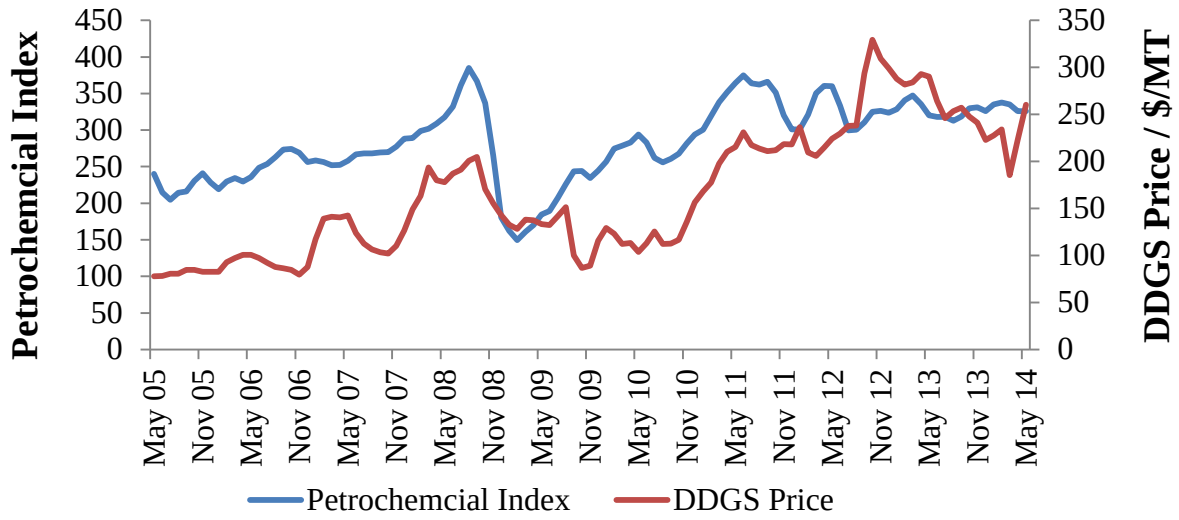

Figure 1. Petrochemical Index and DDGS price at the period of May 2005-May 2014 (data was taken from references [7, 28])

In this study we propose an integrated biorefinery scenario with conventional corn ethanol production followed by DDGS catalytic pyrolysis to produce hydrocarbons. This integrated process was evaluated by modeling with ChemCad^{TM}. Total capital cost, operating cost, and MFSP were calculated to quantify the economic feasibility for the integrated process. Results obtained from the integrated scenario were compared with conventional stand-alone corn ethanol production with DDGS sold as animal feed. The sensitivity of MFSP to various parameters was also discussed along with the result of a Monte Carlo uncertainty analysis.

Methods

Process design

As illustrated in Figure 2, the integrated process includes a conventional corn ethanol facility and an add-on facility to produce hydrocarbons from catalytic pyrolysis of DDGS. The corn ethanol process is a typical dry mill corn ethanol production including processes of corn pretreatment, scarification, sugar fermentation, ethanol distillation, and DDGS

separation. Details about the corn ethanol production process are described in a previous study.[29]

A simplified process flow diagram for an add-on facility processing DDGS is illustrated in Figure 3. DDGS generated from the corn ethanol plant is delivered into pretreatment area for further drying and grinding, where the moisture of DDGS is reduced from 10 wt% to 2 wt%. Pretreated DDGS is sent into a circulating fluidized bed (CFB) reactor with reaction temperature of 600^{o}C. The yield data from DDGS catalytic pyrolysis shown in Table 1 comes from a previous study by our group.[25]

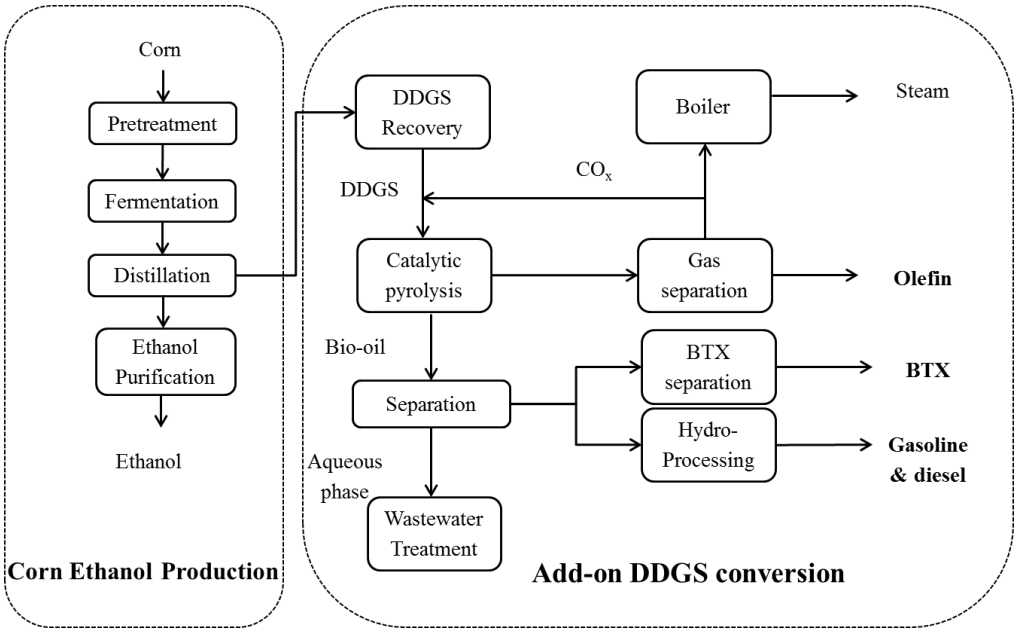

Figure 2. Process diagram for the integrated corn biorefinery (corn ethanol production + DDGS catalytic pyrolysis)

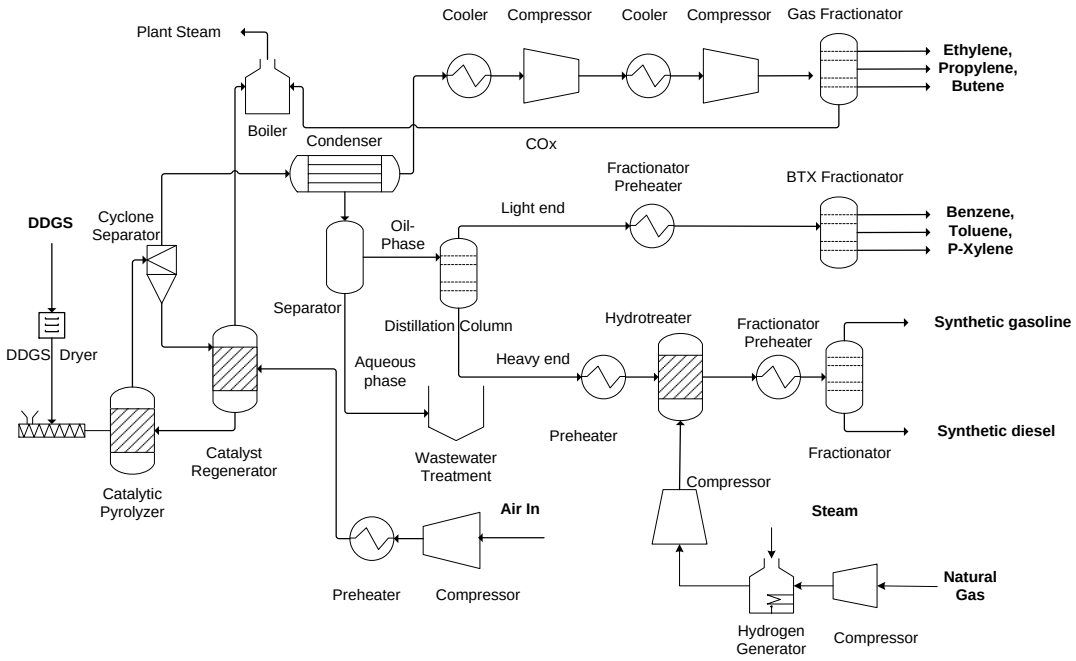

Figure 3. Simplified process flow diagram for processing DDGS to hydrocarbons

Table 1. Product distribution from catalytic pyrolysis of DDGS (data was adapted from reference [25])

Components / % mass fraction of DDGS feedstock	
Bio-oil composition	
benzene	3.30
toluene	7.07
p-xylene	4.86
ethyl-benzene	0.62
o-xylene	1.25
1-ethyl-3-methyl-benzene	0.80
2-ethenyl-1,4-dimethyl-benzene	0.22
indane	0.56
indene	0.51
methyl-indene	0.82
naphthalene	1.21
methyl-naphthalene	1.76

Table 1 (Continued)

ethyl-naphthalene	0.62
dimethyl-naphthalene	0.27
anthracene	0.06
methyl-panthracene	0.26
Gaseous product	
ethylene	3.69
propylene	2.99
butene	0.89
CO	16.20
CO_2	13.12
ammonia	3.99
hydrogen cyanide	0.53
water	12.77
Solid product	
char/coke	15.31
ash	5.53

The reactor configuration widely used for fluidized catalytic cracking in the petroleum industry is also well suited for large-scale biomass catalytic pyrolysis.[30-32] Zeolite catalyst and sand is used as heat carriers. A fraction of waste gas from the olefin fractionator is used as fluidization gas. The superficial velocity of 4 m/s is maintained in reactor modeling.[24, 30] The char/coke, catalyst, and heat carrier are separated from the pyrolysis vapor with high flow gas cyclones operating at 90% efficiency. The catalyst is regenerated in the combustor, where the coke and char are burned out. The heated catalyst and sand are recycled back to the CFB pyrolyzer to provide energy for the catalytic pyrolysis reaction.

Hot pyrolysis vapor exiting the pyrolyzer is a mixture of condensable aromatics and non-condensable gases, water, and nitrogen products. The collection system consisting of two condensers and one ESP collects bio-oil containing aqueous and oil phase. The aqueous phase, including water, dissolved ammonia, and hydrogen cyanide, is separated and pretreated in a wastewater treatment unit as described in literature.[33] The oil phase is separated as light and heavy fractions. Light fraction includes benzene, toluene, and p-xylene, while other aromatics are separated as the heavy fraction. BTX is further separated into pure streams of benzene, toluene, and p-xylene, which is sold as renewable petrochemicals.

Aromatics in the heavy fraction are upgraded in a following hydroprocessing unit to obtain hydrocarbons that can be used as blendstock for gasoline and diesel production. However, there are no publications showing detailed data for upgrading heavy-end streams with compositions similar to those evaluated in this study. The present analysis utilizes the same assumptions as used in the literature [24, 34] to estimate the product yield from hydroprocessing. Table 2 gives the material balance from the hydroprocessing unit. Hydrogen consumed in the hydroprocessing unit is produced by steam reforming of merchant natural gas. The non-condensable gases, consisting of olefin, CO, and $CO_{2,}$ are separated in a cryogenic separation unit widely used in the petrochemical industry.[32, 33] The off-gas stream consisting of CO and CO_2 is sent to a boiler for combustion with off-gas from other processes to provide process heat.

Table 2. Material balance for hyroprocessing of heavy-end aromatics

Components	wt% of DDGS feedstock
Feed hydrogen	0.60
Gasoline fraction	4.90
Diesel fraction	4.29

Economic analysis

Models for both stand-alone and integrated corn biorefinery facilities are constructed using ChemCAD^{TM}. The analysis uses economic assumptions similar to those provided in previous biofuel techno-economic analyses.[24, 29, 35-37] Heat and mass balances are obtained from the ChemCAD^{TM} model in order to calculate equipment capital and operating costs. The process design is based on the current state of technology and is assumed to be an n^{th} plant. Purchase cost of some simple equipment such as pumps and compressors are obtained directly from ChemCAD^{TM}. The pyrolysis reactor cost is based on data from previous studies.[24, 38] In this study, both plants are assumed to have 30-year lifetimes. A modified discounted cash flow rate of return (DCFROR) spreadsheet is employed to calculate the MFSP in this study. Table 3 details the major assumptions employed in this analysis. Financial assumptions include 40% equity with a 7.5% loan interest rate and 10-year loan term. Equipment costs depreciate at a double-declining rate over seven years for the general plant with zero equipment salvage value. The depreciation period for the steam generation plant is 20 years. The income tax rate is 39% and the internal rate of return (IRR) is 10% over a 30-year project lifetime. The facility construction period is three years with capital expenditure percentages of 32%, 60%, and 8% in the first three years, respectively.

Table 3. Major economic analysis assumptions

Plant Life (Years)	30
Operating Hours per Year	7920
Equity	100%
General Plant Depreciation	200 declining balance (DB)
Steam Plant Depreciation	150 DB
Depreciation Period (Years)	
General Plant	7
Steam/Electricity System	20
Construction Period (Years)	2.5
% Spent in Year -3	8.00%
% Spent in Year -2	60.00%
% Spent in Year -1	32.00%
Start-up Time (Years)	0.5
Revenues (% of Normal)	50%
Variable Costs (% of Normal)	75%
Fixed Cost (% of Normal)	100%
IRR	10.00%
Income Tax Rate	39.00%

The sum of purchased equipment costs are reported as total purchased equipment cost (TPEC). All prices are adjusted to 2012 dollars. Total project investment cost is calculated as a function of TPEC based on a cost estimation methodology developed by Peters et al.[39] Table 4 summarizes all of the assumption factors used for capital cost in this analysis. A total installation factor of 3.02 is used to estimate the installed equipment cost for both the corn ethanol plant and the catalytic pyrolysis plant. A Lang Factor of 5.10, which has been employed in previous analyses of biofuel production[24, 29, 36], is employed to estimate total capital investment.

Table 4. Major factors of capital investment estimation for n^{th} plant

Parameter	Assumption
Total purchased equipment cost (TPEC)	100%
Purchased equipment installation	39%
Instrumentation and controls	26%
Piping	31%
Electrical systems	10%
Yard improvement	12%
Service facilities	55%
Total installed cost (TIC)	302% of TPEC
Indirect cost	
Engineering	32%
Construction expenses	34%
Legal expenses	4%
Contractor's fee	19%
Contingency	37%
Indirect cost (IC)	126%
Fixed capital investment (FCI)	428%
Working capital (15% of FCI)	75%
Land use	6% of TPEC
Total capital investment (TCI)	510%

Annual variable operating costs include costs for corn feedstock, natural gas, catalysts and chemicals, waste disposal, electricity, and other utilities. Table 5 details the variable operating parameters employed in the analysis. Since 2011 prices of corn grain and DDGS have ranged widely from \$170-\$363/MT and \$170-\$330/MT, respectively.[7] Based on the 3-year average prices for both, the cost of corn feedstock is assumed to be \$236/MT (\$ 6/bu) and the cost of DDGS to be \$270/MT. Those values are also in line with costs in previous analysis.[29] Average prices of aromatic and olefin hydrocarbons in last three years are

employed in this analysis.[40] Prices of zeolite catalysts, synthetic gasoline/diesel and other chemicals for ethanol production are taken from published literature.[34, 35, 41, 42]

Table 5. Materials and operating parameter employed in the analysis

Material	Price
Feedstock	
Corn	$236/metric ton
Sulfuric acid	$0.28/kg
Alpha-Amylase	$3.96/kg
Glucoamylase	$3.96/kg
Cellulase	$0.39/kg
Yeast	$5.51/kg
Electricity	$0.07/kwh
Catalyst	$13.2/kg
Natural gas	$5.90/MMBTU
Product	
DDGS	$270/metric ton
Benzene	$1316/metric ton
Toluene	$1186/metric ton
p-Xylene	$1404/metric ton
Synthesized gasoline/ diesel	$2.92/gallon
Ethylene	$1289/metric ton
Propylene	$1263/metric ton
Butene[a]	$1263/metric ton

[a]price of propylene was used to denote price of butene due to unavailability of actual data

In addition to variable operating costs, fixed operating costs are also considered. These include labor, overhead, maintenance, insurance, and taxes. Maintenance and insurance are assumed to be 1.5% and 2% of total fixed capital investment. Labor salaries are adapted from the literature [38] and overhead is assumed to be 60% of labor costs.

Sensitivity and uncertainty analysis

Process parameters may vary during operation for the integrated biorefienry. Therefore, sensitivity analysis is employed to evaluate the influences of parameter variation on the MFSP. This is accomplished by evaluating MFSP after changing one parameter while assuming all other parameters remain fixed. In this analysis, the parameters considered are market price of hydrocarbons yield, fixed capital investment, utilities, feedstock cost, and IRR. For those parameters, a ±20% range of values around each case is employed. MFSP is evaluated for the base case, the high-end value, and the low-end value for each parameter.

The sensitivity analysis varies only one parameter while the rest remain fixed. However, in practice, values for several model parameters would vary simultaneously. Thus a Monte Carlo analysis is performed for the integrated facility to evaluate the uncertainty of the result from techno-economic analysis. We employed triangular probability distribution with the same ranges assumed in the sensitivity analysis for corn price, yield of hydrocarbons, fixed capital investment and IRR. The simulation was performed with 3000 trials using Crystal Ball® software and the data is analyzed through Excel® software.

Results and discussion

Process modeling

Table 6 details the input-output mass and energy balances based on high heating value for the stand-alone and integrated scenarios. Ethanol is the main product for both scenarios as measured by mass and energy. The total value of co-products from the integrated scenario is $109 million per year, while that for the stand-alone scenario is $78.5 million per year. Moreover, DDGS is the only co-product for the stand-alone ethanol

production scenario, while co-products from the integrated scenario consist of aromatics, olefins, and synthetic gasoline and diesel. Thus, the integrated scenario has the potential to diversify and bolster the value chain of the corn biorefinery over that of the stand-alone scenario. The mass yield of all hydrocarbons from DDGS is 32 wt%. Of the series of hydrocarbon by-products, BTX are the main ones, the mass production of these being 131 metric ton per day. Energy output of BTX is 228 GJ/h, accounting for 40% of total energy of the co-products stream. Olefin products primarily consist of ethylene and propylene, production of which is 65 metric ton per day. The overall energy efficiency of the add-on facility for DDGS conversion is 58.0% on a high heating value (HHV) basis.

Table 6. Mass and energy balance for the stand-alone and integrated corn biorefinery (data for stand-alone scenario was adapted from reference [29]).

Scenario	Stand-alone				Integrated			
Materials	Mass (t/d)	HHV (MJ/kg)	Energy (GJ/h)	Values ($MM/yr)	Mass (t/d)	HHV (MJ/kg)	Energy (GJ/h)	Values ($MM/yr)
Inputs								
Corn	2000	19.1	1588	208	2000	19.1	1588	208
Electricity	n/a	n/a	24.1		n/a	n/a	85.6	14.7
Natural Gas	85.6	52.2	186		154	52.2	335	
Outputs								
Ethanol	n/a	29.8	1050	n/a		29.8	1050	n/a
DDGS	880	20.3	672	78.4	n/a	n/a	n/a	n/a
BTX	n/a				131	41.8	228	55.5
Olefins	n/a				65	47.2	128	27.4
Gasoline	n/a				43.1	47.3	84.9	14.2
Diesel	n/a				37.8	44.8	70.5	12.5

Economic results

Table 7 details the major economic analysis result for the two scenarios. Total capital investment is the sum of total installed equipment cost, working capital cost, total indirect cost, project contingency, and land use. Estimated installed equipment costs for stand-alone scenario and integrated scenario are $115 million and $237 million, respectively. Thus, the add-on facility for DDGS conversion contributes an extra $122 million of installed equipment cost. Figure 4 details the breakdown of the installed equipment cost for the integrated scenario. Details about installed equipment cost for corn ethanol production were reported in a previous study.[29] Installed equipment cost for pyrolysis is $61 million, which accounts for around half of the installed cost for the add-on DDGS processing facility. Hydroprocessing plus the hydrogen production plant accounts for 27.4% of the installed value of add-on facility with a value of $33 million. The product separation unit accounts for 11% of the installed cost with a value of $14 million. Other equipment cost includes utility and product storages, which constitutes 11% of the total installed cost.

Table 7. Capital investment and annual operating cost for stand-alone and integrated scenarios (data for standalone scenario was adapted from reference [29])

Scenarios	Stand-alone	Integrated
Costs	$ million	$ million
Capital Investment		
Total installed equipment cost	115.0	237.0
Total purchased equipment cost	38.1	67.9
Working capital	28.6	50.9
Total indirect cost	48.0	85.5
Project Contingency	14.1	25.1
Land Use	2.3	4.1
Total Capital Investment	194.2	346.2
Annual operating cost		

Table 7 (Continued)

Feedstock	207.7	207.7
Natural Gas	9.8	14.7
Catalysts & Chemicals	9.1	11.5
Waste Disposal	0.0	3.5
Electricity and other utilities	7.4	18.1
Fixed Costs	8.8	15.7
Capital Depreciation	5.3	11.2
Average Income Tax	7.1	12.2
Average Return on Investment	69.5	55.8
Co-product credit	-78.4	-109
Total Annual Operation Cost	246	241
***MFSP*/** $/gallon ethanol	2.18	2.27

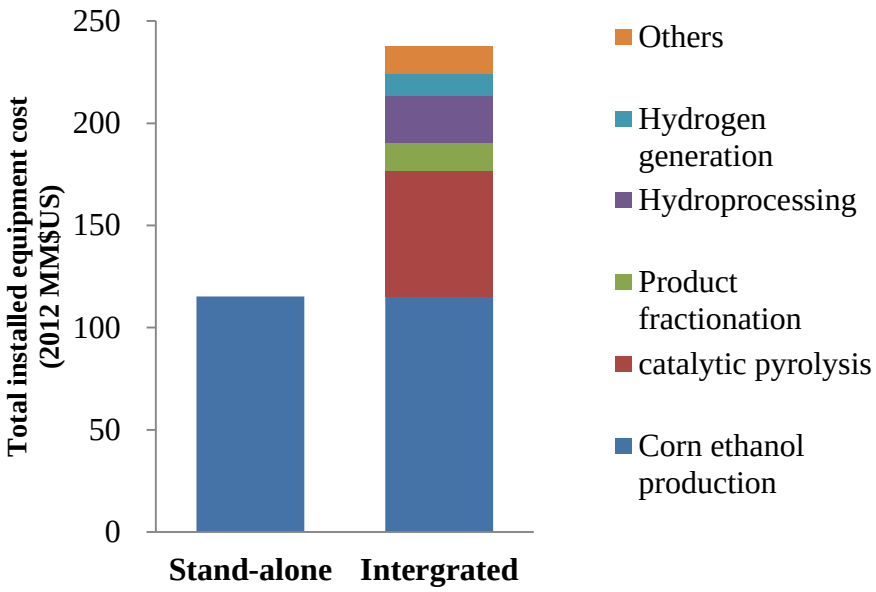

Figure 4. Installed equipment cost for the stand-alone and integrated scenarios (data for stand-alone scenario was adapted from reference [29])

Feedstock cost is the largest contributor for both scenarios. The utilities, including natural gas and electricity, are quite different for the two scenarios. Add-on DDGS

conversion facility significantly increases the usage of those utilities, leading to higher utilities costs for integrated scenario. The annual costs of natural gas and electricity for the integrated scenario are $14.1 million and $18 million, respectively. In contrast, these for the stand-alone scenario are $9.1 million and $7.4 million. For the integrated scenario, more labor is required for operating pyrolysis, product fractionation, and waste water treatment facilities, which results in higher fixed operating costs compared with stand-alone scenario. Fixed operating cost increases from $9 million to $16 million with the add-on facility in operation. The capital depreciation and income tax are also quite different for the two scenarios. Annual capital depreciation, which is directly related to capital investment, is $5.3 million and $11.2 million for stand-alone and integrated scenarios, respectively. Greater net revenue results in a larger income tax burden. Thus the average income tax cost is $7.1 million for stand-alone ethanol production and $13.7 million for the integrated biorefinery scenario. The biggest difference for the two scenarios is the co-product credit. DDGS from stand-alone scenario contribute $78.4 million credit while the hydrocarbons from integrated scenario contribute $109 million credit. The total annual operating costs are estimated at $246 million and $241 million for stand-alone and integrated scenario, respectively.

The MFSP for the integrated scenario is estimated to be $2.27 per gallon, which is comparable to MFSP of $2.18 per gallon for the stand-alone scenario. Figure 5 shows the contributions to the production costs for the two scenarios. The feedstock cost is the largest contributor to the ethanol price cost for both scenarios. One significant difference for the two scenarios is the co-products benefit. Co-product from the stand-alone corn ethanol scenario is DDGS, credit of which is $0.82/gallon ethanol. Catalytic pyrolysis of DDGS generated petrochemicals including BTX, olefin, and synthesis gasoline/diesel derived from

hydroprocessing of heavy-end bio-oil. Those co-products contribute $1.14/gallon credit in total, which is significantly higher compared to the credit from unprocessed DDGS. Waste disposal contributes $0.04/gallon to the production cost of the integrated scenario while it is negligible for stand-alone corn ethanol production.

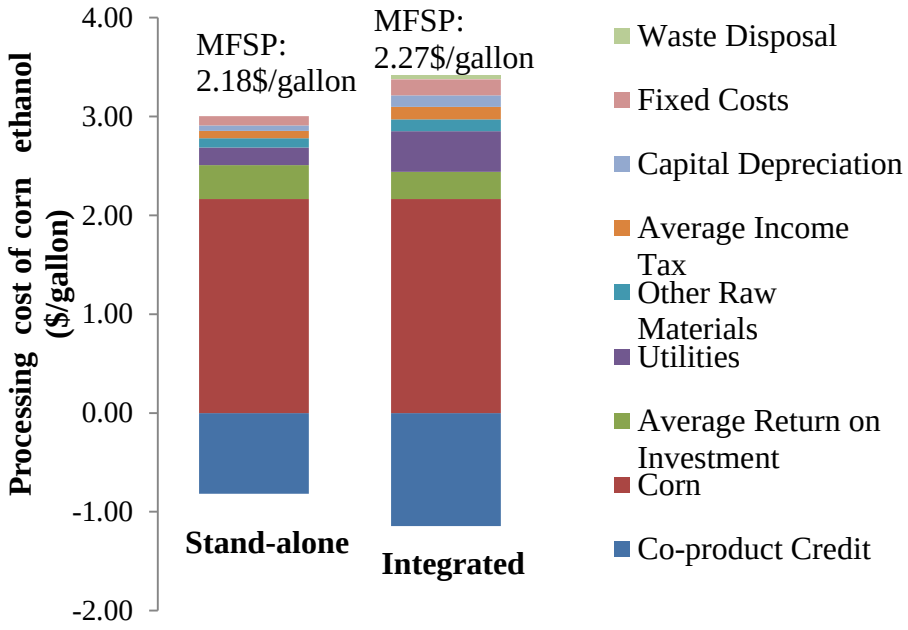

Figure 5. Ethanol fuel conversion cost for stand-alone and integrated corn biorefinery scenario (data for stand-alone scenario was adapted from ref. [29])

Sensitivity and uncertainty analysis

The discussion above is based on an economic analysis that assumes all parameters are precisely known; however, many of the costs and parameters used to evaluate the probability are subject to significant volatility throughout the project's 30-year life. Moreover, the add-on catalytic pyrolysis and hydroprocessing technology is still in early development. The hydrocarbon yields from catalytic pyrolysis have potential to be improved while the facility employed in the future may require more capital investment. Sensitivity analysis is conducted here to investigate the impact of several parameters, including

feedstock cost, yield of co-products, total capital cost, IRR, and income tax rate. Sensitivity analysis result is shown in Figure 6.

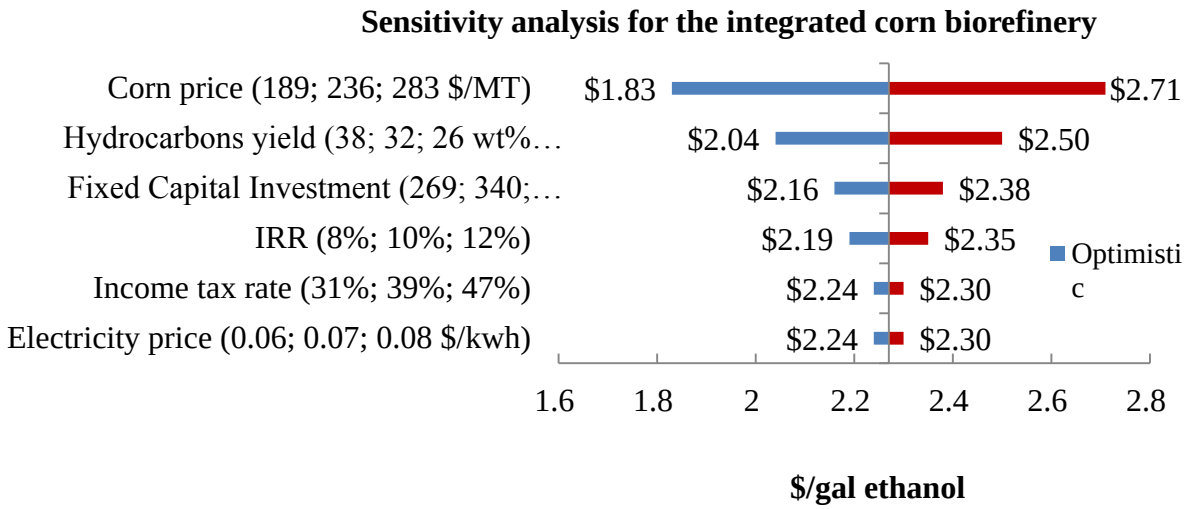

Figure 6. Sensitively analysis for the integrated scenario of corn biorefinery

Feedstock cost has the greatest impact on MFSP. A 20% increase of corn price from $236/MT to $283/MT leads to MFSP increasing from $2.27/gallon to $2.71/gallon. Another key parameter in terms of MFSP sensitivity is hydrocarbon yield. MFSP decreased 10% when overall hydrocarbon yield increased from 32 wt% to 38 wt%. This indicates that future studies to improve the yield of hydrocarbons from catalytic pyrolysis have potential to further reduce MFSP. Modifying catalysts and recycling certain fraction of olefins are two feasible options as suggested in the literature.[21, 43] Fixed capital investment and IRR also have considerable effect on MFSP, while income tax rate and utilities like electricity price have negligible impact.

A Monte Carlo simulation for MFSP distribution was conducted to quantify the uncertainty of the techno-economic analysis results. Sensitivity analysis suggests that feedstock cost, yield of co-products, fixed capital investment, and IRR have the greatest

influence on MFSP. Thus these four model parameters are treated as changing variables in the Monte Carlo simulation. All of these variables are assumed with the same variation range of ±20% used in the sensitivity analysis. Three thousand random MFSP are generated during the simulation. Figure 7 details the cumulative probability of the resulting MFSP, which ranges from $1.69 to $2.85 per gallon with 80% probability of falling in the range of $1.99 to $2.53. MFSP for the integrated scenario has a 50% probability of being less than $2.26 per gallon. This result suggests that ethanol fuel price from the integrated facility is economically competitive with the stand-alone facility. With the benefits of product diversity, the integrated pathway may be more appealing to ethanol producers and policy makers.

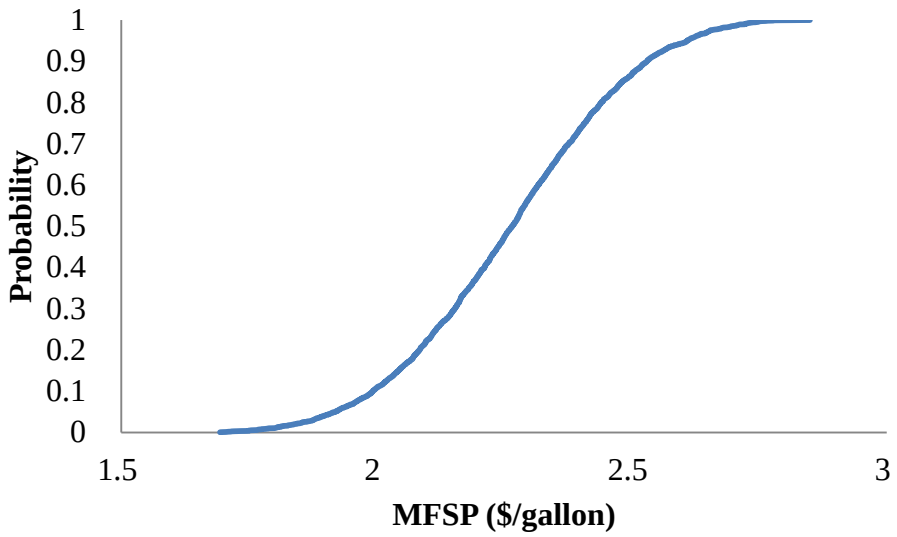

Figure 7. Cumulative probability distribution of MFSP of the integrated scenario

Conclusions

The techno-economic analysis evaluated the economic feasibility of an integrated corn biorefinery process, where DDGS from ethanol production is used as feedstock to produce hydrocarbon fuels and chemicals. The results from the integrated scenario were compared with stand-alone corn ethanol production with DDGS sold as animal feed. The integrated scenario yielded 32 wt% hydrocarbon products from DDGS, including aromatics, olefins, and synthetic gasoline and diesel. Those co-products can be used as "drop in" transportation fuels and value-added petrochemicals. Total values of those by-products are $112 million per year, which is substantially higher than the $78 million per year for unprocessed DDGS. These figures indicate the integrated corn biorefinery may benefit from both product diversity and enhanced values. The total project investment cost for the 2000 metric ton per day integrated facility was $346 million compared with $194 million for stand-alone scenario. The operating cost for the integrated scenario is also higher than that for the stand-alone scenario due to the higher demand for utilities and labor costs for the integrated scenario. With 10% IRR, the MFSP from the integrated scenario is $2.27/gallon, which is comparable to MFSP for the stand-alone scenario. A sensitivity analysis is performed to determine which model parameters have the most influence on the MFSP. Feedstock cost is the greatest contributor followed by hydrocarbons yield. Other key parameters include fixed capital investment and IRR. A Monte Carlo simulation is conducted to calculate a most probable fuel price of $2.26 per gallon, which suggests that the integrated scenario is competitive with the stand-alone scenario.

Acknowledgments

The authors acknowledge the financial support from the Iowa Energy Center (Grant No. 10-02).

References

[1] B. Dinneen, 2013 Ethanol Industry Outlook, in, Renewable Fuels Association, 2013.

[2] T.R. Brown, R.C. Brown, A review of cellulosic biofuel commercial-scale projects in the United States, Biofuels, Bioproducts and Biorefining, 7 (2013) 235-245.
[3] R.C. Brown, Biorenewable Resources: Engineering New Products from Agriculture, Ames,IA, 2003.

[4] S. Naik, V.V. Goud, P.K. Rout, A.K. Dalai, Production of first and second generation biofuels: a comprehensive review, Renewable Sustainable Energy Rev, 14 (2010) 578-597.

[5] T.M. Lammens, M.C.R. Franssen, E.L. Scott, J.P.M. Sanders, Availability of protein-derived amino acids as feedstock for the production of bio-based chemicals, Biomass Bioenerg, 44 (2012) 168-181.

[6] W.G. Hettinga, H.M. Junginger, S.C. Dekker, M. Hoogwijk, A.J. McAloon, K.B. Hicks, Understanding the reductions in US corn ethanol production costs: An experience curve approach, Energ Policy, 37 (2009) 190-203.

[7] D. Hofstrand, A. Johanns, Weekly Ethanol, Distillers Grains, & Corn Prices, in, 2014.

[8] R. Song, Lipid peroxidation in corn dried distillers grains with solubles (DDGS) and effects of feeding a highly oxidized DDGS source to swine, in, THE UNIVERSITY OF MINNESOTA, 2013.

[9] A. Tavasoli, M.G. Ahangari, C. Soni, A.K. Dalai, Production of hydrogen and syngas via gasification of the corn and wheat dry distiller grains (DDGS) in a fixed-bed micro reactor, Fuel Process Technol, 90 (2009) 472-482.

[10] A.A. Boateng, C.A. Mullen, N.M. Goldberg, Producing Stable Pyrolysis Liquids from the Oil-Seed Presscakes of Mustard Family Plants: Pennycress (Thlaspi arvense L.) and Camelina (Camelina sativa)†, Energ Fuel, 24 (2010) 6624-6632.

[11] A. Kumar, K. Eskridge, D.D. Jones, M.A. Hanna, Steam–air fluidized bed gasification of distillers grains: Effects of steam to biomass ratio, equivalence ratio and gasification temperature, Bioresource Technol, 100 (2009) 2062-2068.

[12] R.M. Swanson, A. Platon, J.A. Satrio, R.C. Brown, Techno-economic analysis of biomass-to-liquids production based on gasification, Fuel, 89 (2010) S11-S19.

[13] P.L. Spath, D.C. Dayton, Preliminary screening-technical and economic assessment of synthesis gas to fuels and chemicals with emphasis on the potential for biomass-derived syngas, in, DTIC Document, 2003.

[14] H.W. Lei, S.J. Ren, L. Wang, Q. Bu, J. Julson, J. Holladay, R. Ruan, Microwave pyrolysis of distillers dried grain with solubles (DDGS) for biofuel production, Bioresource Technol, 102 (2011) 6208-6213.

[15] W. Christine, M. Kasiviswanathan, R.K. A., Pyrolysis of Distillers Grains, in: 2012 ASABE Annual International Meeting, American Society of Agricultural and Biological Engineers, Dallas, TX, 2012.
[16] W. Christine, M. Kasiviswanathan, R.K. A., Optimization of the Pyrolysis of Distillers Dried Grains with Solubles, in: 2013 ASABE Annual International Meeting, American Society of Agricultural and Biological Engineers, Kansas City, Missouri, 2013.

[17] C.A. Mullen, A.A. Boateng, K.B. Hicks, N.M. Goldberg, R.A. Moreau, Analysis and Comparison of Bio-Oil Produced by Fast Pyrolysis from Three Barley Biomass/Byproduct Streams, Energ Fuel, 24 (2010) 699-706.

[18] C. Mullen, A. Boateng, Production and Analysis of Fast Pyrolysis Oils from Proteinaceous Biomass, BioEnergy Res, 4 (2011) 303-311.

[19] K. Wang, R.C. Brown, S. Homsy, L. Martinez, S.S. Sidhu, Fast pyrolysis of microalgae remnants in a fluidized bed reactor for bio-oil and biochar production, Bioresource Technol, 127 (2013) 494-499.

[20] T.R. Carlson, G. Tompsett, W. Conner, G. Huber, Aromatic Production from Catalytic Fast Pyrolysis of Biomass-Derived Feedstocks, Topics in Catalysis, 52 (2009) 241-252.

[21] Y.-T. Cheng, J. Jae, J. Shi, W. Fan, G.W. Huber, Production of Renewable Aromatic Compounds by Catalytic Fast Pyrolysis of Lignocellulosic Biomass with Bifunctional Ga/ZSM-5 Catalysts, Angewandte Chemie, 124 (2012) 1416-1419.

[22] K. Wang, K.H. Kim, R.C. Brown, Catalytic pyrolysis of individual components of lignocellulosic biomass, Green Chemistry, 16 (2014) 727-735.

[23] K. Wang, R.C. Brown, Catalytic pyrolysis of microalgae for production of aromatics and ammonia, Green Chemistry, 15 (2013) 675-681.

[24] R. Thilakaratne, T. Brown, Y. Li, G. Hu, R. Brown, Mild catalytic pyrolysis of biomass for production of transportation fuels: a techno-economic analysis, Green Chemistry, 16 (2014) 627-636.

[25] K. Wang, R.C. Brown, Catalytic pyrolysis of corn dry distillers grains with solubles to produce hydrocarbons in, 2014.

[26] D.L. Burdick, W.L. Leffler, Petrochemicals in Nontechnical Language, PennWell Corporation, 2010.

[27] D. Seddon, Petrochemical Economics: Technology Selection in a Carbon Constrained World, Imperial College Press, 2010.

[28] ICIS, ICIS Petrochemcial Index, in, 2014.

[29] L. Ou, T.R. Brown, R. Thilakaratne, G. Hu, R.C. Brown, Techno‐economic analysis of co‐located corn grain and corn stover ethanol plants, Biofuels Bioprod Biorefin, 8 (2014) 412-422.

[30] J.R. Grace, A.A. Avidan, T.M. Knowlton, Circulating Fluidized Beds, Blackie Academic & Professional, 1997.

[31] R. Sadeghbeigi, Fluid Catalytic Cracking Handbook: An Expert Guide to the Practical Operation, Design, and Optimization of FCC Units, Butterworth-Heinemann, 2012.

[32] D.L. Erwin, Industrial Chemical Process Design, McGraw-Hill Professional Publishing, 2002.

[33] R. Meyers, Handbook of Petroleum Refining Processes, McGraw-Hill Education, 2003.

[34] R. Thilakaratne, M.M. Wright, R.C. Brown, A techno-economic analysis of microalgae remnant catalytic pyrolysis and upgrading to fuels, Fuel, 128 (2014) 104-112.

[35] Y. Zhang, T.R. Brown, G. Hu, R.C. Brown, Techno-economic analysis of monosaccharide production via fast pyrolysis of lignocellulose, Bioresource Technol, 127 (2013) 358-365.

[36] T.R. Brown, R. Thilakaratne, R.C. Brown, G. Hu, Techno-economic analysis of biomass to transportation fuels and electricity via fast pyrolysis and hydroprocessing, Fuel, 106 (2013) 463-469.

[37] T.R. Brown, R. Thilakaratne, R.C. Brown, G. Hu, Regional differences in the economic feasibility of advanced biorefineries: Fast pyrolysis and hydroprocessing, Energ Policy, 57 (2013) 234-243.

[38] M.M. Wright, D.E. Daugaard, J.A. Satrio, R.C. Brown, Techno-economic analysis of biomass fast pyrolysis to transportation fuels, Fuel, 89 (2010) S2-S10.

[39] M.S. Peters, K.D. Timmerhaus, R.E. West, Plant Design and Economics for Chemical Engineers, McGraw-Hill Education, 2004.

[40] P. Global, Platts Global Petrochemcial Index, in, 2014.

[41] SRI, PEP Yearbook International 2007, SRI International, Menlo Park, (2007).

[42] A. Aden, Biochemical production of ethanol from corn stover: 2007 state of technology model, in: Technical report NREL/TP-510-43205, National Renewable Energy Laboratory, Golden, CO, 2008.

[43] T.R. Carlson, Y.-T. Cheng, J. Jae, G.W. Huber, Production of green aromatics and olefins by catalytic fast pyrolysis of wood sawdust, Energy Environ Sci, 4 (2011) 145-161.

CHAPTER 8 CONCLUSIONS AND FUTURE WORK

Conclusion

Pyrolysis/catalytic pyrolysis of protein-and lipid- rich biomass was investigated here. The results presented in this dissertation significantly advance the understanding about utilization of protein-rich feedstock. Firstly, catalytic pyrolysis was introduced to conversion of protein-rich biomass into nitrogen-free hydrocarbons, which can be used as drop-in biofuel or value-added chemicals. With adding zeolite catalyst, most of the nitrogen present in biomass was removed as ammonia, which can be recycled as fertilizer for biomass growth. Based on these findings, a nitrogen recycle concept was proposed for processing protein-rich feedstock. Secondly, the study investigated the reaction mechanism during catalytic pyrolysis of nitrogenous biomass. Nitrogenous biomass including microalgae and DDGS was found to produced higher hydrocarbons yield compared with lignocellulosic biomass. Pyrolysis experiment using model compounds for individual components were used to determine the contribution of each component. The results indicate that lignin in biomass mainly contribute to char/coke formation. Protein and lipid produced significant higher yield of both aromatic and olefin hydrocarbons. Lipids in biomass have a positive synergistic effect with other components in the nitrogenous biomass to enhance hydrocarbon yield. Thirdly, *in-situ* and *ex-situ* catalytic pyrolysis was investigated comparatively in a Tandem-micro reactor system. The remarkably high olefin yield from *ex-situ* catalytic pyrolysis suggests the possibility of exploiting the process to preferentially obtain olefins from biomass. A dual catalytic reaction cycle mechanism was introduced to explain the reaction mechanism. Additionally, this study also performed a techno-economic analysis to evaluate the economic feasibility for catalytic pyrolysis protein-rich DDGS for producing hydrocarbon fuels and chemicals. The results

demonstrated that the integrated process with add-on facility for DDGS conversion is competitive with conventional standalone corn ethanol production process.

Future Work

The long-term goal of protein-rich biomass pyrolysis research is to produce drop-in biofuel and chemicals economically and sustainably in industry scales. Researches for this dissertation have focused on mechanism study using micro-scale reactor, which help us to understand the reaction chemistry during this process. However, the knowledge gap between the micro-scale and commercial scale utilization in future will be significant. Continued efforts will likely involve study on continuous bench- or pilot-scale reactors to get bridged the knowledge gap. The result in Chapter 6 has suggest that mass and heat transfer have significantly influence on product distribution from catalytic pyrolysis. Thus heat and mass transfer issues for large scale reactors will be an interesting topic for future study.

Currently, the yield of hydrocarbons from catalytic pyrolysis is significantly lower than the theoretical value. Another issue for catalytic pyrolysis of protein-rich biomass is the formation of toxic hydrogen cyanide. Although the small quantity of cyanide can be removed by passing the pyrolysis vapors through a basic solution or packed bed of metal hydroxide, formation of extremely toxic cyanide will impair the sustainability of the catalytic process anyway. Thus one study I would like to pursue in future is to catalyst modify for increasing the hydrocarbon yield and depressing the cyanide formation, which will enhance the sustainability and economics of the process.

Catalytic pyrolysis is normally operated at inert atmosphere and ambient pressure. The effect of active gases like hydrogen on catalytic pyrolysis is not clear. It will be an

interesting topic to investigate catalytic pyrolysis especially *ex-situ* one with atmosphere of hydrogen, carbon monoxide, methane, etc. Moreover, few researches have been conducted on pyrolysis of protein-rich biomass with high pressure reactive gases, which is normally referred as hydropyrolysis. Hydropyrolysis was first investigated with coal, which produced enhanced yield of hydrocarbons compared with pyrolysis in the absence of hydrogen. We hypothesis that the hydrogen may react with the free radicals from biomass pyrolysis, leading to deoxygenated bio-oil rich in hydrocarbon products. Additionally, formation of hydrogen cyanide will be suppressed in the process. Higher carbon conversion and enhanced economic performance are expected from hydropyrolysis, compared with catalytic pyrolysis with zeolite. Hydropyrolysis of nitrogen-rich biomass will be the focus of my future research.

.